











Review

Concept of Hybrid Drugs and Recent Advancements in Anticancer Hybrids

Ankit Kumar Singh ^{1,†}, Adarsh Kumar ^{1,†}, Harshwardhan Singh ¹, Pankaj Sonawane ¹, Harshali Paliwal ¹, Suresh Thareja ¹, Prateek Pathak ², Maria Grishina ², Mariusz Jaremko ³, Abdul-Hamid Emwas ⁴, Jagat Pal Yadav ^{5,6}, Amita Verma ⁵, Habibullah Khalilullah ⁷ and Pradeep Kumar ^{1,*}

- ¹ Department of Pharmaceutical Sciences and Natural Products, Central University of Punjab, Ghudda, Bathinda 154001, India
 - ² Laboratory of Computational Modeling of Drugs, Higher Medical and Biological School, South Ural State University, 454008 Chelyabinsk, Russia
 - ³ Smart-Health Initiative (SHI) and Red Sea Research Center (RSRC), Division of Biological and Environmental Sciences and Engineering (BESE), King Abdullah University of Science and Technology (KAUST), Thuwal 23955, Saudi Arabia
 - ⁴ Core Laboratories, King Abdullah University of Science and Technology (KAUST), Thuwal 23955, Saudi Arabia
 - ⁵ Bioorganic and Medicinal Chemistry Research Laboratory, Department of Pharmaceutical Sciences, Sam Higginbottom University of Agriculture, Technology and Sciences, Prayagraj 211007, India
 - ⁶ Department of Pharmacology, Kamla Nehru Institute of Management and Technology, Faridipur, Sultanpur 228118, India
 - ⁷ Department of Pharmaceutical Chemistry and Pharmacognosy, Unaizah College of Pharmacy, Qassim University, Unayzah 51911, Saudi Arabia
- * Correspondence: pradeepyadav27@gmail.com or pradeep.kumar@cup.edu.in
† These authors contributed equally to this work.



Citation: Singh, A.K.; Kumar, A.; Singh, H.; Sonawane, P.; Paliwal, H.; Thareja, S.; Pathak, P.; Grishina, M.; Jaremko, M.; Emwas, A.-H.; et al. Concept of Hybrid Drugs and Recent Advancements in Anticancer Hybrids. *Pharmaceuticals* **2022**, *15*, 1071. <https://doi.org/10.3390/ph15091071>

Academic Editors: Parvesh Singh and Vipan Kumar

Received: 30 July 2022

Accepted: 22 August 2022

Published: 28 August 2022

Publisher's Note: MDPI stays neutral with regard to jurisdictional claims in published maps and institutional affiliations.



Copyright: © 2022 by the authors. Licensee MDPI, Basel, Switzerland. This article is an open access article distributed under the terms and conditions of the Creative Commons Attribution (CC BY) license (<https://creativecommons.org/licenses/by/4.0/>).

Abstract: Cancer is a complex disease, and its treatment is a big challenge, with variable efficacy of conventional anticancer drugs. A two-drug cocktail hybrid approach is a potential strategy in recent drug discovery that involves the combination of two drug pharmacophores into a single molecule. The hybrid molecule acts through distinct modes of action on several targets at a given time with more efficacy and less susceptibility to resistance. Thus, there is a huge scope for using hybrid compounds to tackle the present difficulties in cancer medicine. Recent work has applied this technique to uncover some interesting molecules with substantial anticancer properties. In this study, we report data on numerous promising hybrid anti-proliferative/anti-tumor agents developed over the previous 10 years (2011–2021). It includes quinazoline, indole, carbazole, pyrimidine, quinoline, quinone, imidazole, selenium, platinum, hydroxamic acid, ferrocene, curcumin, triazole, benzimidazole, isatin, pyrrolo benzodiazepine (PBD), chalcone, coumarin, nitrogen mustard, pyrazole, and pyridine-based anticancer hybrids produced via molecular hybridization techniques. Overall, this review offers a clear indication of the potential benefits of merging pharmacophoric subunits from multiple different known chemical prototypes to produce more potent and precise hybrid compounds. This provides valuable knowledge for researchers working on complex diseases such as cancer.

Keywords: molecular hybridization; anticancer agents; cell lines; in vitro; pharmacophore

1. Introduction

Cancer is a complex group of multiple diseases characterized by inappropriately controlled cell proliferation and replication eventually resulting in disruption of normal physiology, metabolism, or structure. Benign tumors are self-limited and do not invade or metastasize, but in complex stages groups of cells display uncontrolled growth, invasion and metastasis [1]. In the metastasis stage, cancer cells migrate from one organ (the original tumor site) to another organ of the body through the circulatory and lymphatic systems [2].

Cancer occurs by a series of successive deleterious mutations that change cell functions. These mutations often cause aberrant proliferation [3].

Cancer is a major global health care problem that continues to remain a leading cause of morbidity and mortality, with >277 different cancer types. According to estimates from the World Health Organization (WHO) in 2019, in 112 of 183 countries, cancer is the first or second major cause of death before the age of 70 and ranks third or fourth in a further 23 countries. In 2020, for all cancers, 19,292,789 new cases were estimated globally, with a total of 9,958,133 cancer deaths [4]. According to global demographic trends, 420 million new cancer cases are expected annually by 2025 [5].

Over the past 20 years, cancer treatments have improved significantly, and more potent medications have better safety profiles and more precise molecular targeting. Drug resistance is a major challenge with cancer treatment. During clinical usage, almost all targeted anticancer medications encounter resistance. Numerous processes have been related to drug resistance, including genetic and/or epigenetic mutation, amplification, cancer stem cells (CSCs), efflux transporters, apoptotic dysregulation, and autophagy, among others [6–9].

Cancer chemotherapy with single-agent or single mono functional ‘targeted’ drugs has limited rates of success due to resistance and lack of selectivity. To tackle this limitation, combination therapy (multi-component drugs to treat cancer), was developed [10]. Three alternative combination strategies are used: (a) two or more medicines that operate on distinct sites simultaneously or concurrently; (b) multi-targeting or promiscuous drugs treatment; and (c) hybridization drugs [11].

Tumor heterogeneity, drug-drug interactions, unpredictable pharmacokinetic (PK) safety profiles, and poor patient compliance presents a problem for cancer treatment despite the use of drug-combination medicines. Hence, improving drug selectivity while eliminating drug resistance has become crucial for the successful treatment of cancer patients [10].

There are unique challenges to cancer care in the developing as well as developed countries. These include issues with healthcare financing, patient awareness, and treatment delivery [6,7].

To improve the efficiency of using a two-drug cocktail, one approach involves so-called hybrid drugs [12]. The hybridization of biologically active molecules is a new concept and a powerful tool in drug design and development, used to target a variety of diseases [13]. It is a strategy of rational design of such ligands or prototypes based on the recognition of pharmacophoric sub-units that maintain pre-selected characteristics of the original templates [14].

Hybrid drugs are also termed “single molecule multiple targets” or “multiple ligands”. Hybrid molecules imply that one molecule shows structural features of two “parent” molecules. Two parent biologically active molecules (pharmacophores) that independently act at two distinct pharmacological targets. Molecular hybrids designed in a manner to maintain their activities [15] by merging or blending of two or more bioactive compounds or their pharmacophoric subunits into in a new molecular structure with a dual mode of action. The presence of two or more pharmacophores in a single unit leads to a pharmacological potency greater than the sum of each individual moiety’s potencies [16,17].

Additionally, it is important to note that hybrid drugs usually have high molecular mass and lipophilicity; they violate Lipinski’s and Veber’s rules [17]. However, hybrid anticancer drugs have remarkable advantages over conventional anticancer drugs because they are designed to act on a different bio target or interact with numerous targets simultaneously, reducing the likelihood of drug-drug interactions, with reduced side effects and reduced propensity to elicit resistance relative to the parent drugs. These novel hybrid molecules have improved affinity, enhanced efficacy and improved safety [14,18].

Nowadays, hybrid drugs have drawn interest in the purposeful and logical design of ligands functioning selectively on multiple targets, and this has been reflected by an increase in the number of relevant publications in the field. In this review, we have compiled

recent findings from 2011 to 2021 on novel hybrid compounds for different drug classes that exhibit promising anticancer activities. This analysis highlights in vitro anticancer activity of synthesized anticancer hybrids on different cell lines.

2. The Concept of Hybrid Drugs in Anticancer Agent Development

Hybrid drugs are categorized based on the manner in which they are connected to each other. The concept of design and preparation of hybrid molecules is achieved using two strategies, which are described as follows:

1. Combining drug pharmacophoric moieties with: (a) two pharmacophoric groups directly linked; (b) two pharmacophoric groups linked by a spacer.

These approaches are achieved by: (i) the merging of two pharmacophoric groups from two different drugs acting through the same mechanism of action; (ii) the merging of pharmacophoric groups from two drugs acting through different mechanisms of action.

This is the integration of multiple pharmacophores in a single molecule. In this scenario, the starting point is to choose two established pharmacophores with high selectivity for their respective targets and a proper linker is selected to connect these two pharmacophores. This strategy is used to design new anticancer hybrids and is based on the ability of a combination of pharmacophoric moieties on a new molecular structure to retain their affinity and activity for the biological targets (Figure 1).

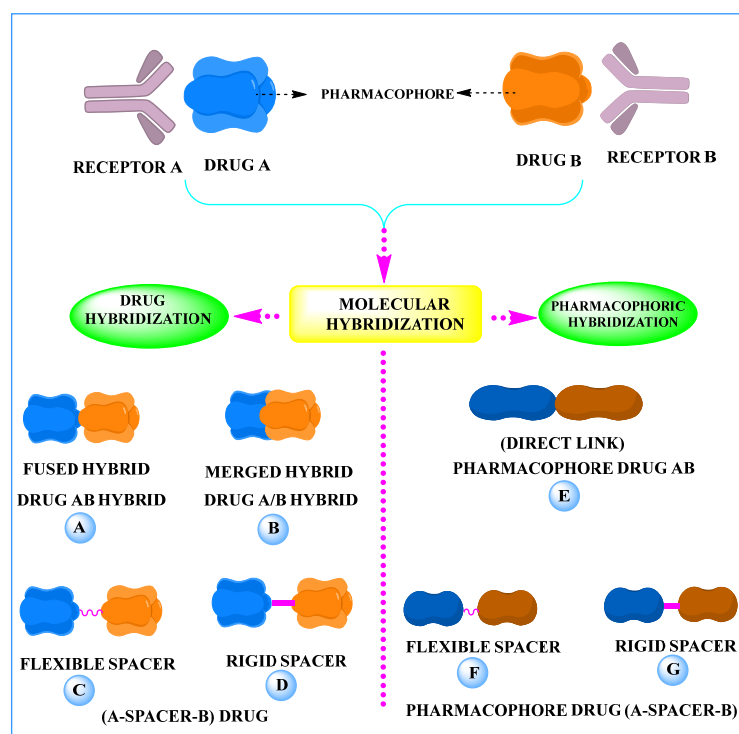


Figure 1. Different methods of molecular hybridization. (A) Drug A and B are directly linked to each other; (B) drug A and B are merged with each other; (C) drug A and B are connected by a flexible spacer; (D) drug A and B are connected through a rigid spacer; (E) two pharmacophoric moieties are directly connected to each other; (F) two pharmacophoric moieties are connected by a flexible spacer; (G) two pharmacophoric moieties are connected by a rigid spacer.

2. Combining two or more entire drugs: the second approach combines two or more entire medications that can be connected either directly or indirectly using a spacer or linker. The following categories apply:

(a) Directly linked hybrid drugs: each molecule is connected via a functional group. Notable examples are mostly enzymatically hydrolysable esters, and carbamateoramide.

(b) Merged or overlapped hybrid drugs: these types of hybrid agents are obtained by overlapping structural motifs or pharmacophores of two drugs. These hybrid agents differ significantly in their structures compared to the drugs from which they were designed. The hybrid agents may retain the functional properties of either or both of the overlapping drugs.

(c) Spacer linked hybrid drugs: the main purpose of using a linker or spacer is to provide a bridge to connect two drugs and modulate the release of individual drugs in vivo. These molecules can be classified as cleavable and non-cleavable.

(1) Non-cleavable hybrid drugs: non-cleavable linkers are connected with non-hydrolysable chemical bonds to create chemically as well as enzymatically stable linkers. This strategy is also based on the ability of the different molecules to retain their biological activity, specificity and respective affinity for their biological targets.

(2) Cleavable hybrid drugs: a cleavable linker is based on the release of two parental molecular structures under physiological or enzymatic conditions that prevail at the site of activity. The majority of cleavable conjugates have an ester linkage that plasma esterases can cleave to release two separate medicines with independent actions (Figure 1).

The purpose of cleavable hybrid drugs is to either improve poor pharmacokinetic properties and slowly deliver the two therapeutic entities in the body (e.g., ester, amide or carbamate), or to improve the selectivity and the antineoplastic activity of the drugs and release the two drugs directly in the targeted tissues (e.g., phosphorylated DES (Diethylstilbestrol) prodrugs for prostate cancer).

Hybrids drugs have been formed by connecting two drugs with the same mechanism of action or by connecting two drugs with different mechanisms of action. The aim of connecting two drugs is to target specific biological tissues [12,19–22].

3. Recent Advances in Anticancer Hybrids

3.1. Quinazoline Based Hybrids

Quinazoline is a heterocyclic compound and potent bioactive scaffold that has been associated with anticonvulsant, anticancer, analgesic, sedative, anti-hypertensive, anti-inflammatory, anti-histaminic, antimicrobial, anti-viral and anti-tubercular properties. Quinazoline containing compounds were investigated for their inhibition of kinases, which are major explored targets of cancer medicine development [23,24].

Cheng et al. (2015) synthesized and explored quinazoline based imidazole hybrids and evaluated their anticancer activity against Epidermal Growth Factor Receptor (EGFR) and HT-29 cells (in normoxic and hypoxic conditions). Most of the synthesized compounds displayed potent anticancer activity. Among them, compound 1(a) showed excellent activity with an IC_{50} of 0.47 nM, 2.21 μ M and 1.61 μ M, respectively compared to the gefitinib control with an IC_{50} of 0.45 nM, 3.63 and 5.21 μ M, respectively. The structure of quinazoline based imidazole hybrids is given in Figure 2. Table 1 shows in vitro antiproliferative activity against the human cancer cell line HT-29 and EGFR inhibitory activity (nM) of compounds 1(b–e) [25].

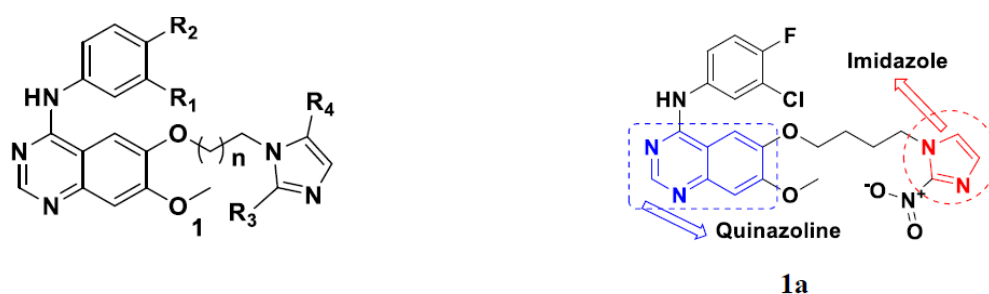
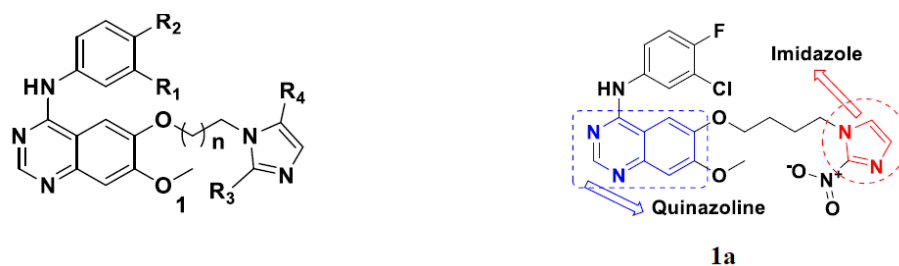


Figure 2. Structure of quinazoline-based imidazole hybrids and the most promising compound 1a.

Table 1. In vitro cytotoxic activities of hybrid compounds 1(b–e).

Compound No.	R ₁	R ₂	R ₃	R ₄	n	EGFR (IC ₅₀ nM)	HT-29 (IC ₅₀ μM)	
							Normoxia	Hypoxia
1b	Cl	F	NO ₂	H	5	0.32	12.89	9.81
1c	Br	H	NO ₂	H	2	0.66	4.48	4.01
1d	ethynyl	H	NO ₂	H	3	0.56	10.08	5.96
1e	ethynyl	H	NO ₂	H	5	0.50	2.93	3.46
Gefitinib						0.45	3.63	5.21

Zhang Y et al. (2017) synthesized and evaluated anticancer activity of quinazoline-based deoxyjirimycin hybrids against Epidermal Growth Factor Receptor (EGFR) and α -glucosidase. Most of the synthesized compounds displayed potent anticancer activity. Among them, compound 2(a) showed excellent activity with an IC₅₀ 1.79 nM and 0.39 μM, respectively (the control gefitinib had an (–IC₅₀ of = 3.32 nM and >100 μM, respectively). The structure of a quinazoline-based deoxyjirimycin hybrid is given in Figure 3 and in vitro EGFR and α -glucosidase inhibitory activity of compounds 2(b–e) against human cancer cell lines is shown in Table 2 [26].

**Figure 3.** Structure of quinazoline-based deoxyjirimycin hybrids and the most promising compound 2a.**Table 2.** In vitro cytotoxic activities of hybrid compounds 2(b–e).

Compound No.	R ₁	R ₂	R ₃	EGFR (IC ₅₀ nM)	α -Glucosidase (IC ₅₀ μM)
2b	3-Cl, 4-(3-fluorobenzoyloxy)			4.53	0.14
2c	3-ethynyl			4.87	0.09
2d	3-ethynyl			ND *	6.25
2e	3-Cl, 4-F			10.71	4.34
Gefitinib				3.32	≥100

* Not determined.

Quinazoline based urea hybrids were synthesized by Zhang et al. (2016) and evaluated for their ability to inhibit EGFR and Vascular Endothelial Growth Factor Receptor-2 (VEGFR-2). Most of the synthesized compounds displayed potent anticancer activity. Among them, compound 3(a) showed excellent activity with an IC₅₀ of 1.0 nM and 79 nM, respectively, when the control vandetanib had an IC₅₀ of 11 nM and >15 nM, respectively.

The structure of a quinazoline-based urea hybrid is given in Figure 4 and in vitro EGFR and VEGFR-2 inhibitory activity of compounds 3(b–e) against human cancer cell lines is shown in Table 3 [27].

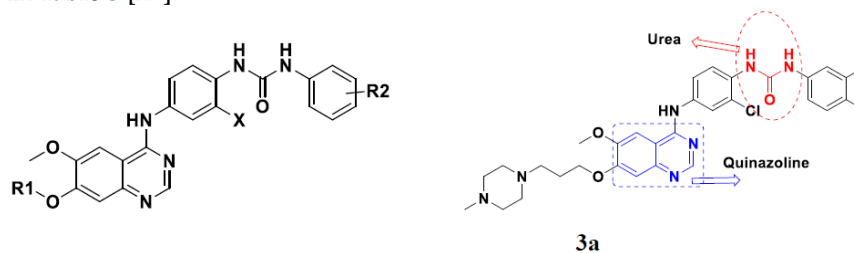


Figure 4. Structure of quinazoline-based urea hybrids and the most promising compound 3a.

Table 3. In vitro cytotoxic activities of hybrid compounds 3(b–e).

Compound No.	R ₁	R ₂	X	EGFR (IC ₅₀ nM)	VEGFR-2 (IC ₅₀ nM)
3b		m-Cl, p-F	Cl	14	14
3c		m-CH ₃ , p-CH ₃	Cl	78	51
3d		o-CH ₃	Cl	15	178
3e		H	Cl	14	261
vandetanib				11	15

Yadav et al. (2016) synthesized substituted quinazoline based aryl hybrids and evaluated their anticancer activity. Most of the synthesized compounds showed excellent activity against different isoforms of PI3K, but compound 4(a) showed 3.7 times more potent activity against Phosphoinositide 3-Kinase(PI3K) α (IC₅₀ = 0.201 μ M) than γ isoform (IC₅₀ = 0.75 μ M), and was a selective inhibitor of MCF-7 cells (human breast adenocarcinoma) with GI50 7 μ M. Compound 4(a) also did not show any cytotoxicity to normal human cells. It inhibited 37% and 62% triglyceride (TGI) at 25 mg/kg dose in Ehrlich solid tumor and Ehrlich ascites carcinoma tumor models, respectively, with a control of 5-fluorouracil at 22 and 20 mg/kg dose with TGI inhibition 50 and 96%, respectively. The structure of quinazoline-based aryl hybrids is given in Figure 5 and the in vitro cytotoxicity of compounds 4(b–e) against human cancer cell lines is shown in Table 4 [28].

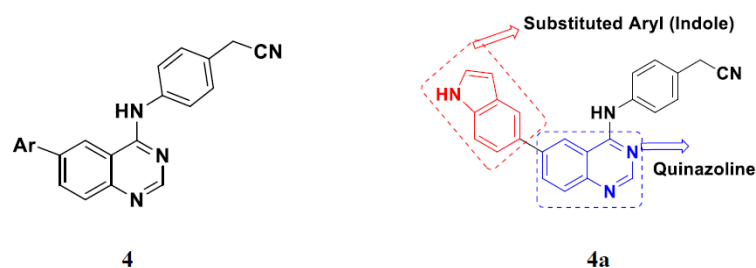
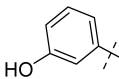
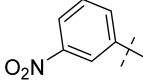
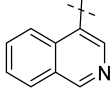
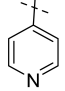
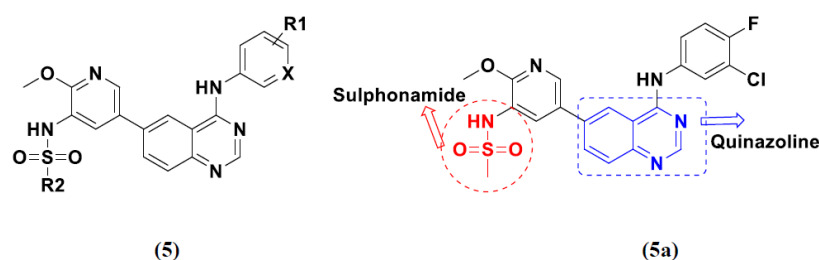


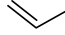
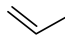
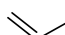
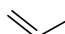
Figure 5. Structure of quinazoline-based aryl hybrids and the most promising compound 4a.

Table 4. In vitro cytotoxic activities of hybrid compounds 4 (b–e).

Compound No.	Ar.	MCF-7 (GI50 μM)	PI3K (IC ₅₀ μM)		
			A	β	γ
4b		15	5.3	16	2.3
4c		12	22.2	1.9	22.2
4d		12	133	56	5.9
4e		32	14.2	0.5	14.2

Ding et al. (2018) synthesized and reported aminoquinazoline-sulphonamide based hybrids and evaluated their anticancer activity. Most of these compounds showed dual inhibitory activity against EGFR and PI3K α . Compound 5(a) showed excellent activity with an IC₅₀ of 2.4 and 317 nM, compared to controls gefitinib (IC₅₀ 2.4 nM) and dactolisib (IC₅₀ 16.4 nM). Compound 5(a) exhibited potent activity against a panel of cell lines including adenocarcinomic human alveolar basal epithelial cells (A549 IC₅₀ = 8.23 μM), epithelial cells (BT549, IC₅₀ = 1.02 μM), human colon cancer cells (HCT-116, IC₅₀ = 5.60 μM), breast cancer cells (MCF-7, IC₅₀ = 5.59 μM), human hepatic adenocarcinoma cells (SK-HEP-1, IC₅₀ = 6.10 μM), and gastric carcinoma cells (SNU638, IC₅₀ = 4.10 μM). For comparison, the controls gefitinib and dactolisib had IC₅₀ doses of 8.27, 6.56, 5.98, 26.7, 10.1, and 7.56 μM or 0.62, 0.74, 0.84, 1.33, 1.82, and 1.24 μM in the same cell lines, respectively. The structure of aminoquinazoline-sulphonamide based hybrids is given in Figure 6 and in vitro cytotoxicity (IC₅₀, μM) of compounds 5(b–e) against human cancer cell lines is shown in Table 5 [29].

**Figure 6.** Structure of aminoquinazoline-sulphonamide hybrids and the most promising compound 5a.**Table 5.** In vitro cytotoxic activities of hybrid compounds 5(b–e).

Compounds No.	R ₁	R ₂	X	A549 (μM)	BT549 (μM)	HCT-116 (μM)	MCF-7 (μM)	SK-HEP-1 (μM)	SNU638 (μM)
5b	3-COOCH		CH	1.10	1.08	0.40	10.1	2.40	1.12
5c	3-COOCH ₃ -4-Cl		CH	2.13	2.36	3.13	1.43	7.06	2.20
5d	4-OCH ₃		CH	3.58	1.88	3.49	1.79	1.61	3.97
5e	2,4-diF		CH	4.71	2.48	4.01	1.61	2.49	2.05
Gefitinib				8.27	6.56	5.98	26.7	10.1	7.56
Dactolisib				0.62	0.74	0.84	1.33	1.82	1.24

Continuing the work of Ding et al. (2018), Fan et al. synthesized amino quinazoline based hybrids and evaluated their anticancer activity. Most of these compounds showed inhibitory activity against PI3K. Compound **6(a)** showed excellent activity towards PI3K α with an IC₅₀ 13.6 nM in comparison to other isoforms of PI3K including PI3K β , PI3K γ and PI3K δ , which had IC₅₀ of 396.2, 117.5, and 101.8 nM. Compound **6(a)** exhibited potent activity against a panel of cell lines including HCT-116, SK-HEP1, MDA-MB-231 (epithelial, human breast cancer cells), SNU638, A549, and MCF-7 with IC₅₀ values 0.16, 0.28, 0.28, 0.48, 1.32, and 3.24 μ M. Control BEZ235 had IC₅₀ values of 0.84, 1.82, 0.18, 1.24, 0.62, and 1.33 μ M. The structure of quinazoline-amino sulphonamide based hybrid is given in Figure 7 and in vitro cytotoxicity (IC₅₀, μ M) of compounds **6(b–e)** against human cancer cell lines is shown in Table 6 [30].

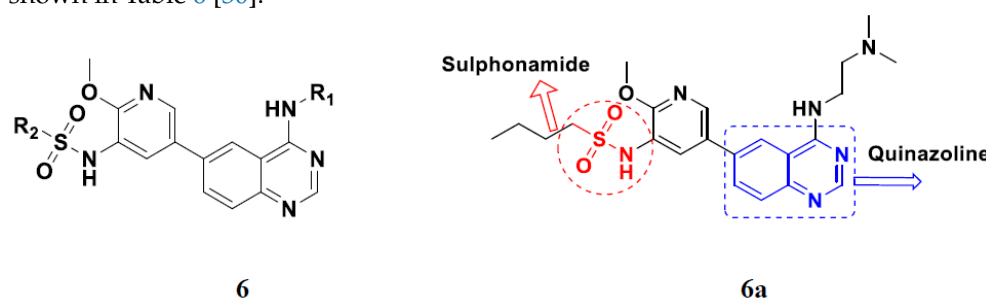


Figure 7. Structure of quinazoline-amino sulphonamide based hybrids and the most promising compound **6a**.

Table 6. In vitro cytotoxic activities of hybrid compounds **6(b–e)**.

Compound No.	R1	R2	HCT-116 (μ M)	SK-HEP1 (μ M)	MDA-MB-231 (μ M)	SNU638 (μ M)	A549 (μ M)	MCF-7 (μ M)
6b			1.44	4.72	0.71	0.62	0.94	1.02
6c			0.49	0.86	0.88	1.26	3.52	4.73
6d			0.59	0.44	0.42	0.61	1.56	10.8
6e			1.74	1.14	2.58	0.98	3.14	4.59
BEZ235			0.84	1.82	0.18	1.24	0.62	1.33

Frohlich et al. (2017) synthesized hybrids of quinazoline with artemisinin and evaluated their in vitro anticancer activity on CCRF-CEM (lymphoblastoid cell) and CEM/ADR5000 (leukemia cells). Most of the synthesized compounds showed potent anticancer activity; out of them, compound **7** (Figure 8) showed excellent activity with an EC₅₀ of 2.8 and 0.6 μ M. Control doxorubicin had an EC₅₀ of 0.009 and 23.27 μ M, respectively [31].

Yang et al. (2018) synthesized quinazoline based hybrids and evaluated them for their Bromodomain-containing protein 4 (BRD4) inhibitory activity. SAR studies revealed that the phenylmorpholine along with the pyrazole skeleton showed potent activity against BRD4. Compound **8(a)** showed potent activity against human AML cells (MV4-11) with an IC₅₀ value of 1.10 μ M (K_d 66 nM) when control BET760 had an IC₅₀ 0.80 μ M (K_d 37 nM). The structure of quinazoline-phenyl morpholine based hybrids is given in Figure 9 and in vitro cytotoxicity of compounds **8(b–e)** against human cancer cell lines is shown in Table 7 [32].

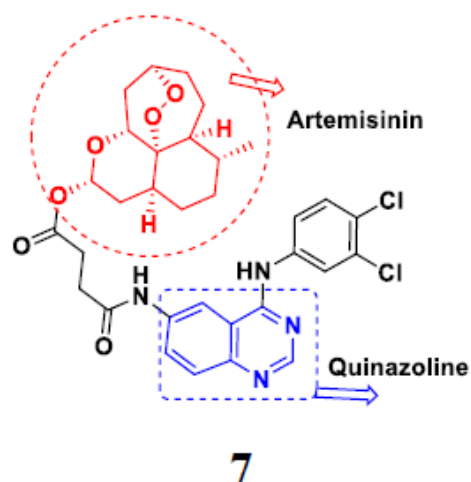


Figure 8. Structure of quinazoline-artemisinin based hybrid 7.

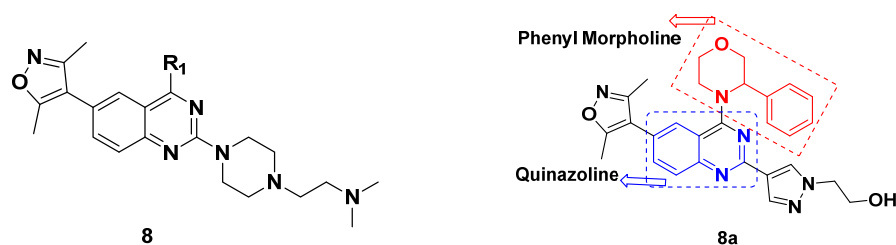


Figure 9. Structure of quinazoline phenyl morpholine based hybrids and the most promising compound 8a.

Table 7. In vitro cytotoxic activities of hybrid compounds 8(b–e).

Compound No.	R ₁	BRD4 K _d (nM)	MV4-11, IC ₅₀ (μM)
8b		480	4.88
8c		250	2.54
8d		60	5.07
8e		28	1.83
BET760	-	37	0.80

Quinazoline-Based Hybrids That Are FDA Approved or under Clinical Trial

The hybrids of quinazoline have been evaluated in various clinical trials in recent years, with several of them showing promising results. In addition, the Food and Drug Administration (FDA) approved certain quinazoline-based enzyme inhibitors for the management of various malignancies. Dacomitinib, erlotinib, gefitinib, afatinib, and lapatinib are the quinazoline based hybrid drugs approved by the FDA for management of different types of cancers (Figure 10). Additionally, in Table 8, we have summarized quinazoline-based hybrid molecules under clinical trials for the treatment of different types of cancer.

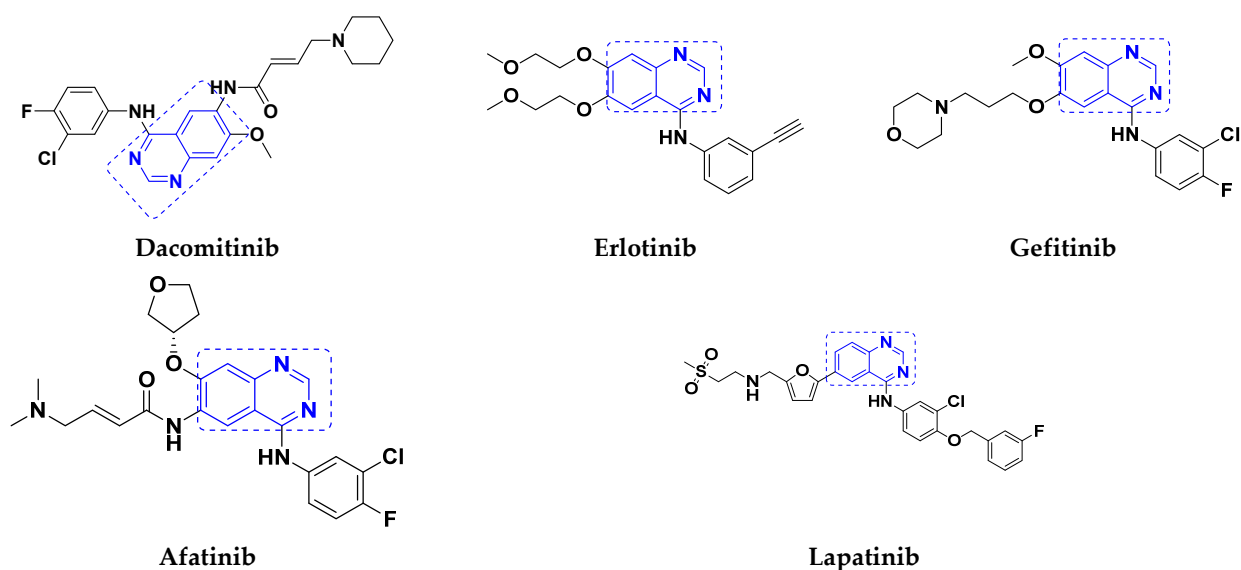


Figure 10. FDA approved/clinical trial drugs with quinazoline hybrids.

Table 8. Quinazoline-based compounds approved/under clinical trial with their current status.

Company Name	Compound Name	Drug Target	Type of Cancer	Status	References
AstraZeneca	Vandetanib	Kinase inhibitor	Medullary thyroid cancer	Approved	[33]
Boehringer Ingelheim	Afatinib	Tyrosine kinase	Non-small cell lung Carcinoma	Approved	[34]
Pfizer	Dacomitinib	EGFR inhibitor	Non-small cell lung carcinoma	Approved	[10]
AstraZeneca and Teva	Gefitinib	EGFR inhibitor	Breast and Lung cancer	Approved	[35]
Roche Pharmaceuticals	Erlotinib	EGFR inhibitor	pancreatic cancer and non-small cell lung cancer	Approved	[36]
GlaxoSmith Kline (GSK)	Lapatinib	Dual tyrosine kinase inhibitor	solid tumors and Breast cancer	Approved	[37]
AstraZeneca	Sapitinib (AZD 8931)	Erb8 receptor tyrosine kinase	Breast cancer and metastatic cancer	Clinical trials	[10]
Array Biopharma	Tucatinib (ARRY 380)	Kinase inhibitor	Breast cancer	Approved	[10]
Selleck chemicals	Barasertib (AZD 1152)	Aurora Kinase	Tumor lymphoma, solid tumors and myeloid leukemia	Clinical trials	[38]
Spectrum Pharmaceuticals	Poziotinib	Tyrosine kinase	Breast cancer	Clinical trials	[10]
AstraZeneca	AZD 3759	EGFR antagonist	Non-small cell lung Cancer	Clinical trials	[10]
Curis Inc.	CUDC-101	By inhibiting Histone deacetylase, EGFR and HER2	Advanced /Liver/Neck/Gastric/Head/ non-small cell lung cancer and Breast	Clinical trials	[39]
Beta-Phama	Icotinib	EGFR-TK1 inhibitor	Non-small cell lung cancer	Approved	[40]

3.2. Indole-Based Hybrids

Indole is a remarkable and adaptable heterocycle that has been used to create important biological scaffolds in pharmaceutical research. Indole/indole derivatives have many reported therapeutic properties, such as anti-virals, anti-convulsants, antibacterials, anti-

microbials, anticancer agents, anti-malarials, anti-inflammatories, anti-oxidants, and anti-diabetics. Different natural and synthesized indole motifs have demonstrated considerable anticancer potential. Such substances have been found to act on a variety of protein targets, including sirtuins, PIM (proviral integration site for Moloney murine leukemia virus) kinases, HDACs (histone deacetylases) and DNA topoisomerase [41,42].

Zhang et al. (2013) synthesized hybrids of indole with hydroxycinnamide, and evaluated their anticancer activity against different cell lines. Most of the synthesized compounds showed potent anticancer activity. Among them, compound 9(a) exhibited excellent activity against various cell lines including human myeloid leukemia (U937), prostate adenocarcinoma (PC-3), A549, ovarian carcinoma (ES-2), MDA-MB-231, and HCT116 at IC₅₀ 1.8, 3.7, 4.4, 5.4, 3.1, and 5.5 μM, respectively with control suberoylanilide hydroxamic acid (SAHA) had IC₅₀ values of 2.3, 9.9, 3.8, 12.7, 5.6, and 6.0 μM, respectively. Furthermore, compound 9(a) showed excellent HDAC (histone deacetylase) inhibitory activity against different isoforms of HDAC including HDAC1, HDAC2, HDAC3, and HDAC6 with IC₅₀ values of 0.39, 1.42, 0.28, and 0.94 μM compared to control SAHA at IC₅₀ values of 0.076, 0.256, 0.028, and 0.118 μM, respectively. The structure of indole with hydroxycinnamide hybrids is shown in Figure 11 and in vitro cytotoxicity of compounds 9(b–e) against human cancer cell lines is shown in Table 9 [43].

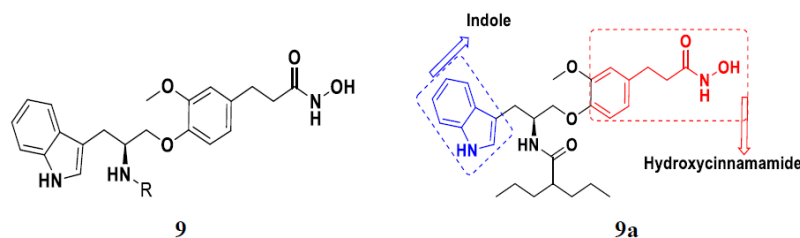


Figure 11. Structure of indole with hydroxycinnamide hybrid and the most promising compound 9a.

Table 9. In vitro cytotoxicity (IC₅₀) of hybrid compounds 9(b–e).

Compound No.	R	U937 (μM)	PC-3 (μM)	A549 (μM)	ES-2 (μM)	MDA-MB-231 (μM)	HCT116 (μM)
9b		3.1	10.5	11.8	29.2	7.2	6.0
9c		2.2	10.4	4.2	25.1	4.5	3.8
9d		2.2	5.8	1.6	4.4	6.8	5.9
9e		2.7	5.4	7.0	8.9	7.2	2.4
SAHA	-	2.3	9.9	3.8	12.7	5.6	6.0

Zhang et al. (2013) synthesized and explored hybrids of indole with hydroxycinnamide, evaluating their anticancer activity against different cell lines. Most of the synthesized compounds showed potent anticancer activity. Among them, compound 10(a) exhibited excellent activity against various cell lines including U937, K562 (myelogenous leukemia cells), HEL (human erythroleukemia cells), KG1 (myeloid leukemia cells), HL60 (promyelocytic leukemia cells), MDA-MB-231, PC-3, MCF-7, HCT116, and A549 with IC₅₀

values 0.16, 0.51, 0.19, 0.22, 1.69, 0.22, 0.46, 2.68, 0.52, and 2.74 μM , respectively. Furthermore, compound **10a** showed excellent HDAC selectivity against different isoforms of HDAC including HDAC1, HDAC2, HDAC3, and HDAC6 with IC_{50} values 11.8, 498.1, 3.9, and 308.2 nM with control SAHA had IC_{50} values of 34.6, 184.7, 90.1, and 63.0 nM, respectively. The T structure of indole and hydroxycinnamamide hybrids is shown in Figure 12 and the in vitro cytotoxicity of compounds **10(b–e)** against human cancer cell lines is shown in Table 10 [44].

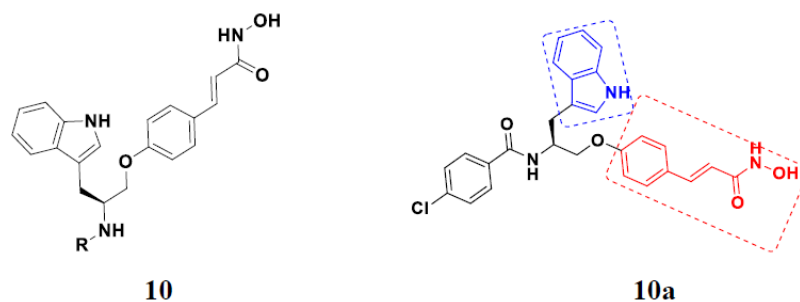


Figure 12. Structure of indole with hydroxycinnamamide hybrids and the most promising compound **10a**.

Table 10. In vitro cytotoxic activities of hybrid compounds **10(b–e)**.

Compound No.	R	U937 (μM)	K562 (μM)	HEL (μM)	KG1 (μM)	HL60 (μM)	MDA-MB-231 (μM)	PC-3 (μM)	MCF-7 (μM)	HCT116 (μM)	A549 (μM)
10b		0.33	0.79	0.20	0.39	2.11	0.24	0.33	3.47	0.37	3.39
10c		0.32	0.68	0.27	0.72	1.59	0.41	0.53	2.95	0.57	3.91
10d		0.18	1.01	0.19	0.24	1.04	0.27	0.51	2.7	0.37	2.96
10e		0.34	0.89	0.16	0.47	1.68	0.15	0.29	2.32	0.22	3.27
SAHA		1.45	3.24	0.49	1.59	4.26	1.72	3.57	3.78	2.81	3.9

Mehndiratta et al. (2014) synthesized hybrids of indole with sulphonamides, and evaluated their anticancer and anti-inflammatory activity. Most of the synthesized compounds showed potent anticancer activity. Among them, compound **11(a)** showed excellent activity against HeLa nuclear HDAC enzyme with an IC_{50} of 7.9 nM. The structure of indole and sulphonamide hybrids is shown in Figure 13 and the in vitro cytotoxicity of compounds **11(b–e)** against human cancer cell lines is shown in Table 11 [45].

Panathur et al. (2013) synthesized indole based hybrids, and evaluated them for anticancer activity against three cancer cell lines including K562, MDA-MB 231 and LNCaP (androgen-sensitive human prostate adenocarcinoma cells). Most of the synthesized compounds showed potent anticancer activity; among them, 9 compounds showed excellent activity against MDA-MB 231, with three compounds inhibiting growth of LNCaP cell up to 50% at 10 μM . Furthermore, the lead molecule **12(a)** showed SIRT1 (Sirtuin 1) inhibitory activity up to 70% with control finasteride (growth inhibition 56%) at 40 μM . The structure of indole-triazole based hybrids is given in Figure 14 and the in vitro cytotoxicity of compounds **12(b–e)** against human cancer cell lines is shown in Table 12 [46].

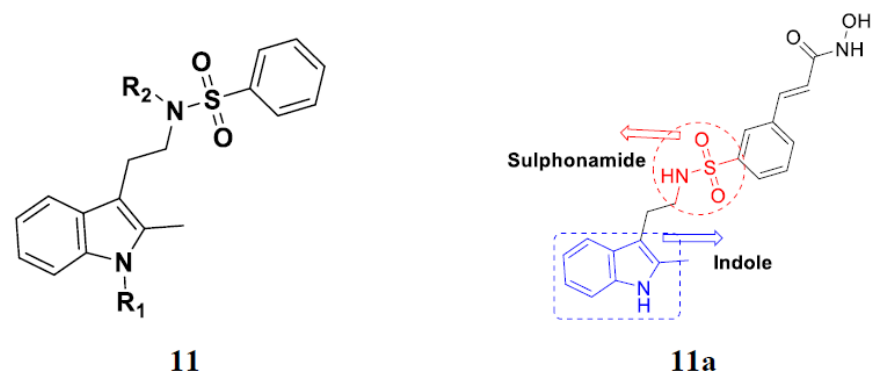


Figure 13. Structure of indole with sulphonamide hybrids and the most promising compound **11a**.

Table 11. In vitro cytotoxic activities of hybrid compounds **11(b–e)**.

Compound No.	R ₁	R ₂	R ₃	HeLa Nuclear HDAC (nM)
11b	H	H	4'-(N-3-hydroxyacrylamide)	2.8
11c	CH ₃	H	4'-(N-3-hydroxyacrylamide)	3.3
11d	CH ₂ CH ₃	H	4'-(N-3-hydroxyacrylamide)	3.4
11e	H	CH ₃	4'-(N-3-hydroxyacrylamide)	47.4
LBH589.HCl				7.5

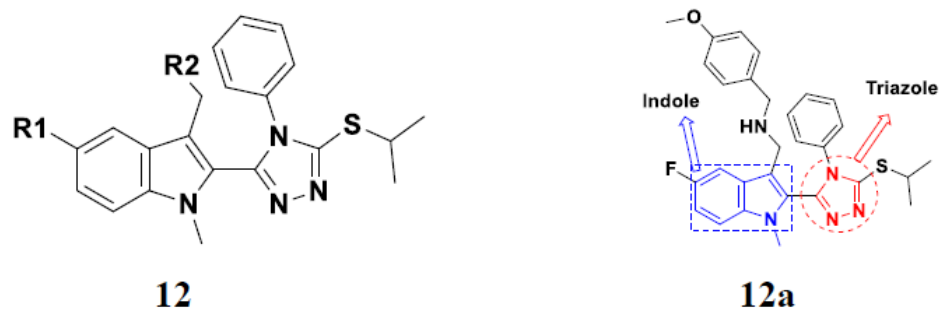


Figure 14. Structure of indole-triazole based hybrids and the most promising compound **12a**.

Table 12. In vitro cytotoxic activities of indole-triazole based hybrid compounds **12(b–e)**.

Compound No.	R ₁	R ₂	K562 (Upto %)	MDA-MB 231 (μM)	LNCaP (μM)
12b	H		88	2	32
12c	H		87	28	38
12d	F		64	58	24
12e	F		67	68	35

Lee et al. (2014) synthesized indole based hybrids and evaluated their proto-oncogene serine/threonine-protein kinase (PIM) kinase selectivity against different forms of PIM kinase including PIM1, PIM2, and PIM3. Compound **13(a)** showed excellent selectivity towards PIM1 with IC_{50} values of 0.058, 0.52, and 0.16 μ M. Furthermore, the lead molecule **13(a)** was tested against different cell lines, including MV-4-11 (acute myeloid leukemia cell), Jurkat (T lymphocyte cells), and K562, and was found to be very selective towards MV-4-11 in a cell viability assay. The lead molecule also showed binding interaction with Lys67 and Glu89 in the active site of PIM1 (ATP-binding). The structure of an indole-pyrimidine based hybrid is shown in Figure 15, and the in vitro cytotoxicity of compounds **13(b–e)** against human cancer cell lines is shown in Table 13 [47].

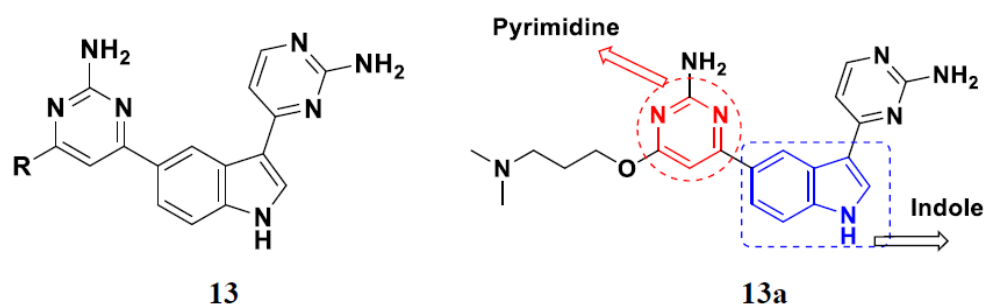


Figure 15. Structure of indole-pyrimidine based hybrids and the most promising compound **13a**.

Table 13. In vitro cytotoxic activities of indole-pyrimidine based hybrid compounds **13(b–e)**.

Compound No.	R	PIM (μ M)		
		PIM1	PIM2	PIM3
13b	$Me_2N(CH_2)_2O$	0.30	1.40	0.50
13c	$Et_2N(CH_2)_2O$	0.14	0.84	0.27
13d	$Et_2N(CH_2)_3O$	0.11	0.38	0.081
13e	$Et_2N(CH_2)_3NH$	0.067	3.16	0.61

Mirzaei et al. (2017) synthesized and explored indole-chalcone based hybrids and evaluated their anticancer activity against various cell lines including A549, MCF7, SKOV3 (human ovarian cancer cell), and NIH3T3 (embryonic fibroblast cells), finding IC_{50} values of 4.3, 100, 20.2, and 154.6 μ g/mL with control etoposide IC_{50} of 7.8, 9.9, 8.5, and 118.0 μ g/mL, respectively. Furthermore, the lead molecule **14(a)** was subjected to a tubulin polymerization inhibitory assay, with results revealing that the lead molecule showed excellent inhibitory activity, having an IC_{50} of 17.8 μ M with control colchicine, having an IC_{50} of 2.3 μ M. The structure of indole-chalcone based hybrids is shown in Figure 16 and the in vitro cytotoxicity of compounds **14(b–e)** against human cancer cell lines is shown in Table 14 [48].

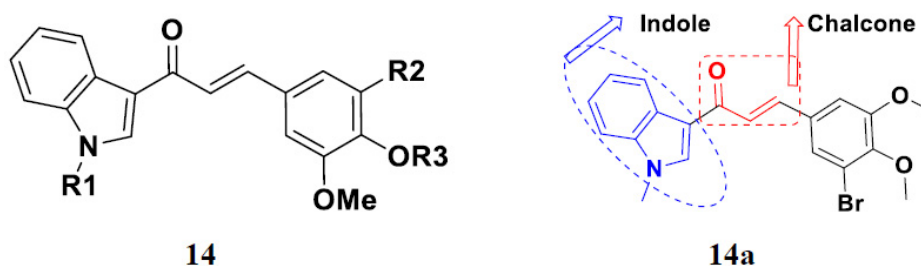
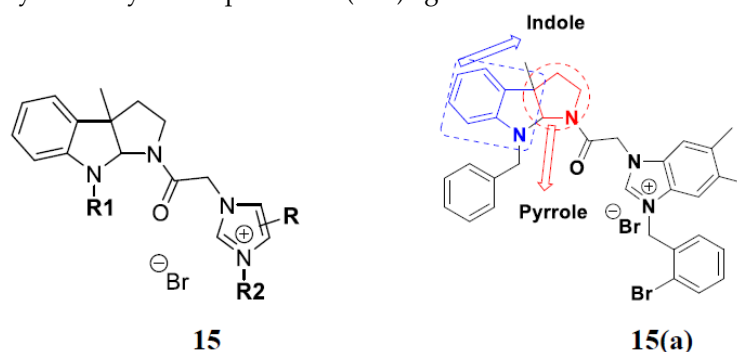


Figure 16. Structure of indole-chalcone based hybrids and the most promising compound **14a**.

Table 14. In vitro cytotoxic activities of indole-chalcone based hybrid compounds 14(b–e).

Compound No.	R1	R2	R3	A549 (µg/mL)	MCF7 (µg/mL)	SKOV3 (µg/mL)	NIH3T3 (µg/mL)
14b	C ₂ H ₅	Br	Me	4.9	50.1	68.8	52.0
14c	H	Br	n-Bu	8.0	54.0	74.1	141.3
14d	Me	OMe	Me	5.1	36.2	53.0	–
14e	H	Br	Me	27.9	28.0	52.0	–
Etoposide				7.8	9.9	8.5	118.0

Zhou et al. (2016) synthesized and explored hybrids of indole with pyrrole and evaluated their anticancer activity against various cell lines including HL-60, SMMC-7721 (hepatocarcinoma cells), A-549, MCF-7, and SW480 (colon carcinoma cell). Most of the synthesized compounds showed potent anticancer activity. Among them, compound 15(a) showed excellent activity having IC₅₀ values of 1.27, 1.72, 2.68, 1.78, and 1.44 µM with control cisplatin (DDP) having IC₅₀ values of 1.16, 8.08, 7.10, 10.45, and 8.88 µM, respectively. The structure of indole-pyrrole based hybrids is shown in Figure 17 and the in vitro cytotoxicity of compounds 15(b–e) against human cancer cell lines is shown in Table 15 [49].

**Figure 17.** Structure of indole-pyrrole based hybrids and the most promising compound 15a.**Table 15.** In vitro cytotoxic activities of indole-pyrrole based hybrid compounds 15(b–e).

Compound No.	R ₁	R ₂	R ₃	HL-60 (µM)	SMMC-7721 (µM)	A-549 (µM)	MCF-7 (µM)	SW480 (µM)
15b	Bn	Benzimidazole	2-Bromobenzyl	1.21	4.69	6.76	2.23	6.35
15c	Bn	Benzimidazole	4-Methylbenzyl	1.20	4.98	6.23	2.72	6.57
15d	Bn	5,6-Dimethylbenzimidazole	2-Naphthylmethyl	1.21	2.27	4.80	1.68	1.76
15e	Me	5,6-Dimethylbenzimidazole	2-Naphthylmethyl	1.35	4.03	6.18	1.84	4.5
DPP	–	–	–	1.16	8.08	7.10	10.45	8.88

Kumar et al. (2014) synthesized indole based chalcone hybrids and evaluated their antiproliferative activity against A549, PC3 and PaCa2 (pancreatic cancer) cell lines. Among the synthesized derivatives, compound 16(a) showed potent activity having IC₅₀ values of 2.4 and 0.8, 36.0 and 22.5, and >50 µM, respectively (with control mitomycin C having an IC₅₀ = of 0.45 µM against A549 at 24h). The structure of indole-chalcone based hybrids is shown in Figure 18 and the in vitro cytotoxicity of compounds 16(b–e) against human cancer cell lines is shown in Table 16 [50].

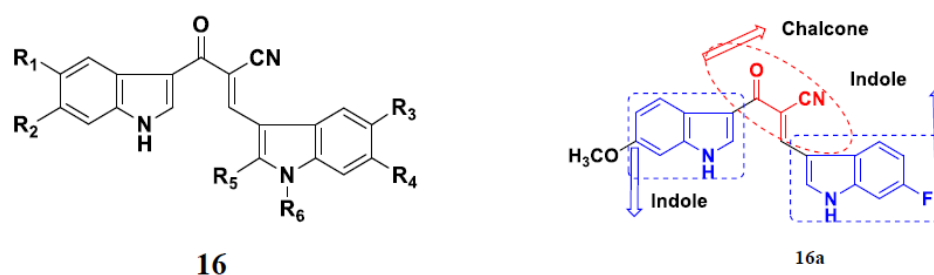


Figure 18. Structure of indole-chalcone based hybrids and the most promising compound 16a.

Table 16. In vitro cytotoxic activities of indole-chalcone based hybrid compounds 16(b–e).

Compound No.	R ₁	R ₂	R ₃	R ₄	R ₅	R ₆	A549 (μM)		PC3 (μM)		PaCa2 (μM)	
							24 h	48 h	24 h	48 h	24 h	48 h
16b	H	H	H	OCH ₃	H	H	9.6	5.8	33.3	12.5	27.5	>50
16c	H	OCH ₃	H	H	H	H	6.4	7.5	>50	12.0	13.5	>50
16d	H	OCH ₃	OCH ₃	H	H	H	3.7	5.5	31.1	37.1	>50	>50
16e							4.9	3.0	17.2	8.1	24.0	>50
Mitomycin C							0.45					

Kumar et al. (2018) synthesized and explored indole-ospemifene-triazole based hybrids and evaluated their anticancer activity against MCF-7 and MDA-MB-231. Most of the synthesized compounds showed good anticancer activity, compound 17(a) exhibited excellent activity at IC₅₀ 1.56 and 48.46 μM controls included ospemifene (IC₅₀ 55 and 50 μM), tamoxifen (IC₅₀ 3.5 and >100 μM), and plumbagin (IC₅₀ 75 and 4.4 μM). The structure of the indole-ospemifene-triazole based hybrid is shown in Figure 19 and the in vitro cytotoxicity of compounds 17(b–e) against human cancer cell lines is shown in Table 17 [51].

Table 17. In vitro cytotoxic activities of indole-ospemifene-triazole based hybrid compounds 17(b–e).

Compound No.	R	MCF-7 (μM)	MDA-MB-231 (μM)
17b		≥100	71.40
17c		16.50	≥100
17d		10.99	71.40
17e		≥100	≥100
Ospemifene		55	50
Tamoxifen		3.5	≥100
Plumbagin		75	4.4

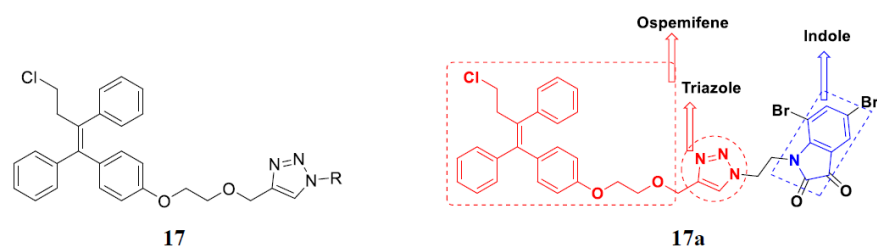


Figure 19. Structure of indole-ospemifene-triazole based hybrids and the most promising compound 17a.

Kumar et al. (2018), and Sharma et al. (2019) synthesized indole-isatin based triazole hybrids and evaluated their anticancer activity. Among the synthesized compounds, compound 18(a) showed excellent activity against MCF-7 and MDA-MB-231 cell lines with IC_{50} values of 37.42 and >100 μ M. Control included plumbagin (IC_{50} 3.5 μ M), peganumine A (IC_{50} 38.5 μ M and not observed) and tamoxifen (IC_{50} 50 and 75 μ M), respectively. Furthermore, the biological activity was validated by docking studies. The structure of the indole-isatin-triazole based hybrid is shown in Figure 20, and the *in vitro* cytotoxicity (μ M) of compounds 18(b–c) against human cancer cell lines is shown in Table 18 [52].

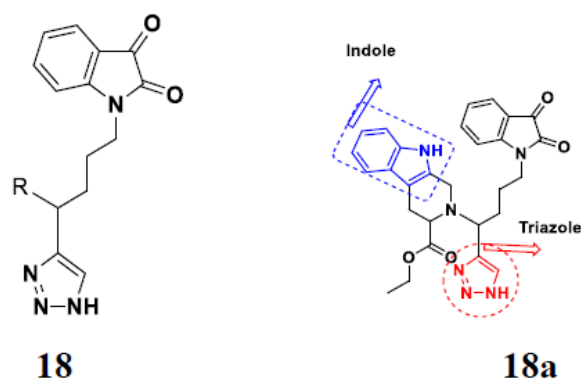


Figure 20. Structure of indole-ospemifene-triazole based hybrids and the most promising compound 18a.

Table 18. *In vitro* cytotoxic activities of indole-isatin-triazole based hybrid compounds 18(b–c).

Compound No.	R	MCF-7 (μ M)	MDA-MB-231 (μ M)
18b		50	>100
18c		>100	>100
Plumbagin		3.5	4.4
Peganumine A		38.5	Not observed
Tamoxifen		50	75

3.3. Indole-Based Hybrids That Are FDA Approved or under Clinical Trial

Dacinostat (LAQ824), an indole-based hybrid molecule, is approved for the management of breast and prostate cancer, whereas panobinostat (LBH-589) is a marketed medicine for numerous malignancies. Quisinostat (JNJ-26481585), a synthetic indole-hydroxamic acid molecule (hybrid) with putative antitumor action is an orally available 2nd gener-

ation molecule to inhibit HDAC. Cediranib is a tyrosine kinase inhibitor which affects the function and development of endothelial cells in human kidney tumors. Anlotinib (AL3818) is a potent kinase inhibitor with potential antitumor as well as antiproliferative efficacy currently in clinical trials. Figure 21, shows chemical structures of indole-based FDA approved/clinical trial drugs and Table 19 gives descriptions of them.

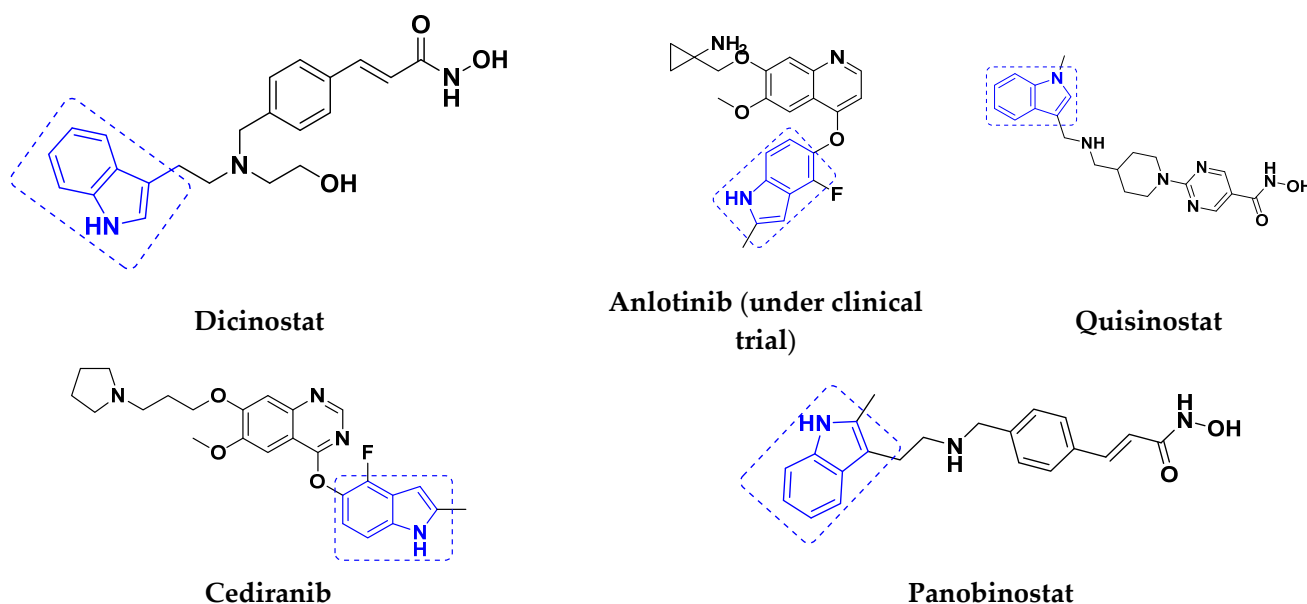


Figure 21. FDA approved/clinical trial drugs with indole hybrids.

Table 19. Current status of indole-based hybrids that are approved or/-under clinical trials.

Company Name	Compound Name	Drug Target	Type of Cancer	Status	Reference
AstraZeneca	Cediranib	VEGFR tyrosine kinases	Glioblastoma	Approved	[53]
Chia-tai Tianqing Pharmaceutical Co.	AL 3818 (Anlotinib)	Tyrosine kinase	Synovial sarcoma, Advanced alveolar soft part sarcoma	Clinical trials	[54]
Janssen pharmaceuticals	Quisinostat	HDAC inhibitor	Multiple myeloma	Approved	[55]
Novartis	Panobinostat (LBH-589)	Non-selective HDAC inhibitor	Multiple myeloma	Approved	[56]
Selleck	Dacinostat (LAQ824)	Histone deacetylase inhibitor	Breast and Prostate cancer	Approved	[57]

3.4. Carbazole Based Hybrids

Carbazole is a key scaffold found in a wide range of physiologically potent chemicals, including natural and synthetic analogues. Anticancer, antifungal, antibacterial, anti-HIV, anti-inflammatory, anti-protozoan, anti-psychotic, antidiabetic and anticonvulsant properties are found in molecules with a chemically modified carbazole moiety. The first carbazole compounds, celiptium and ellipticine, targeted topoisomerase II and cytochrome P450, respectively, and are used to combat cancer (metastatic breast cancer). An investigation of the carbazole nucleus for the production of novel structural scaffolds has led to the development of a number of available anti-tumor hybrids [58,59].

Liu et al. (2015) synthesized and evaluated the anticancer activity of carbazole derivatives against various cell lines including HL-60, SMMC-7721, A549, MCF-7 and SW480. Among the synthesized carbazole derivatives, compound 19(a) showed potent activity with IC_{50} values of 0.51, 2.38, 3.12, 1.40, and 2.48 μ M, where control cisplatin (DDP) had IC_{50}

values of 1.32, 6.24, 11.83, 15.17, and 12.95 μM , respectively. Compound 19(a) showed cell cycle arrest in SMMC-7721 cells. The structure of carbazole-imidazole based hybrids is shown in Figure 22 and the in vitro cytotoxicity of compounds 20(b–e) against human cancer cell lines is shown in Table 20 [60].

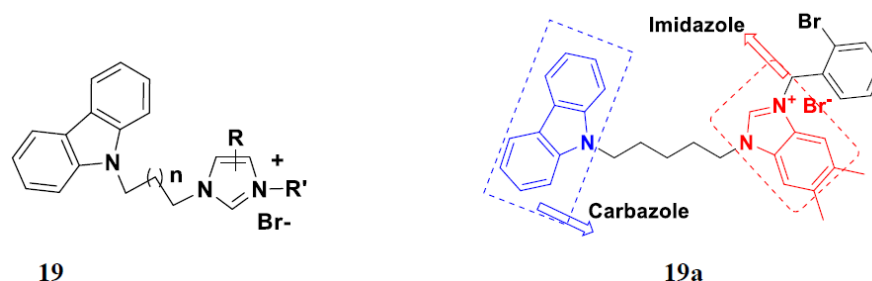


Figure 22. Structure of carbazole-imidazole based hybrids and the most promising compound 19a.

Table 20. In vitro cytotoxic activities of carbazole-imidazole based hybrid compounds 19(b–e).

Compound No.	n	R	R'	HL-60 (μM)	SMMC-7721 (μM)	A549 (μM)	MCF-7 (μM)	SW480 (μM)
19b	2	Benzimidazole	-	3.11	3.21	12.36	5.06	18.25
19c	2	imidazole	4-methylbenzyl	0.84	5.74	3.92	2.24	9.56
19d	2	benzimidazole	2-bromobenzyl	0.71	3.66	3.58	2.14	3.08
19e	3	benzimidazole	4-methylbenzyl	0.57	2.55	2.65	2.82	3.19
DDP				1.32	6.24	11.83	15.17	12.95

Mongre et al. (2019) synthesized a potent novel hybrid (20) of carbazole and piperazine and evaluated its anticancer activity against various cell lines including A549, NCI-H1299 (non-small cell lung carcinoma cells), HT-29, MCF-7, Hela (cervical carcinoma), and U2OS (osteosarcoma cells). The IC_{50} values in these cell lined were 1.779, 2.270, 2.20, 2.637, 3.072 and 2.739 μM , respectively. The molecule also showed potent cell cycle arresting activity at concentrations of 0.5, 1.0 and 2.0 μM by affecting G2/M cell cycle transition. Hybrid (20) also inhibited tumor progression in a xenograft model (BALB/c-nu nude mouse) at a dose of 3 mg/kg body weight without any toxicity. A carbazole-piperazine hybrid is depicted in Figure 23 [61].

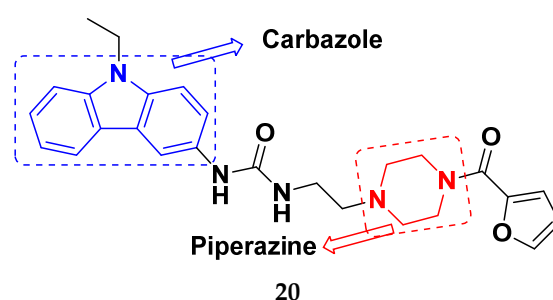


Figure 23. A carbazole-piperazine hybrid (20).

Carbazole-Based Hybrids That Are FDA Approved or under Clinical Trial

Some well-known carbazole-based hybrids with potential anticancer effects have been published [59,62–64]. Some carbazole-based hybrids are FDA approved medications or in clinical studies for cancer treatment. Alectinib was licensed by the US Food and Drug Administration (FDA) and the European Medicines Agency (EMA) in 2015 for the management of anaplastic lymphoma kinase-positive progressive non-small cell lung cancer (NSCLC). Midostaurin is a carbazole hybrid that was approved by the FDA and the European Medicines Agency (EMA) in 2017. It is used to treat recently diagnosed advanced systemic mastocytosis and acute myeloid leukemia [65,66].

Currently, four hybrids of carbazole are being tested in clinical studies including becatecarin and edotecarin, which have been proven to intercalate DNA and maintain the DNA-topo I complex, and are currently in Phase II and Phase III clinical studies, respectively. CEP-2563 is a strong inhibitor of platelet derived growth factor (PDGF) and tyrosine kinase that is now in a Phase I clinical development for medullary thyroid cancer. UCN-01 is now being tested in a Phase II clinical study for breast cancer, lymphoma, and pancreatic by acting upon protein kinases. The structure of FDA approved/clinical trials drugs with carbazole hybrids is given in Figure 24 and their current status is shown in Table 21.

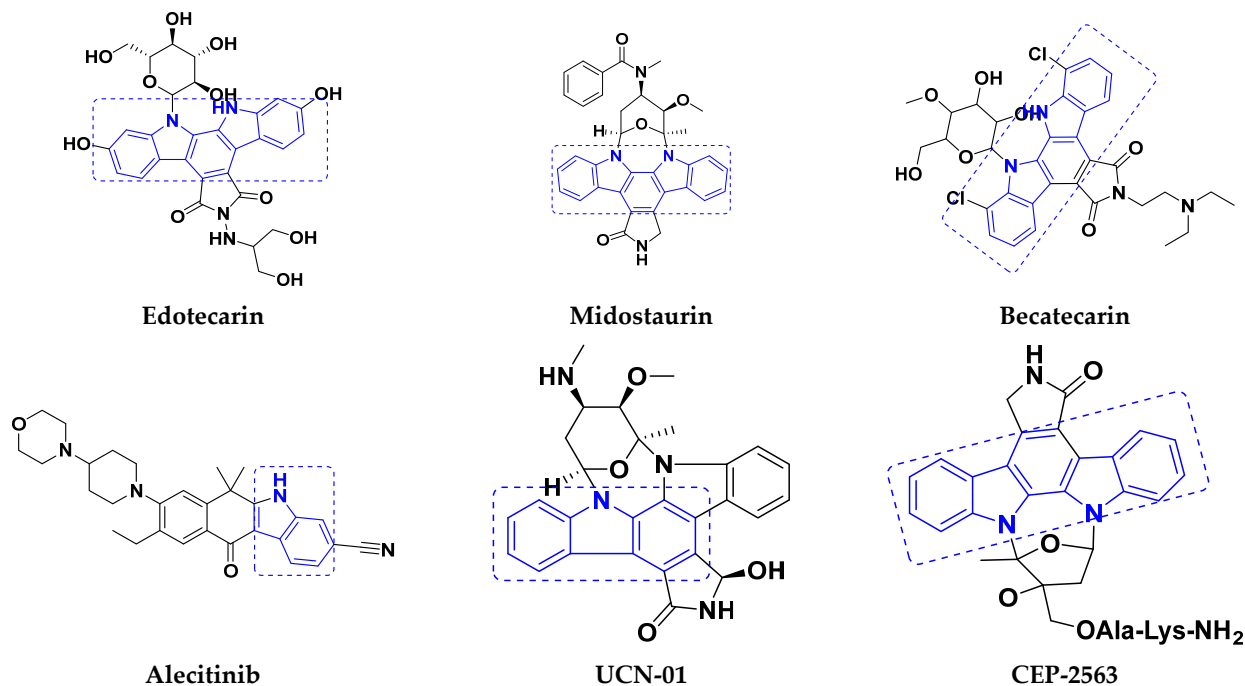


Figure 24. Carbazole hybrids that are FDA approved/or under clinical trials.

Table 21. Current status of carbazole-based hybrid drugs that are approved/or under clinical trials.

Company Name	Compound Name	Drug Target	Type of Cancer	Status	References
Novartis Pharmaceutical Corporation	Midostaurin	Kinase inhibitor	Advanced systemic mastocytosis, myelodysplastic syndrome	Approved	[67]
Chugai Pharmaceuticals Co. Schwarz Pharma	Alectinib	Tyrosine kinase	Non-small cell lung cancer	Approved	[68]
	CEP-2563	Tyrosine kinase	Solid tumors	Clinical trials	[10]
Cayman Chemicals	UCN-01	Tyrosine kinase	Pancreatic, malignant melanoma, ovarian Cancer and small cell lung	Clinical trials	[69]
Helsinn Healthcare	Becatecarin	Topoisomerase-I	Leukemia and gastric cancer	Clinical Trials	[10]
Pfizer Pharmaceutical Co.	Edotecarin	Topoisomerase-I	Oesophageal cancer and solid tumors	Clinical trials	[10]

3.5. Pyrimidine-Based Hybrids

The basic structure of RNA, DNA, and nucleic acids is the heterocyclic pyrimidine ring. Pyrimidine and its conjugated counterparts possess antiviral, antibacterial, anticancer, analgesic, anti-inflammatory, antimalarial and antioxidant activities. Anticancer action is the most often described therapeutic property of pyrimidine because it interacts with a variety of targets, as well as receptors to cause cell death. Multiple studies on the anticancer

efficacy of pyrimidine compounds, as well as their therapeutic use, have supported their position as a prospective drug development nucleus [70,71].

Combs et al. (2015) synthesized and patented aminopyrimidine hybrids and evaluated their P13K enzyme as well as cell proliferation inhibitory potential in 96-well plates using scintillation counting. Compound **21** (Figure 25) showed potent activity with $IC_{50} < 20$ nM [72].

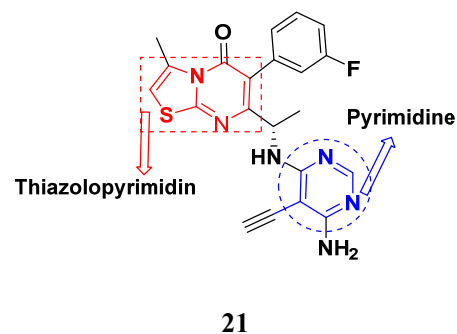


Figure 25. A pyrimidine hybrid (21).

Bolour et al. (2012) synthesized and patented pyrimidine-indazole based hybrids as VEGFR2 inhibitors. Compound **22** showed potent activity with an $IC_{50} < 50$ μ M. Furthermore, the lead compound **22** (Figure 26) was evaluated in an endothelial cell proliferation assay where it displayed activity with IC_{50} s of 1–200 nM [73].

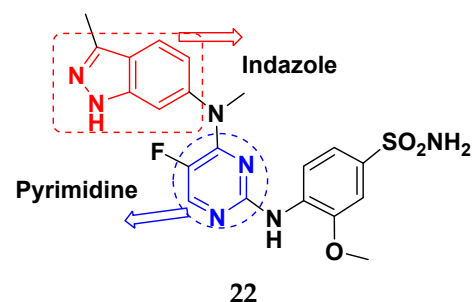


Figure 26. A pyrimidine-indazole based hybrid 22.

Hogberg et al. (2012) developed and patented indole based pyrimidine hybrids and evaluated their anticancer activity as tubulin inhibitors. Among the synthesized compounds, compound **23** (Figure 27) showed potent activity on CCRFCEM (T lymphoblastoid cells) with an EC_{50} value of 0.015 μ M [74].

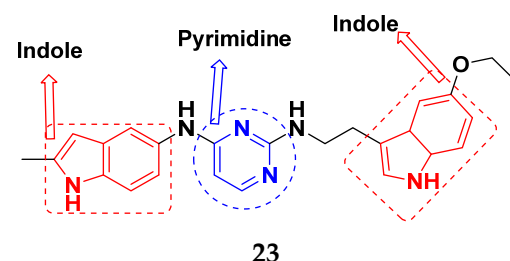


Figure 27. A pyrimidine-di-indazole based hybrid (23).

Mao et al. (2012) synthesized and patented pyrimidine-pyrazole based hybrid molecules and evaluated their anticancer activity against H1993 cells. The synthesized compounds did not show desirable activity on representative cell line. Furthermore, potent compound **24** (Figure 28) was subjected to enzymatic assay on cMet protein and displayed excellent activity, having an IC_{50} in the nM range [75].

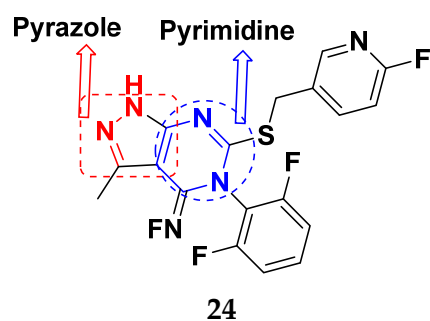


Figure 28. A pyrimidine hybrid (24).

Tanaka et al. (2012) synthesized and patented pyrimidine-pyrazole based hybrid molecules and evaluated their anticancer activity as Fyn inhibitors. Among the synthesized compounds, compound 25 (Figure 29) showed excellent activity with an IC_{50} of 3 nM. Furthermore, 26 (Figure 29) showed excellent activity on carbonyl reductase 1 with an IC_{50} of 28 nM [76].

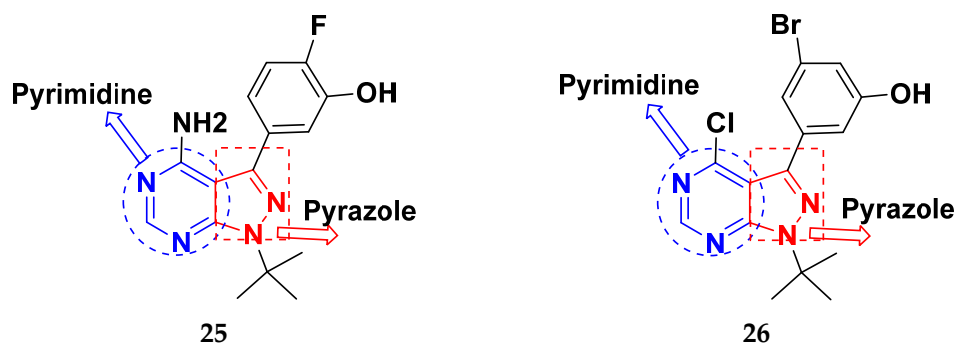


Figure 29. Pyrimidine-pyrazole based hybrid (25 and 26).

Liang et al. (2013) synthesized and patented pyrimidine-pyrazole based hybrid molecules, and evaluated their anticancer activity as mammalian target of rapamycin mTOR inhibitors. Compound 27 (Figure 30) showed potent activity on A549 and U-87MG (glioma cells) with an $IC_{50} < 1 \mu\text{M}$ [77].

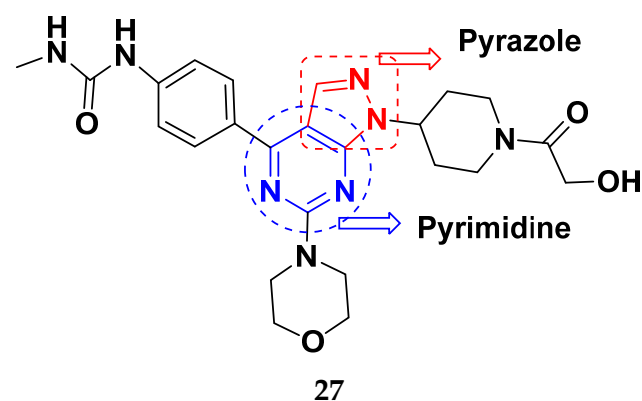


Figure 30. A Pyrimidine-pyrazole based hybrid (27).

Dorsch et al. (2013) synthesized and patented pyrimidine-triazole based hybrids and evaluated their anticancer activity as general control non-derepressible 2 (GCN2) inhibitors of U2OS human cells. Among the synthesized hybrids, the compound 28 (Figure 31) showed excellent activity with $IC_{50} \leq 0.3 \mu\text{M}$ [78].

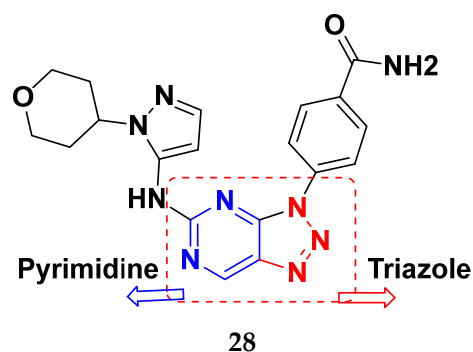


Figure 31. A pyrimidine-triazole based hybrid (**28**).

El-Sayed et al. (2011) synthesized sulfonamide-thiazole fused pyrimidine derivatives, and evaluated their anticancer activity in amethyl green/DNA displacement assay. Among the synthesized compounds, compound **29a** showed potent activity with an IC_{50} of 40 $\mu\text{g}/\text{mL}$ and high DNA binding affinity. Furthermore, in vivo studies showed that the compound **29a** increased the % lifespan of mice by 42.86% over standard fluorouracil. The structure of sulfonamide-thiazole fused pyrimidine derivatives is shown in Figure 32 and the in vitro cytotoxicity of compounds **29(b–e)** against human cancer cell lines is shown in Table 22 [79].

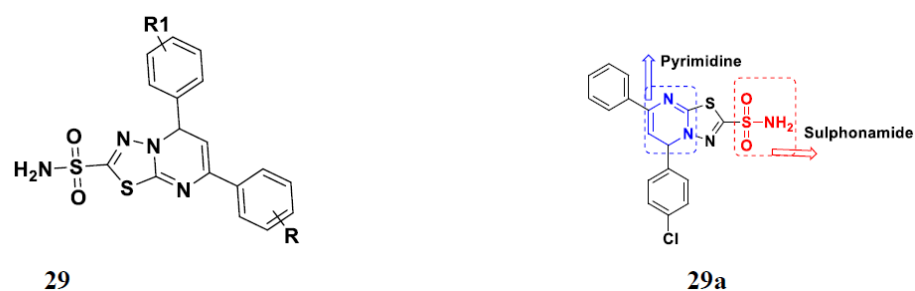


Figure 32. Structure of sulfonamide-thiazole fused pyrimidine hybrids and the most promising compound **29a**.

Table 22. In vitro cytotoxic activities of sulfonamide-thiazole fused pyrimidine hybrid compounds **29(b–e)**.

Compound No.	R	R ₁	DNA Displacement Assay ($\mu\text{g}/\text{mL}$)	DNA Binding Affinity
29b	4-H	4-Br	74	High
29c	4-H	4-NO ₂	81	weak
29d	4-H	4-OCH ₃	81	Moderate
29e	4-H	3,4-diOMe	62	High
Ethidium bromide	-	-	1.4	-

Shao et al. (2013) synthesized tri-substituted pyrimidine based hybrid derivatives, and evaluated their anticancer activity as cyclin-dependent kinase (CDK) inhibitors. Most of the synthesized compounds showed potent anticancer activity. Among them, compound **30a** showed potent kinase inhibition against CDK9T1, CDK1B, CDK2A, CDK7H with K_i of 14, 262, 316, and 163 nM, and cell toxicity activity against HCT-116, and MCF-7 cell lines with IC_{50} value of 0.79, and 0.64 μM , respectively. Furthermore, compound **30a** showed potent activity of Mal-1 and caspase-3 inhibition by down regulation of apoptotic protein. The structure of substituted pyrimidine derivatives is shown in Figure 33 and the in vitro cytotoxicity of compounds **30(b–e)** against human cancer cell lines is shown in Table 23 [80].

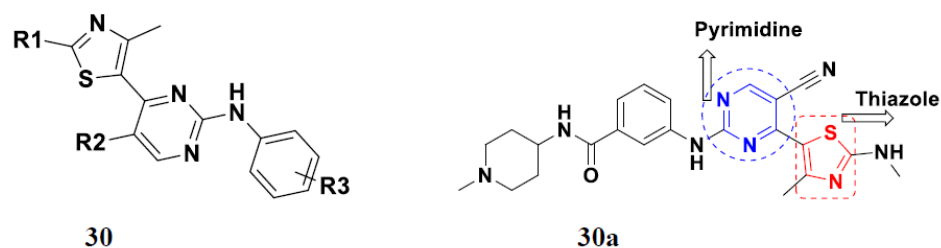


Figure 33. Structure of tri-substituted pyrimidine hybrids and the most promising compound 30a.

Table 23. In vitro cytotoxic activities of tri-substituted pyrimidine hybrid compounds 30(b–e).

Compound No.	R ₁	R ₂	R ₃	CDK9T1 (μM)	CDK1B (μM)	CDK2A (μM)	CDK7H (μM)	HCT-116 (μM)	MCF-7 (μM)
30b	NH ₂	F	m-SO ₂ NH ₂	3	7	3	252	0.05	0.41
30c	NHMe	CN	m-SO ₂ Me	5	19	43	110	0.20	0.43
30d	NHMe	F	m-SO ₂ NH(CH ₂) ₂ OCH ₃	3	10	6	30	0.30	0.72
30e	NHMe	CN	p-CO-N-(1-methylpiperidin-4-yl)	8	43	32	304	0.18	0.5

Fares et al. (2014) synthesized pyrimidine-based triazole hybrid derivatives and evaluated their anticancer activity. Most of the synthesized compounds showed potent anticancer activity. Among them, compound 31(a) showed excellent activity against various cell lines including MCF-7, human hepatoma carcinoma cells (HEPG2), A-549, and (PC-3) with IC₅₀ of 37.96, 56.65, 0.41, and 0.36 μM. Furthermore, compound 31a was screened in a CDK4 and CDK6 inhibition assay and compound showed 0 and 2% inhibition at 1 μM, 5 and 1% inhibition at 10 μM and 21 and 17% inhibition at 100 μM with control staurosporine having 93 and 90% inhibition at 1 μM. The structure of pyrimidine-triazole based hybrid derivatives is shown in Figure 34 and the in vitro cytotoxicity (μM) of compounds 31(b–e) against human cancer cell lines is shown in Table 24 [81].

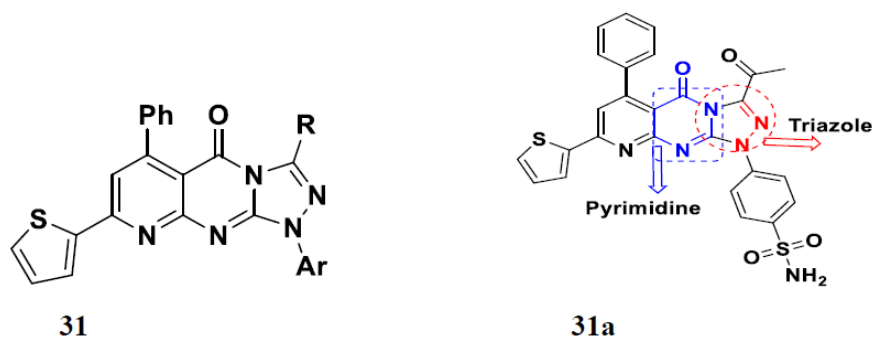


Figure 34. Structure of a pyrimidine-triazole based hybrids and the most promising compound 31a.

Table 24. In vitro cytotoxic activities of pyrimidine-triazole hybrid compounds 31(b–e).

Compound No.	Ar	R	A-549 (IC ₅₀ (μM))	PC-3
31b	4-MeC ₆ H ₄	COCH ₃	19.33	16.92
31c	C ₆ H ₅	COOC ₂ H ₅	26.64	33.56
31d	4-SO ₂ NH ₂ C ₆ H ₄	COOC ₂ H ₅	16.42	7.15
31d	4-ClC ₆ H ₄	COCH ₃	30.56	22.90
5-FU			4.21	12.00

Kurumurthy et al. (2019) synthesized pyrimidine based triazole hybrids and evaluated their anticancer activity. Most of the synthesized compounds showed potent anticancer

activity. Among them, compound **32(a)** showed excellent activity against various cell lines including U₉₃₇, THP-1 and Colo205 cells having IC₅₀ values of 6.20, 11.27, and 15.01 µg/mL with control etoposide having IC₅₀ values of 17.94, 2.16, 7.24, and 1.26 µg/mL, respectively. The structure of pyrimidine-triazole based hybrid derivatives is shown in Figure 35 and the in vitro cytotoxicity of compounds **32(b–e)** against human cancer cell lines is shown in Table 25 [82].

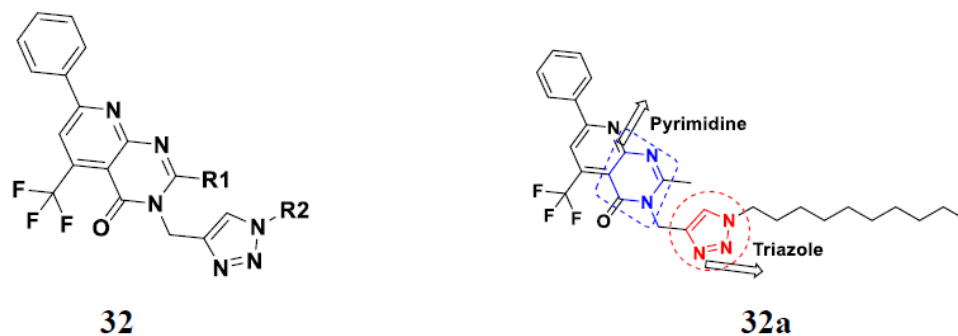


Figure 35. Structure of pyrimidine-triazole based hybrids and the most promising compound **32a**.

Table 25. In vitro cytotoxic activities of pyrimidine-triazole hybrid compounds **32(b–e)**.

Compound No.	R1	R2	U ₉₃₇ (µg/mL)	THP-1 (µg/mL)	Colo205 (µg/mL)
32b	H	CH ₃ -(CH ₂) ₈ -CH ₂ -	8.16	16.91	19.25
32c	CH ₃ -(CH ₂) ₄ -CH ₂ -	6F ₁₃ -CH ₂ -CH ₂ -	7.56	-	132.42
32c	(CH ₃) ₂ CH-	8F ₁₇ -CH ₂ -CH ₂ -	8.35	142.23	-
32d	C ₂ H ₅	CH ₃ -(CH ₂) ₈ -CH ₂ -	17.83	82.65	-
Etoposide			17.94	2.16	7.24

Nagendra et al. (2014) synthesized pyrimidine based pyrazole hybrids and evaluated their anticancer activity. Most of the synthesized compounds showed potent anticancer activity. Among them, compound **33(a)** showed excellent activity against various cell lines including A549, MCF7, DU145 (prostate cancer cell) and HeLa with IC₅₀ values of 4.2, 37.2, 5.8, and 34.3 µM and control 5-FU having IC₅₀ values of 1.3, 1.4, 1.5, and 1.3 µM, respectively. The structure of pyrimidine-pyrazole based hybrid derivatives is shown in Figure 36 and the in vitro cytotoxicity (µM) of compounds **33(b–e)** against human cancer cell lines is shown in Table 26 [83].

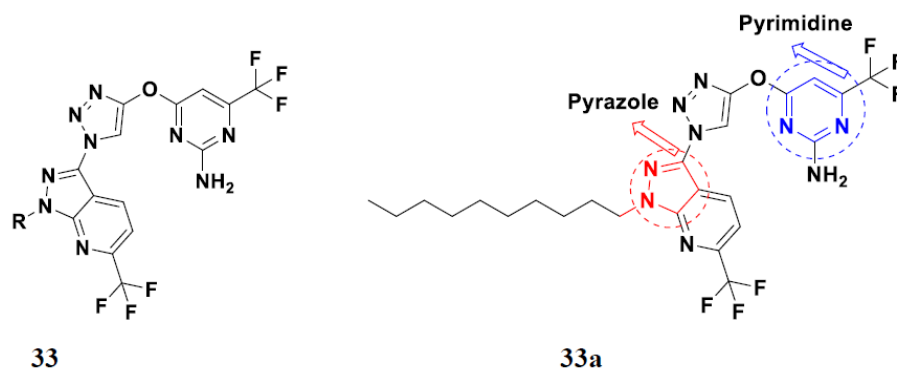
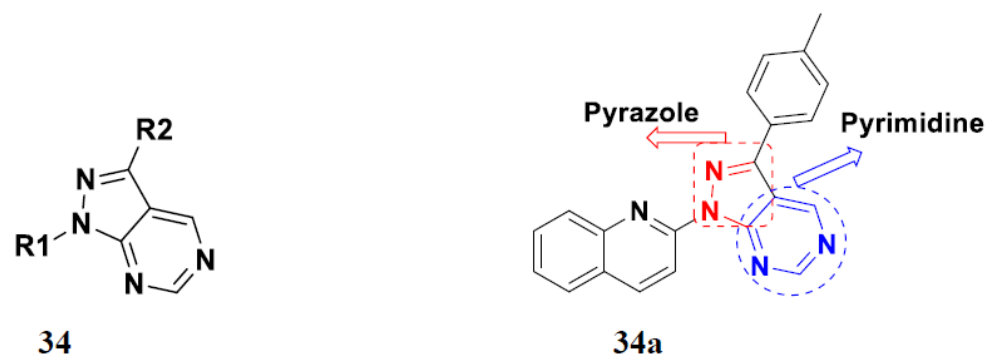


Figure 36. Structure of pyrimidine-pyrazole based hybrids and the most promising compound **33a**.

Table 26. In vitro cytotoxic activities of pyrimidine-pyrazole based hybrid compounds 33(b–e).

Compound No.	R	A549 (μM)	MCF7 (μM)	DU145 (μM)	HeLa (μM)
33b	CH ₃ CH ₂ OC(O)CH ₂ -	16.3	12.4	18.2	9.8
33c	CH ₃ (CH ₂) ₆ CH ₂ -	5.7	24.7	6.3	22.7
33d	CF ₃ (CF ₂) ₇ CH ₂ CH ₂ -	33.7	-	37.7	-
33e		4.1	-	4.7	-
5-FU	-	1.3	1.4	1.5	1.3

Huang et al. (2012) synthesized pyrimidine based pyrazole hybrids and evaluated their anticancer activity. Most of the synthesized compounds showed potent anticancer activity. Among them, compound 34(a) showed excellent activity against various cell lines including NCI-H226 (human lung squamous carcinoma cells), NPC-TW01 (nasopharyngeal carcinoma), and Jurkat having GI₅₀ 29, 30, and 54 μM, respectively. The structure of pyrimidine-pyrazole based hybrid derivatives is shown in Figure 37, and the in vitro cytotoxicity of compounds 34(b–e) against human cancer cell lines is shown in Table 27 [84].

**Figure 37.** Structure of pyrimidine-pyrazole based hybrids and the most promising compound 34a.**Table 27.** In vitro cytotoxic activities of pyrimidine-pyrazole based hybrid compounds 34(b–e).

Compound No.	R ₁	R ₂	NCI-H226 (μM)	NPC-TW01 (μM)	Jurkat
34b	Ph	p-Me-Ph	35	49	48
34c	2-Quinolinylnyl	p-Cl-Ph	39	35	69
34d	2-Quinolinylnyl	p-OMe-Ph	37	36	>100
34e	Ph	p-Cl-Ph	18	23	36
N0-(4-formyl-1,3-diphenyl-1H-pyrazol-5-yl)-N,N-dimethyl-methanimidamide			9.3	31.4	23.5

FDA Approved Pyrimidine Based Hybrids

Ceritinib, palbociclib, and ibrutinib are three hybrids which contain pyrimidine scaffold that have received US-FDA approval for their antitumor effects against non-small cell lung cancer, advanced breast cancer and leukemia, respectively. Pyrimidine-based FDA approved drugs are depicted in Figure 38 and their details are shown in Table 28.

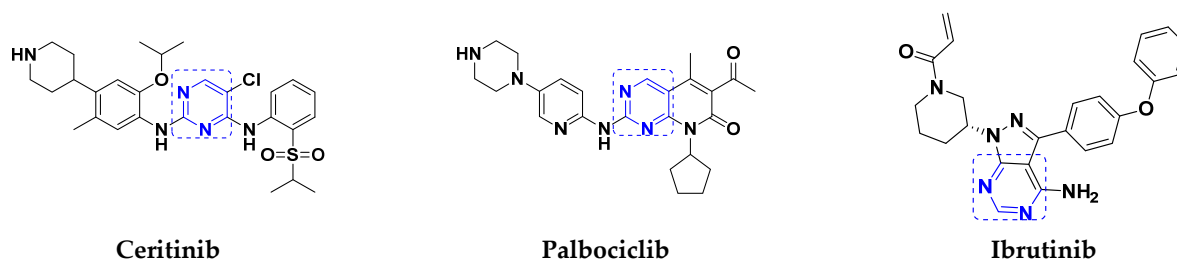


Figure 38. Pyrimidine based FDA approved drugs.

Table 28. FDA approved pyrimidine based hybrids.

Company Name	Compound Name	Drug Target	Type of Cancer	Status	Reference
Novartis	Ceritinib	Abnormal ALK-gene	Non-Small cell lung Cancer	Approved	[85]
Pfizer Pharmaceutical company	Palbociclib	CDK4/6 inhibitor	Breast cancer	Approved	[86]
AbbVie Pharmaceuticals	Ibrutinib	Tyrosine kinase	Mantle cell lymphoma	Approved	[87,88]

3.6. Quinoline-Based Hybrids

Quinoline has been identified as a major scaffold with huge therapeutic potential, including antibacterial, anti-viral, anti-helminthic, anti-malarial and anti-prozoal activities. Due to its derivatives having demonstrated outstanding effects against cancerous cells via various mechanisms, the quinoline nucleus has played a crucial role in the research and development of chemotherapeutic agents. Camptothecin is a natural anticancer agent with the capacity to obstruct DNA topoisomerase [89–91].

Sidoryk et al. (2015), synthesized quinoline based guanidine hybrids and evaluated their anticancer activity. Most of the synthesized compounds showed potent anticancer activity. Among them, compound 35 showed excellent activity against BALB/3T3, A549, MCF-7, LoVo, and KB cell lines (Table 29). Furthermore, compound 35 (Figure 39) showed excellent activity in a DNA displacement assay and potent activity in G2/M phase of the cell cycle [92].

Table 29. In vitro cytotoxic activities of quinoline-pyrimidine based hybrid compounds 35.

Compounds No.	BALB/3T3 (μM)	A549 (μM)	MCF-7 (μM)	LoVo (μM)	KB (μM)
35	30.04	3.24	0.81	9.38	0.87
Doxorubicin	1.08	0.33	0.44	0.11	0.84
DiMIQ	5.77	2.19	1.54	0.20	1.14

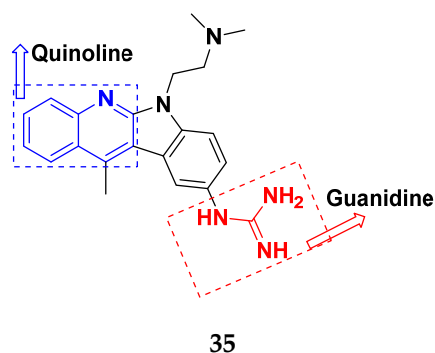


Figure 39. Structure of quinoline-guanidine based hybrid 35.

Gedawy et al. (2015) synthesized tetrahydro-pyrimido-quinoline based hybrids and evaluated their anticancer activity. Most of the synthesized compounds showed potent anticancer activity. Among them, compound 36 (Figure 40) showed excellent activity against HCT-116, and MCF-7 (Table 30) [93].

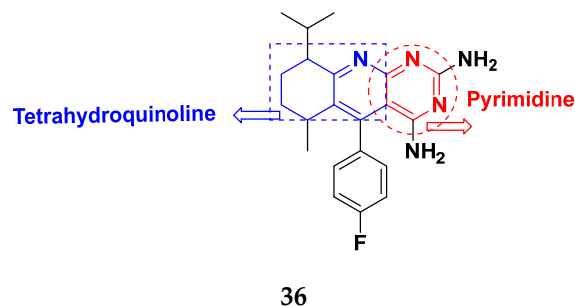


Figure 40. Structure of tetrahydro-pyrimido-quinoline based hybrid 36.

Table 30. In vitro cytotoxic activities of tetrahydro-pyrimido-quinoline based hybrid compound 36.

Compound No.	HCT116 (μM)	MCF7 (μM)
36	16.33	27.26
Imatinib	34.40	-
Tamoxifen	-	34.30

Sanchez et al. (2011) synthesized quinoline-based thiazole hybrids based on the structure of m-Amsacrine (37, Figure 41), and evaluated their anticancer activity against cancerous (K-562) and non-cancerous (PMBCs) cells. Compound 37a showed excellent activity with IC_{50} values of 28.7 and 7.82 μM , respectively, compared to a control of Paclitaxel (IC_{50} 0.25 μM). Mechanistically, compound 36(a) induced apoptotic cell death via caspase activation with an IC_{50} of 7.8 μM [94].

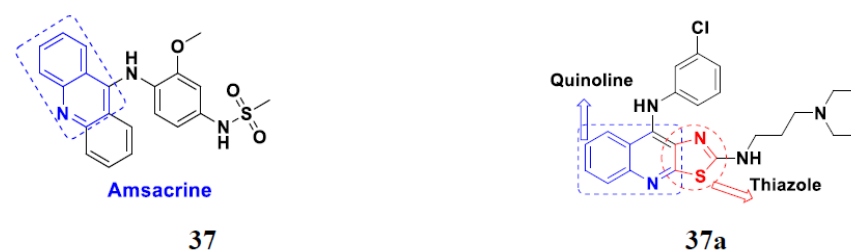


Figure 41. Structure of quinoline hybrid amsacrine 37 and the most promising compound 37a.

Luniewski et al. (2012) synthesized quinoline based indole hybrids and evaluated their anticancer activity. Most of the synthesized compounds showed potent anticancer activity. Among them, compound 38(a) showed excellent activity against KB, A-549, MCF-7, Hs294T, and BALB/3T3 cell lines having IC_{50} values of 0.15, 0.24, 0.38, 0.62, and 0.31 μM with control 5,11-dimethyl-5H-indolo [2,3-b]quinoline (DIMIQ) at IC_{50} values 1.14, 2.19, 1.50, 9.70, and 5.70 μM , respectively. Furthermore, compound 38a showed excellent topo II inhibitory activity at concentration of 0.05 μM with control DIMIQ (Conc. 0.5 μM), m-AMSA (Conc. 0.05 μM), and daunorubicin (Conc. 0.5 μM) and cell cycle inhibitory activity at a concentration of 0.10 μM with control DIMIQ (Conc. 1.02 μM). Additionally, it showed positive inhibitory results in the G2M phase of the cell cycle. The structure of quinoline-indole based hybrid derivatives is given in Figure 42 and the in vitro cytotoxicity of compounds 38(b–e) against human cancer cell lines is shown in Table 31 [95].

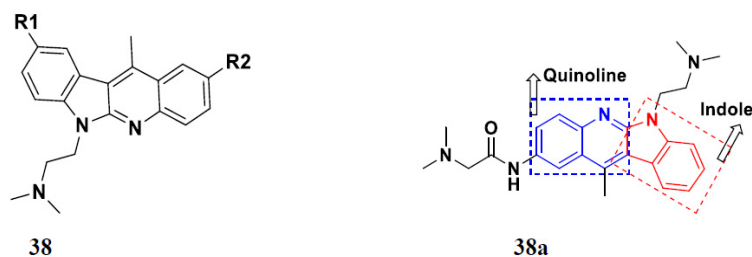


Figure 42. Structure of quinoline-indole based hybrids and the most promising compound 38a.

Table 31. In vitro cytotoxic activities of quinoline-indole based hybrid compounds 38(b–e).

Compound No.	R ₁	R ₂	KB (μM)	A-549 (μM)	MCF-7 (μM)	Hs294T (μM)	BALB/3T3 (μM)
38b		H	0.15	0.81	0.79	0.64	0.67
38c		H	0.36	0.29	0.99	0.72	0.60
38d	H		0.64	0.17	0.47	0.35	0.34
38e	H		0.08	0.19	0.66	0.76	0.57
DIMIQ			1.14	2.19	1.50	9.70	5.70

Jin et al. (2019) synthesized quinoline-based ursolic acid hybrids and evaluated their anticancer activity. Most of the synthesized compounds showed potent anticancer activity. Among them, compound 39(a) showed excellent activity against MDA-MB-231, HeLa, SMMC-7721, and QSG-7701 (hepatocyte cell line) at IC₅₀ 0.12, 0.08, 0.34, and 10.76 μM with control Etoposide with IC₅₀ values of 5.26, 2.98, 3.48, and 28.75 μM, respectively. Furthermore, compound 39(a) showed excellent activity apoptosis-inducing activity in on HeLa cell lines (for 48 h). The structure of quinolinebased ursolic acid hybrids derivatives is shown in Figure 43, and the in vitro cytotoxicity (μM) of compounds 39(b–e) against human cancer cell lines is shown in Table 32 [96].

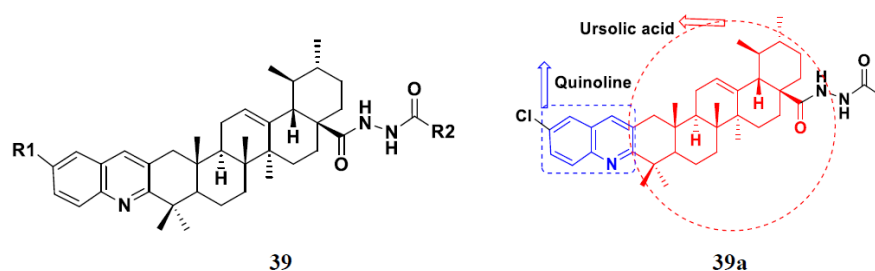


Figure 43. Structure of quinoline based ursolic acid hybrids and the most promising compound 39a.

Table 32. In vitro cytotoxic activities of quinoline based ursolic acid hybrids compounds 39(b–e).

Compound No.	R ₁	R ₂	MDA-MB-231(μM)	HeLa (μM)	SMMC-7721(μM)	QSG-7701(μM)
39b	H	CH ₃	1.84	1.18	17.48	40.59
39c	OCH ₃	CH ₃	1.42	0.83	17.65	45.20
39d	F	CH ₃	1.16	0.99	19.41	>50
39e	H	n-C ₄ H ₉	>50	>50	>50	Not tested
Etoposide	-	-	5.26	2.98	3.48	28.75

Solomon et al. (2019) synthesized quinoline based sulphonamide/piperazine hybrids and evaluated their anticancer activity. Most of the synthesized compounds showed potent anticancer activity. Among them, compound **40(a)** showed excellent activity against MB231, MB468, MCF7, 184B5 (normal mammary tissue), and MCF10A cell lines, having GI_{50} values of 3.4, 0.7, 2.3, 9.0, and 12.3 μM . Control chloroquine, had GI_{50} values of 22.5, 28.6, 38.4, 76.1, and 81.26 μM and Cisplatin having GI_{50} value 23.7, 31.0, 25.8, 25.5, and 51.51 μM , respectively. Furthermore, compound **40(a)** showed cell cycle interruption at the meta phase, and also increased the liposomal volume in cancerous cells which led to cell death. The structure of quinoline based piperazine hybrids is given in Figure 44 and the in vitro cytotoxicity (μM) of compounds **40(b–e)** against human cancer cell lines is shown in Table 33 [97].

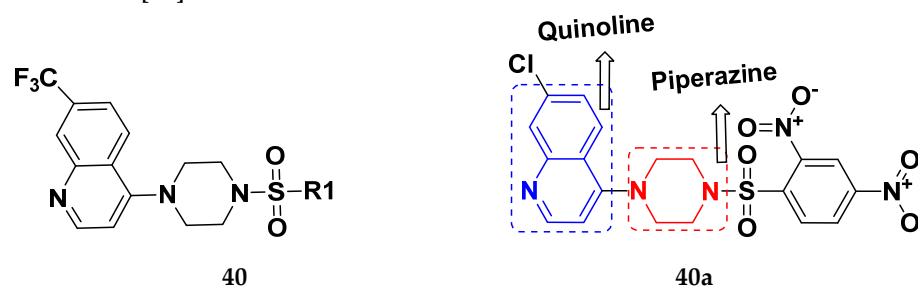


Figure 44. Structure of quinolone-based piperazine hybrids and the most promising compound **40a**.

Table 33. In vitro cytotoxic activities of quinoline based piperazine hybrids compounds **40(b–e)**.

Compound No.	R ₁	MB231 (GI_{50} μM)	MB468 (GI_{50} μM)	MCF-7 (GI_{50} μM)	184B5 (GI_{50} μM)	MCF10A (GI_{50} μM)
40b	2,4-Dinitrophenyl	24.3	19.2	10.8	37.8	35.4
40c	3-Nitrophenyl	32.2	18.6	9.4	17.7	15.4
40d	2,4-Dichlorophenyl	20.3	18.6	16.7	20.4	15.6
40e	Biphenyl	27.2	20.5	14.8	19.1	15.5
Chloroquine	-	22.5	28.6	38.4	76.1	81.26
Cisplatin	-	23.7	31.0	25.8	25.5	51.51

Kumar et al. (2014) synthesized quinoline-based gallium(III) hybrids and evaluated their anticancer activity. Synthesized hybrid **41** showed potent activity against HCT-116, Caco-2 (human colon cancer cell), HT-29, and CCD-18C (colonic fibroblasts), having IC_{50} values of 14.26, 19.56, 19.66, and 28.28 μM , respectively. Control etoposide had comparative values of 38.10, 32.90, 35.10, and 58.90 μM , respectively. Furthermore, hybrid **41** was evaluated for anti-malarial activity, showing more potent activity than lumefantrine on the 3D7 strain of Plasmodium falciparum. A quinoline-based gallium(III) hybrid is depicted in Figure 45 [98].

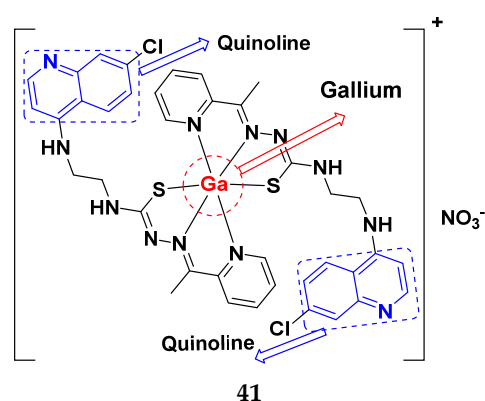


Figure 45. Quinoline-based gallium(III) hybrid (**41**).

Quinoline-Based FDA Approved Drugs

Quinoline containing drugs that have received FDA approval include lenvatinib, cabozantinib, and bosutinib which are protein kinase inhibitors and are used to cure medullary thyroid cancer and chronic myelogenous leukemia accordingly. FDA approved drugs with quinoline hybrids are depicted in Figure 46 and their details are shown in Table 34.

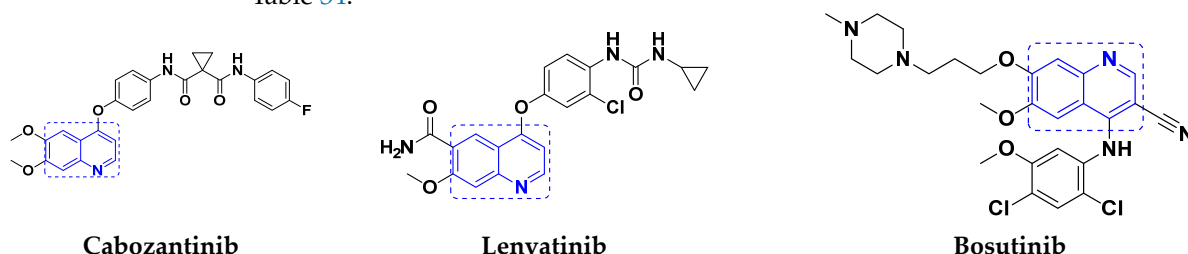


Figure 46. FDA approved drugs with quinoline hybrids.

Table 34. Quinoline based FDA approved hybrids.

Company Name	Compound Name	Drug Target	Type of Cancer	Status	Reference
Eisai Co.	Lenvatinib	Kinase inhibitor	Thyroid cancer	Approved	[99]
Exelixis Inc.	Cabozantinib	Tyrosine-kinase	Thyroid cancer and renal carcinoma	Approved	[68]
Wyeth and Pfizer	Bosutinib	BCR and Src tyrosine kinase	myelogenous leukemia	Approved	[100]

3.7. Quinone Hybrids

Quinones are found in all living beings; particularly animals, plant and microbes. Through serving as crucial links in the cell nucleus respiratory cycle, they play a vital role in the power generation of such species. Numerous distinct medicinal uses of quinones have been noted, such as antiviral, antithrombotic, antiplatelet, antibacterial, antifungal, anti-inflammatory, and antiallergic properties [101,102].

Markovic et al. (2015) synthesized quinone based chalcone hybrids and evaluated their anticancer activity. Most of the synthesized compounds showed potent anticancer activity. Among them, compound 42(a) showed excellent activity against HeLa, LS174 (colorectal cancer cells), A549, and MRC-5 (multipotent stem cells) with IC₅₀ values of 2.73, 6.44, 28.84, and 48.76, respectively. Furthermore, compound 42(a) showed caspase based apoptosis in G2/M and S phase of cell division. The structure of quinone-based chalcone hybrids derivatives is given in Figure 47 and the in vitro cytotoxicity of compounds 42(b–e) against human cancer cell lines is shown in Table 35 [103].

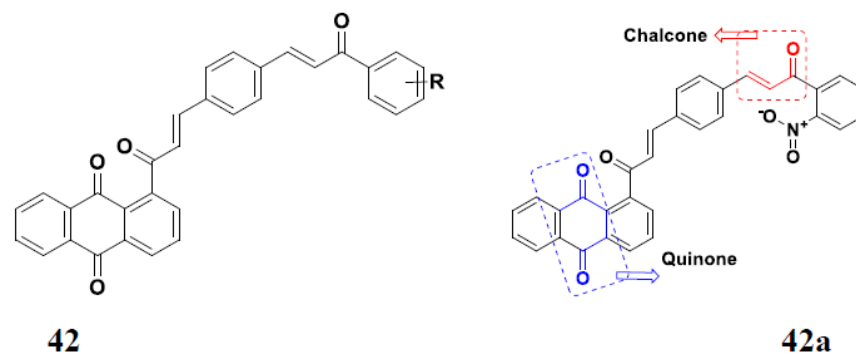
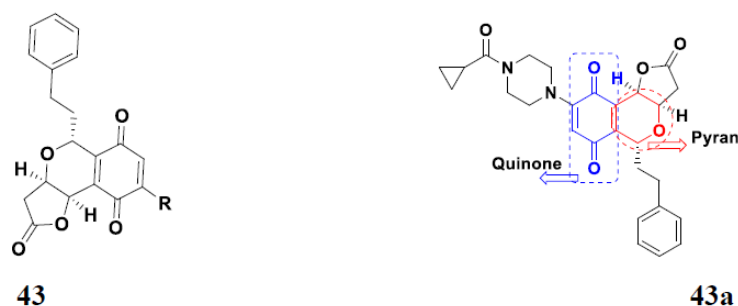


Figure 47. Structure of quinone-based chalcone hybrids and the most promising compound 42a.

Table 35. In vitro cytotoxic activities of quinone based chalcone hybrid compounds 42(b–e).

Compound No.	R	HeLa (μM)	LS174 (μM)	A549 (μM)	MRC-5 (μM)
42b	H	2.41	4.56	26.20	33.57
42c	2-CH ₃	2.36	3.13	29.05	41.87
42d	3-CH ₃	2.45	11.79	33.70	52.00
42e	4-CH ₃	2.64	22.63	24.15	38.49
cisplatin	-	2.10	5.54	11.92	14.21

Jiang et al. (2015) synthesized quinone based pyran hybrids and evaluated their anticancer activity. Most of the synthesized compounds showed potent anticancer activity. Among them, compound 43(a) showed excellent activity against KB (throat cancer cells), KB/VCR (colon cancer cells), A549, and HL60, with IC₅₀ values 4.05, 1.28, 0.62, and 1.73 $\mu\text{g}/\text{mL}$. A control vincristine had IC₅₀ values of 0.46, 0.26, and 12.09 $\mu\text{g}/\text{mL}$ (for KB, KB/VCR, A549), respectively, and adriamycin had an IC₅₀ value 0.02 $\mu\text{g}/\text{mL}$ (HL60). The structure of quinone-based pyran hybrid derivatives is given in Figure 48 and the in vitro cytotoxicity ($\mu\text{g}/\text{mL}$) of compounds 43(b–e) against human cancer cell lines is shown in Table 36 [104].

**Figure 48.** Structure of quinone based pyran hybrids and the most promising compound 43a.**Table 36.** In vitro cytotoxic activities of quinone based pyran hybrid compounds 43(b–e).

Compound No.	R	KB ($\mu\text{g}/\text{mL}$)	KB/VCR ($\mu\text{g}/\text{mL}$)	A549 ($\mu\text{g}/\text{mL}$)	HL60 ($\mu\text{g}/\text{mL}$)
43b		4.31	2.21	6.58	4.45
43c		>8.00	>8.00	>8.00	>8.00
43d		>8.60	8.52	4.49	4.46
Vincristine	-	0.46	0.26	12.09	-
Adriamycin I	-	-	-	-	0.02

Quinone Containing FDA Approved Drugs

Doxorubicin, daunorubicin, and mitoxantrone drugs are used to treat several types of cancer. These drugs are shown in Figure 49 [101].

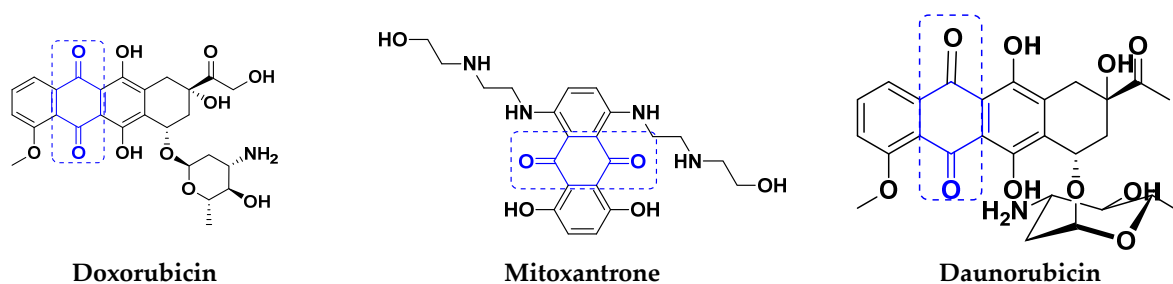


Figure 49. FDA approved drugs with Quinone hybrids.

3.8. Imidazole Based Hybrids

The imidazole derivatives have recently gained a lot of interest and are already present in many existing treatments. Imidazole was first synthesized in 1858 using glyoxal and formaldehyde by Heinrich Debus [105]. Various medicinal properties of imidazole based hybrid molecules have been reported; especially as antitumor [106], anti-diabetic, anti-HIV, anti-protozoal, anti-mycobacterial, anti-inflammatory, analgesic, and anti-protozoal agents [107,108].

Xiao-Dong Yang et al. (2012) synthesized different derivatives of novel hybrid compounds between 2-phenylbenzofuran and imidazole. Myeloid liver carcinoma (SMMC-7721), colon carcinoma (SW480), breast carcinoma (MCF-7), lung carcinoma (A549) and leukemia (HL-60) cell lines were used for in vitro study of the cytotoxic effects of synthesized hybrids with cisplatin (DPP) as the standard drug. Five derivatives showed more potent cytotoxic activity than standard DPP. The structure of imidazole based benzofuran hybrid derivatives are given in Figure 50 and the in vitro cytotoxic activities of hybrid compounds 44(a–e) (IC_{50} , μM) are listed in Table 37 [109].

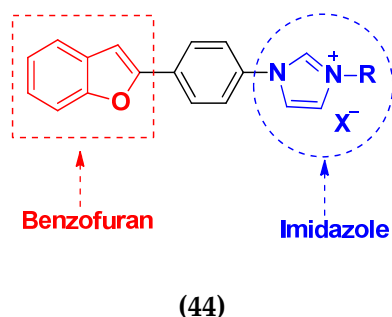


Figure 50. Structure of imidazole-based benzofuran hybrid derivatives (44).

Table 37. In vitro cytotoxic activities of imidazole based benzofuran hybrid compounds 44(a–e).

Compound No.	R	X	SMMC-7721 (μM)	SW480 (μM)	MCF-7 (μM)	A549 (μM)	HL-60 (μM)
44a	2-Bromobenzyl	Br	4.38	12.71	14.29	9.77	1.97
44b	Phenacyl	Br	3.71	10.34	11.90	12.94	2.61
44c	4-Bromophenacyl	Br	3.39	2.85	2.84	8.46	3.15
44d	Naphthyl acyl	Br	1.65	3.38	5.87	10.93	2.49
44e	2'-Phenyl-phenacyl	Br	3.31	6.93	6.90	6.79	2.70
DPP	-	-	8.86	15.92	16.65	11.68	1.81

Wen Chen et al. (2013) synthesized numerous derivatives of novel hybrid 2-phenyl-3-alkylbenzofuran and imidazole compounds. Myeloid liver carcinoma (SMMC-7721), colon carcinoma (SW480), breast carcinoma (MCF-7), lung carcinoma (A549) and leukemia (HL-60) cell lines were used for in vitro cytotoxic testing of synthesized hybrids, with

DPP as the standard drug. They found that five derivatives showed more potent cytotoxic activity than standard DPP. The structure of imidazole based benzofuran hybrid derivatives is given in Figure 51 and the in vitro cytotoxic activities of hybrid compounds 45(a–e) (IC_{50} , μM) are listed in Table 38 [110].

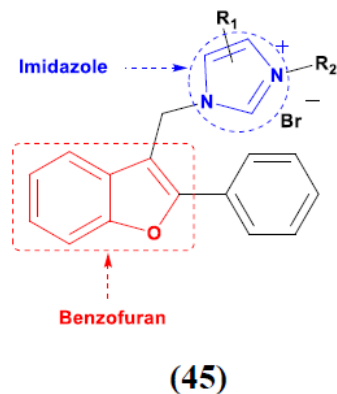


Figure 51. Structure of imidazole based benzofuran hybrid derivatives (45).

Table 38. In vitro cytotoxic activities of imidazole based benzofuran hybrid compounds 45(a–e).

Compound No.	R ₁	R ₂	SMMC-7721 (μM)	SW480 (μM)	MCF-7 (μM)	A549 (μM)	HL-60 (μM)
45a	Benzimidazole	2-Bromobenzyl	2.10	5.56	4.78	3.34	0.64
45b	2-Ethylimidazole	4-Hydroxyphenacyl	11.81	5.69	3.17	12.90	0.58
45c	2-Ethylimidazole	4-Bromophenacyl	6.07	3.58	2.89	12.76	0.72
45d	2-Ethylimidazole	Naphthylacyl	2.30	3.14	3.03	5.35	0.61
45e	2-Ethylimidazole	2-Bromobenzyl	0.52	0.47	0.51	0.55	0.08
DPP			1.69	12.49	14.09	20.82	18.85

Al-blewi et al. (2013) synthesized numerous derivatives of novel imidazole-1,2,3-triazole hybrids. The synthesized compounds were screened for their anticancer activity against three different types of cancer, namely human colon carcinoma (Caco2 and HCT116), human cervical carcinoma (HeLa) and human breast adenocarcinoma (MCF-7) cancer cells-, using doxorubicin as a standard drug. They found that these derivatives showed potent more cytotoxic activity than standard doxorubicin. The structure of imidazole based triazole hybrid derivatives is given in Figure 52 and in vitro cytotoxic activities of hybrid compounds 46(a–e) are listed in Table 39 [111].

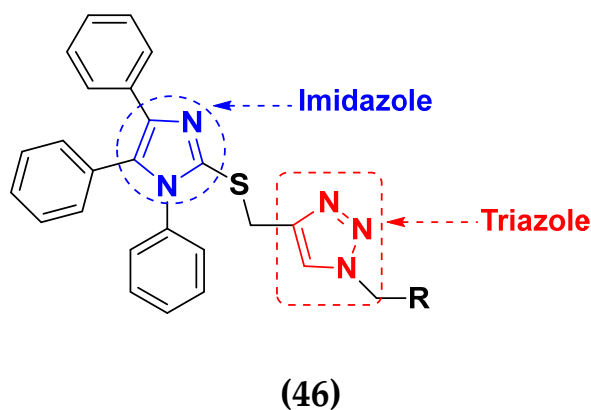
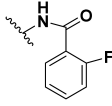
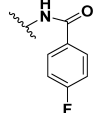
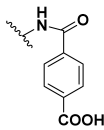
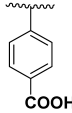
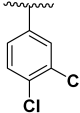
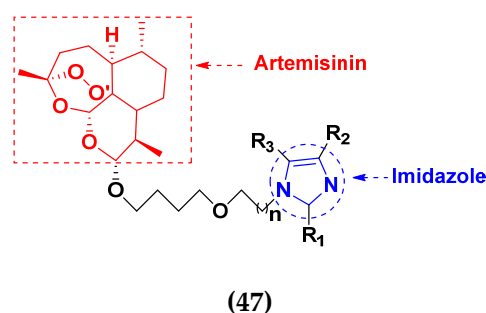


Figure 52. Structure of imidazole based triazole hybrid derivatives (46).

Table 39. In vitro cytotoxic activities of imidazole based triazole hybrid compounds 46(a–e).

Compound No.	R	Caco2 (μM)	HCT116 (μM)	HeLa (μM)	MCF-7 (μM)
46a		6.31	12.04	7.91	3.80
46b		8.45	18.32	9.45	4.45
46c		4.67	16.78	6.87	0.38
46d		5.22	18.70	8.42	3.87
46e		10.87	30.98	20.34	15.56
Doxorubicin	-	5.17	5.64	1.25	0.65

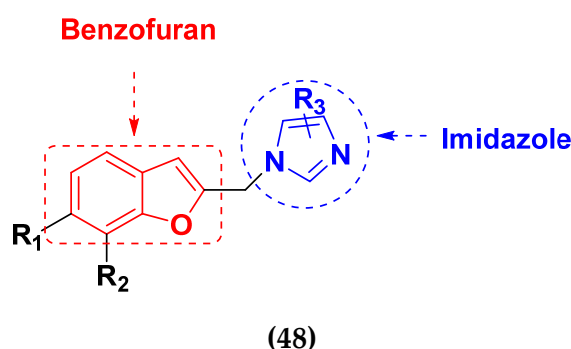
Yanping Hu et al. (2019) designed and synthesized a series of artemisinin-imidazole hybrids derivatives with multidrug resistance (MDR) reversal activity. All hybrids were screened in vitro for anticancer activities against four human cancer cell lines, human breast cancer (MCF-7), human non-small-cell lung (A549), (HEPG-2), breast cancer (MDA-MB-231) and normal human hepatic cells (L02). Adriamycin was used as reference drug. They found that most of the synthesized compounds showed higher anticancer activities than artemisinin. The structure of imidazole based artemisinin hybrid derivatives is given in Figure 53 and the in vitro cytotoxic activities of hybrid compounds 47(a–e) are listed in Table 40 [112].

**Figure 53.** Structure of imidazole-based artemisinin hybrid derivatives (47).

Wen-Jian Song et al. (2012) designed and synthesized a series of novel hybrid compounds of 2-substituted benzofuran and imidazole. In vitro anticancer activity of synthesized hybrids against a panel of human tumor cell lines i.e., ovarian carcinoma cell line (Skov-3), leukemia (HL-60) and breast carcinoma (MCF-7) was evaluated. They found that the hybrid compounds were more selective than standard DPP. The structure of imidazole based benzofuran hybrid derivatives is given in Figure 54 and the in vitro cytotoxic activities of hybrid compounds 48(a–e) are listed in Table 41 [113].

Table 40. In vitro cytotoxic activities of imidazole-based artemisinin hybrid compounds 47(a–e).

Compound No.	R ₁	R ₂	R ₃	n	MCF-7 (μM)	A549 (μM)	HEPG-2 (μM)	MDA-MB-231 (μM)	LO2 (μM)
47a	H	CN	CN	1	10.75	12.36	25.59	>100	49.05
47b	H	NO ₂	H	2	12.86	20.95	39.30	>100	46.37
47c	H	H	Br	2	12.40	26.02	41.59	80.92	>100
47d	H	H	NO ₂	2	12.69	19.97	33.33	80.92	34.32
47e	H	NO ₂	H	3	9.78	16.53	21.25	85.20	45.74
Andriamycin	-	-	-		0.67	1.13	0.85	2.94	0.79

**Figure 54.** Structure of imidazole based benzofuran hybrid derivative 48.**Table 41.** In vitro cytotoxic activities of imidazole-based benzofuran hybrid compounds 48(a–e).

Compounds No.	R ₁	R ₂	R ₃ (Imidazole)	SKOV-3 (μM)	HL-60 (μM)	MCF-7 (μM)
48a	H	H	Benzimidazole	9.5	8.4	11.8
48b	H	Allyl	Benzimidazole	7.9	>40	>40
48c	OMe	Allyl	Imidazole	36.2	>40	>40
48d	OMe	Allyl	Benzimidazole	9.3	>40	>40
48e	H	H	Imidazole	>40	>40	>40
DDP	-	-	-	8.9	5.5	13.0

Imidazole Based Hybrids That Are FDA Approved or under clinical Trial

Different imidazole-based anticancer hybrid drugs that are FDA approved/or under clinical trials are shown in (Figure 55), and their chemical structures brand/company name and targets are in Table 42.

3.9. Selenium-Based Hybrids

Selenium (Se) is a unique trace element. Se directly or indirectly exerts antioxidant functions in the human body. However, during recent years, researchers reported that Se containing compounds exhibit superior anticancer effects, with high efficacy and selectivity [117]. It has been reported that a variety of organic selenium compounds, including selenoesters, selenocyanates, methylseleninic acid, isoselenocyanates, diselenides, and endocyclic selenium, have anticancer properties [118].

Organic Se compounds have lower systemic effects, fewer side effects, and strong anti-tumor action. They also have a greater ability to inhibit metastasis. Several novel organic Se compounds have been synthesized in order to further improve the selectivity, specificity and efficacy and to lower the toxicity [119].

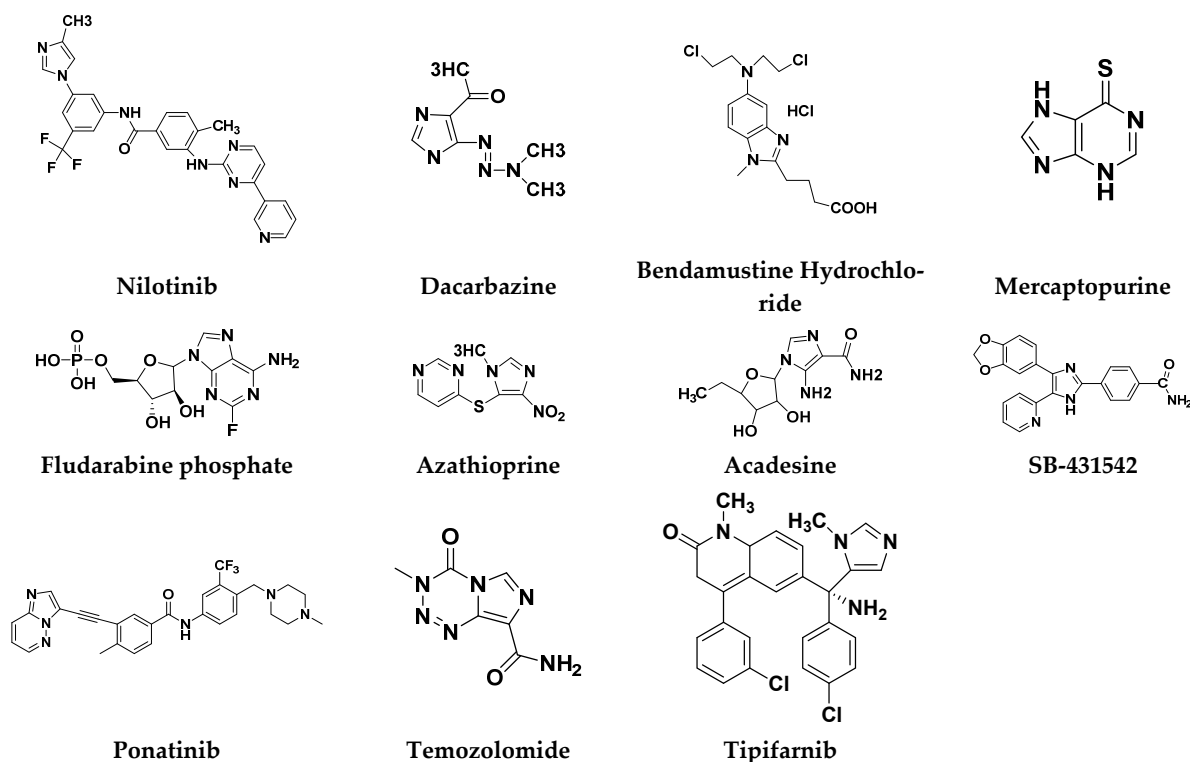


Figure 55. Imidazole based anticancer drugs that are FDA approved or in clinical trials.

Table 42. Imidazole based anticancer drugs with brand/company name, specific cancer types and targets.

Brand/Company Name	Compound Name	Drug Target	Type of Cancer	Status	References
AdisInsight-springer/Ligand pharmaceuticals	Acadesine	AMP-activated protein kinase	Acute lymphoblastic leukemia	Phase-III	[105]
Tasigna/Novartis	Nilotinib	BCR-ABL	Leukemia	FDA approved	[114]
Hikma Pharmaceuticals	Dacarbazine	DNA synthesis	Melanoma; Lymphoma	FDA approved	[115]
Janssen Pharmaceutical	Tipifarnib	Farnesyltransferase inhibitors (FTIs)	Breast cancer	phase II trials	[116]
Treanda	Bendamustine hydrochloride	DNA synthesis	Leukemia; Lymphoma	FDA approved	[115]
Astellas Pharma	Fludarabine phosphate	DNA synthesis	Leukemia	FDA approved	[115]
Oforta/Sanofi pharma	Azathioprine	Thiopurine	Childhood acute lymphoblastic leukemia	Discontinued	[115]
Nova Laboratories, Ltd.	prodrug of mercaptopurine	S-methyltransferase (TPMT)	Childhood acute lymphoblastic leukemia	FDA approved	[115]
Iclusig/Otsuka	Ponatinib	BCR-ABL	Leukemia	FDA approved	[115]
Pharmaceutical	Temodar/Ranbaxy (UK)	DNA synthesis	Brain cancer	FDA approved	[115]
Puri-nethol/German Remedies Limited	Mercaptopurine	HPRT1	Leukemia	FDA approved	[115]
GlaxoSmithKline (GSK)	SB-431542	Activin receptor-like kinase (ALK) receptors	Childhood acute lymphoblastic leukemia	No clinical trials	[105]

Xianran He et al. (2020) synthesized organoselenium (SeCF_3) derivatives as potential anticancer agents. The anticancer activity of the synthesized compounds was assessed using human cancer cell lines, human colon adenocarcinoma cells (SW480), human cervical cancer cells (HeLa), human lung carcinoma cells (A549), human breast adenocarcinoma cells (MCF-7). The in vitro biological evaluation was conducted at 24, 48 and 72 h intervals, and it was found that the organoselenium hybrid compounds were more selective than standard Fluorouracil (5FU). The structure of organoselenium hybrid derivatives is given in Figure 56 and the in vitro cytotoxic activities of hybrid compounds 49(a–c) are listed in Table 43 [118].

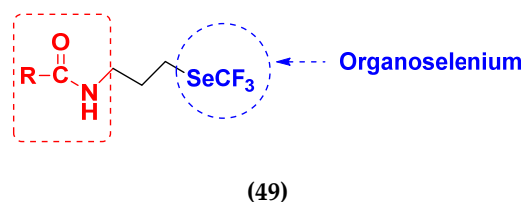


Figure 56. Organoselenium hybrid derivatives (49).

Table 43. In vitro cytotoxic activities of organoselenium hybrid compounds 49(a–c).

Compound No.	Structure	h	SW480 (μM)	HeLa (μM)	A549 (μM)	MCF-7 (μM)
49a		24	13.4	24.3	9.4	8.2
		48	11.4	15.1	11.3	6.4
		72	10.1	19.4	7.4	10.4
49b		24	8.2	19.6	13.1	8.6
		48	7.4	17.5	18.4	9.3
		72	6.5	28.7	22.6	9.5
49c		24	4.9	11.5	9.4	3.4
		48	3.3	17.4	15.2	4.3
		72	4.2	19.7	18.5	2.8
Fluorouracil (5FU)	-	24	15.3	20.6	25.3	8.5
		48	12.4	15.5	22.5	10.4
		72	13.1	12.7	17.3	12.6

Guilherme A. Jardim et al. (2017) synthesized selenium-containing quinone-based 1,2,3-triazoles with potential antitumor activity via rhodium-catalyzed C-H bond activation and click reactions. All compounds were evaluated against five types of cancer cell lines: human promyelocytic leukemia cells (HL-60), human colon carcinoma cells (HCT-116), human glioblastoma cells (SF295), human lung cells (NCIH-460) and human prostate cancer cells (PC3), using paclitaxel as a positive control. L929 cells were also used to test the cytotoxic potential of the naphthoquinoidal derivatives in non-tumor cells. Overall, these compounds represented promising new lead derivatives with potential antitumor activity. The structure of selenium based quinone triazole hybrids is given in Figure 57 and in vitro cytotoxic activities of hybrid compounds 50(a–e) are listed in Table 44 [120].

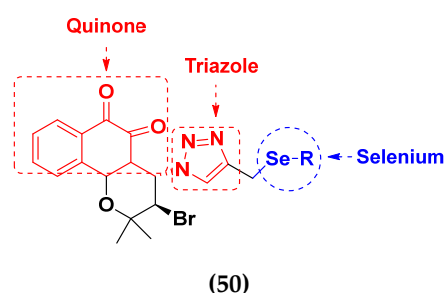
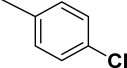
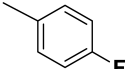
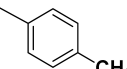
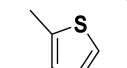

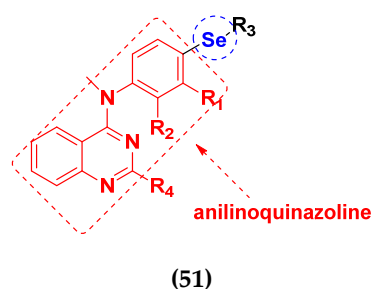


Figure 57. Structure of selenium-based quinone triazole hybrid derivatives (50).

Table 44. In vitro cytotoxic activities of selenium based quinone triazole hybrid compounds 50(a–e).

Compound No.	R	HL-60 (μM)	HCT-116 (μM)	SF295 (μM)	NCIH-460 (μM)	PC3 (μM)	L929 (μM)
50a		0.81	78.0	2.60	2.06	2.03	0.52
50b		0.59	0.37	1.48	1.32	1.06	0.36
50c		1.0	2.03	3.12	3.26	2.70	0.61
50d		0.53	78.0	2.13	2.75	2.47	3.16
50e		0.71	0.97	3.43	2.64	1.64	2.12
DOXO	-	0.02	0.21	0.41	0.15	0.76	1.72

An B et al. (2018) synthesized selenium-containing 4-anilinoquinazoline hybrids and evaluated them as tubulin polymerization inhibitors. All the synthesized compounds were screened against a panel of six human tumor cell lines, human colon cancer cells (RKO), HEPG2, breast adenocarcinoma (MCF-7), human epithelial cervical cancer cells (HeLa), human colon cancer cells (HCT116), and human gastric cancer cells (MGC803). An antiproliferative activity assay showed that most of compounds inhibited human cancer cells at low nano-molar concentrations. These compounds disturbed microtubule dynamics, lowered mitochondrial membrane potential, and stopped HeLa cells in the G2/M phase, ultimately leading to apoptosis. The structure of selenium based anilino quinazoline hybrids is given in Figure 58 and the in vitro cytotoxic activities of hybrid compounds 51(a–e) are listed in Table 45 [121].

**Figure 58.** Structure of selenium based anilino quinazoline hybrid derivatives (51).**Table 45.** In vitro cytotoxic activities of selenium based anilino quinazoline hybrid compounds 51(a–e).

Compound No.	R ₁	R ₂	R ₃	R ₄	RKO (nM)	HGPG2 (nM)	MCF7 (nM)	HELA (nM)	HCT116 (nM)	MGC803 (nM)
51a	H	H	-CN	Cl	3.39	5.24	9.98	2.09	4.97	3.54
51b	CH ₃	H	-CN	Cl	6.01	6.79	18.9	8.73	22.7	16.5
51c	Cl	H	-CN	Cl	3.42	6.78	10.6	6.78	9.17	9.67
51d	F	H	-Se-CH ₃	Cl	7.87	13.2	22.5	9.28	12.3	14.8
51e	H	H	-Se-CH ₃	-OCH ₃	7.85	8.92	22.7	9.15	11.4	4.78
EP128495	-	-	-	-	4.22	6.47	5.61	5.11	8.27	6.23

Hairong Tang et al. (2021) synthesized novel selenium-containing chiral 1,4-diarylazetidino-2-ones and biologically evaluated for antitumor activities. All the newly synthesized selenium-containing compounds were screened for their antiproliferative activity against

four human cancer cell lines, human epithelial cervical cancer cells (HeLa), human hepatoma cells (HUH-7), ovarian carcinoma cells (Skov-3) and human ovarian cancer cells (A2780), using paclitaxel as the positive control. The structure of Selenium based arylazetidins hybrids is shown in Figure 59 and the in vitro cytotoxic activities of hybrid compounds 51(a–d) are listed in Table 46 [122].

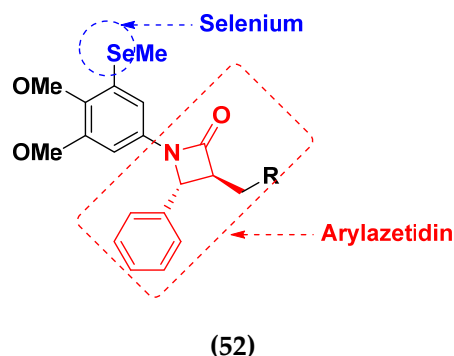


Figure 59. Structure of selenium based anilino quinazoline hybrid derivatives (52).

Table 46. In vitro cytotoxic activities of selenium based anilino quinazoline hybrid compounds 52(a–d).

Comound No.	R	HeLa (nM)	HUH-7 (nM)	SKOV3 (nM)	A2780 (nM)
52a	OH	3.3	2.3	1.6	2.0
52b	F	2.0	6.7	8.5	7.9
52c	Cl	6.1	3.7	1.0	5.9
52d	I	9.2	17.1	9.4	8.2
Paclitaxol	-	2.1	3.2	2.2	3.2

Sheng Huang et al. (2021) designed and synthesized fourteen novel selenium N-heterocyclic carbene (Se-NHC) compounds derived from 4,5-diarylimidazole and evaluated their antiproliferative activity towards ovarian cancer cells (A2780) and normal ovarian epithelial cells (IOSE80). Most of them were more effective towards ovarian cancer cells (A2780) than HepG2 hepatocellular carcinoma (HCC) cells. In addition, compound 53 displayed more than two-fold higher cytotoxicity to A2780 cells than to normal ovarian epithelial cells (IOSE80). Further research demonstrated that these inhibitors generated reactive oxygen species (ROS), harmed mitochondrial membrane potential (MMP), stopped cells from entering G0/G1 phase, and ultimately promoted apoptosis in the A2780 cells. The structure of selenium-based diarylimidazole hybrids is shown in Figure 60 and the in vitro cytotoxic activities of hybrid compounds 53(a–e) are listed in Table 47 [123].

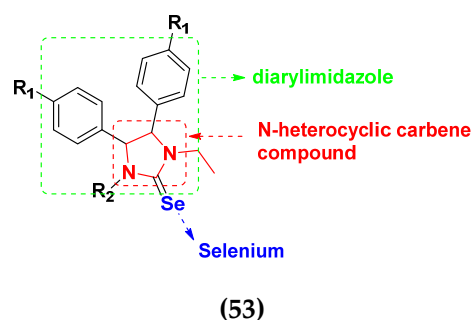


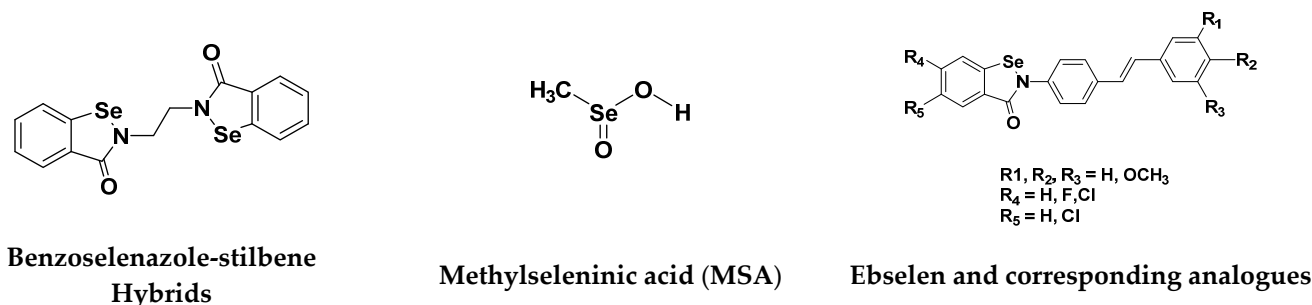
Figure 60. Structure of selenium-based diaryl imidazole hybrid derivatives (53).

Table 47. In vitro cytotoxic activities of selenium based diaryl imidazole hybrid compounds 53(a–e).

Compound No.	R ₁	R ₂	A 2780 (nM)	IOSE 80(nM)
53a	OMe	Et	9.7	51.3
53b	OMe		6.4	11.0
53c	F		19.1	34.8
53d	F		13.0	29.4
53e	Br	Et	21.1	43.7
Ebselen	-	-	25.4	55.4

Selenium-Based Hybrids That Are FDA Approved or under Clinical Trials

Different selenium-based potent anticancer drugs their chemical structure (Figure 61), mode of action and doses are shown in Table 48.

**Figure 61.** Selenium based potent anticancer compounds.**Table 48.** Selenium-based potent compounds with mode of action, specific cancer types and doses.

Compound Name	Mode of Action	Type of Cancer	Dose (Conc.) *	References
Methylseleninic Acid (MSA)	Apoptosis mediated by caspases, ER stress, UPR, mitochondrial dysfunction/signaling and PARP cleavage Anoikis, whereby cell detachment is a prerequisite for caspase activation and PARP cleavage	Breast, Colon Lung, Lymphoma Pancreatic	Medium to Low In pancreatic Very low-Low	[119]
Ebselen and corresponding Analogues	Not determined. Compounds have antioxidant activity	Breast, Liver, Promyelocytic Leukemia, Prostate	Medium-high	[119]
Benzoselenazole-stilbene hybrids	Apoptosis mediated by thioredoxin reductase inhibition and oxidative stress	Breast, Cervical, Liver, Lung	Very low-low	[119]

* Effective Dose in vitro (48–72 h IC₅₀) low (0.1–2 μM) (1–20 μM) Medium (10–100 μM) High (100+ μM).

3.10. Platinum-Based Hybrids

Platinum (Pt) medicines are still among the most often used anticancer treatments after more than 40 years of use. It is not unexpected that new research into changes in DNA repair pathways provides a reasonable explanation for Pt medicines' efficacy since they primarily target DNA [124]. The first platinum drug, cisplatin, was discovered by Barnett

Rosenberg in 1960 [125] and received FDA approval in 1978 for the treatment of advanced ovarian, bladder and testicular cancer [126]. Oxaliplatin and carboplatin are also platinum containing clinical drugs. Despite the widespread use of platinum medicines in cancer treatment regimens, there are several associated drawbacks. It is associated with severe side effects such as nephrotoxicity, neurotoxicity, and ototoxicity [127]. Additionally, using platinum medications has a number of adverse effects that range in intensity from mild to toxic (at high doses). In an attempt to circumvent these problems, a large number of platinum complexes have been prepared and tested for anticancer activity [128].

A. Graham et al. (2012) synthesized platinum–acridine hybrid anticancer agents. In vitro cytotoxicity activity was evaluated on different cell lines, ovarian cancer (OVCAR-3), breast cancer (MCF-7, MDA-MB231), pancreatic (PANC1) and non-small cell lung cancer cells (NCI-H460) using cisplatin as the positive control. The structure of Platinum–acridine hybrids is given in Figure 62 and in vitro cytotoxic activities of hybrid compounds 54(a–e) are listed in Table 49 [129].

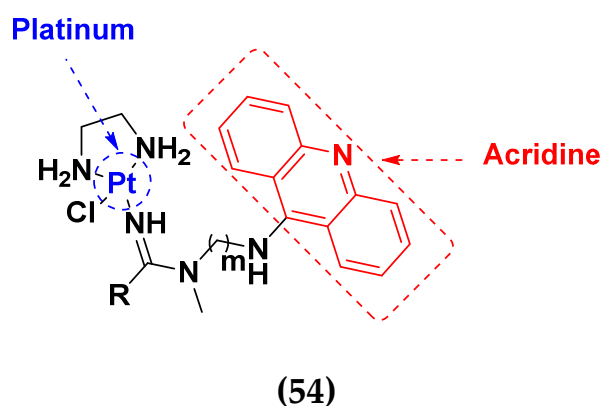


Figure 62. Structure of Platinum–acridine hybrid derivatives (54).

Table 49. In vitro cytotoxic activities of Platinum–acridine hybrid compounds 54(a–e).

Compound No.	R	m	OVCAR-3 (μM)	MCF-7 (μM)	MDA-MB231 (μM)	PANC1 (μM)	NCI-H460 (μM)
54a	CH ₃	2	1.1	2.5	15	0.09	0.008
54b	CH ₃	3	33	11	37	4.4	0.052
54c	(CH ₂)(CO)OCH ₃	2	-	-	-	-	0.036
54d	(CH ₂) ₂ (CO)OCH ₃	2	1.9	3.6	9.9	0.086	0.011
54e	(CH ₂) ₂ (CO)OCH ₃	3	150	19	36	2.2	0.065
Cisplatin	-	-	3.3	12	60	6.6	1.2

Jian Zhao et al. (2012) designed and synthesized six novel platinum (II) complexes 1–6 bearing different furoxan moieties as nitric oxide (NO) donors. The furoxan groups were introduced to the platinum complexes to release NO, which may have synergistic action with the platinum-based moieties on the tumor cells. It was found that all compounds exhibited higher cytotoxicity against human cancer cell lines HCT-116 and SGC-7901 compared to standard carboplatin, and oxaliplatin. The structure of platinum hybrids is shown in Figure 63 and the in vitro cytotoxic activities of hybrid compounds (55–60) are listed in Table 50 [130].

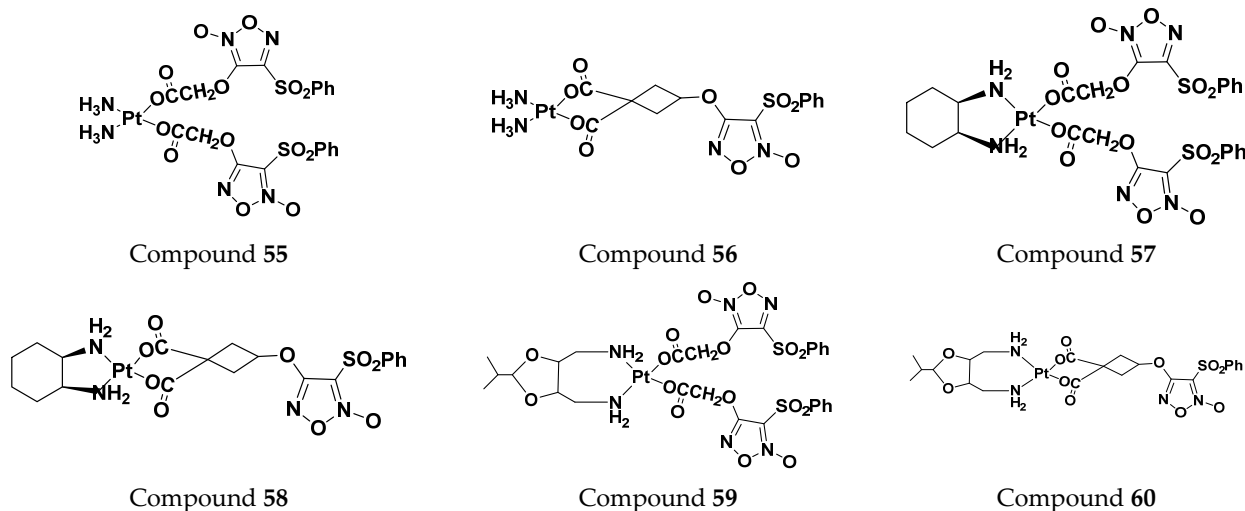


Figure 63. Platinum hybrid derivatives (55–60).

Table 50. In vitro cytotoxic activities of Platinum hybrid compounds (55–60).

Compounds No.	HCT-116 (μM)	SGC (μM)
55	64.06	217.93
56	57.21	94.23
57	39.43	34.64
58	111.91	248.07
59	142.15	59.10
60	87.06	70.83
carboplatin	273.05	58.11
oxaliplatin	57.04	17.35

Liu Z et al. (2021) prepared dihydro-2-quinolone (DHQLO) platinum (IV) compounds. Cytotoxic profiles of DHQLO platinum (IV) complexes were tested against five carcinoma cell lines including, ovarian cancer (SKOV-3), human cervical cancer cell (HeLa), human lung cancer (A549), murine colon cancer (CT-26), a cisplatin resistant cell line (A549R), and one normal human embryonic kidney cell line (293T). The antitumor activities of DHQLO platinum (IV) compounds were tested using the MTT assay with cisplatin and oxaliplatin as reference drugs. Cells were treated with drugs at different concentrations for 48 h, and the results were given as IC_{50} values. The structure of Platinum (iv) dihydro-2-quinolone hybrids is given in Figure 64 and the in vitro cytotoxic activities of hybrid compounds 61(a–e) are listed in Table 51 [131].

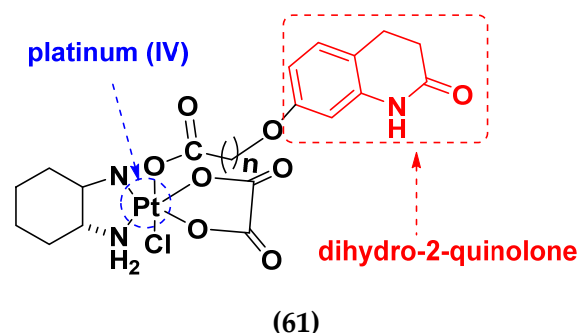
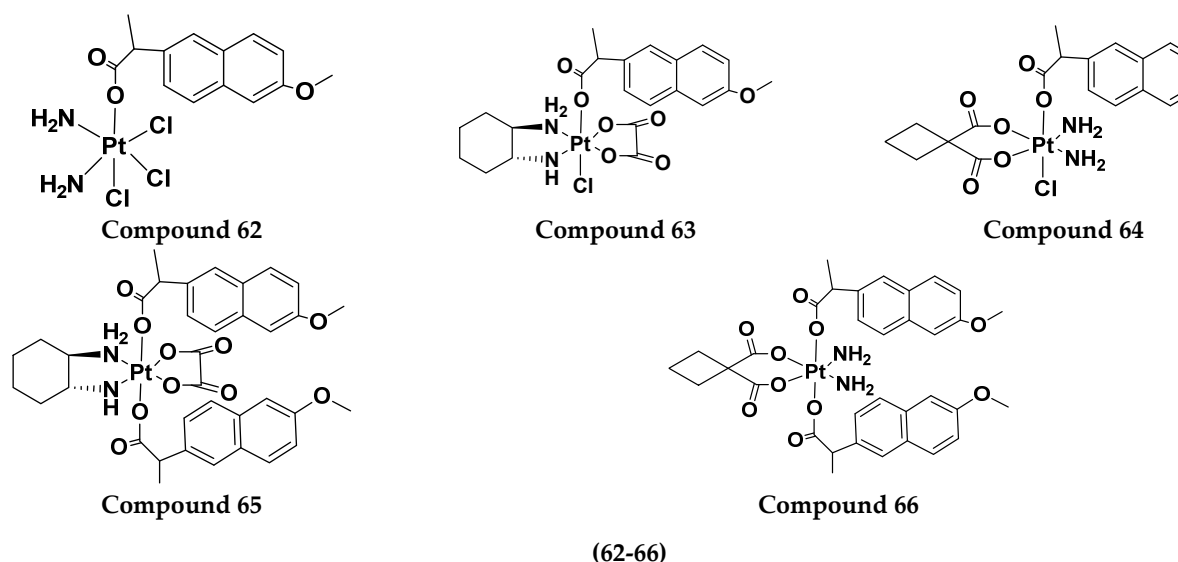


Figure 64. Structure of Platinum (iv) dihydro-2-quinolone hybrid derivatives (61).

Table 51. In vitro cytotoxic activities of Platinum (iv) dihydro-2-quinolone hybrid compounds 61(a–c).

Compound No.	n	CT26 (μM)	SKOV-3 (μM)	HeLa (μM)	A549 (μM)	A549R (μM)
61a	01	5.0	4.0	3.2	9.8	23.4
61b	03	11.7	2.7	2.6	8.6	8.3
61c	04	9.2	3.5	2.5	6.1	8.9
Cisplatin	-	5.3	2.4	2.4	13.5	22.6
Oxaliplatin	-	3.9	5.3	7.4	26.8	22.2

Yan Chen et al. (2020) synthesized naproxen platinum(IV) hybrids (62–66, Figure 65) that inhibited, matrix metalloproteinases and caused DNA damage. The antitumor activities of naproxen platinum(IV) compounds (62–66) were tested against four tumor cell lines including human lung cancer (A549), human ovarian cancer (SKOV-3), murine colon cancer (CT-26) and a cisplatin resistant cell line (A549R). A human normal liver cell LO-2 was also evaluated. The results are given in Table 52. It was observed that compounds 62–66 displayed moderate to effective antitumor activities against the tested tumor cell lines [132].

**Figure 65.** Structure of naproxen platinum (IV) hybrid derivatives.**Table 52.** In vitro cytotoxic activities of naproxen platinum (IV) hybrid compounds (62–66).

Compound No.	A549 (μM)	A549R (μM)	SKOV-3 (μM)	CT-26 (μM)	LO-2 (μM)
62	2.2	19.7	14.4	0.2	1.9
63	5.2	4.8	8.5	2.9	4.8
64	47.2	62.2	26.0	26.1	39.9
65	10.2	12.0	11.3	8.2	15.3
66	27.3	83.0	48.9	48.9	26.3
Cisplatin	4.8	15.1	2.5	0.3	3.0
Oxaliplatin	8.4	7.3	9.4	2.3	3.6
Carboplatin	79.6	60.6	38.1	46.2	70.7

Raffaella Cincinelli et al. (2013) designed and synthesized camptothecin-linked platinum anticancer agents. Biological activity was tested on different cell lines, including non-small cell lung cancer (H460), osteosarcoma (U2OS), cell carcinoma cells (A431), and ovarian carcinoma (IGROV-1, A2780). These compounds showed growth inhibitory activity against a panel of human tumor cell lines, including sublines resistant to topotecan and

platinum compounds. A general reduced potency with respect to TPT was observed in ovarian carcinoma IGROV-1 and A2780 cell lines. The structure of camptothecin-linked platinum anticancer hybrids is given in Figure 66 and the in vitro cytotoxic activities of hybrid compounds (67–69) are listed in Table 53 [133].

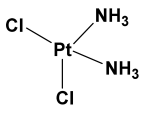
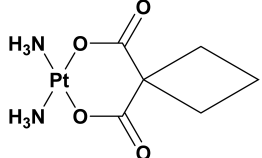
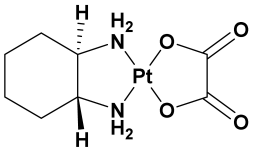
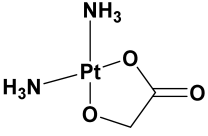
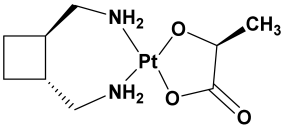
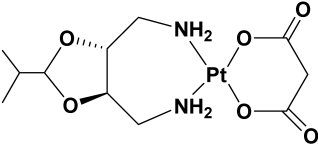
Table 53. In vitro cytotoxic activities of camptothecin-linked platinum hybrid compounds (67–69).

Compound No.	H460 (μM)	U20S (μM)	A431 (μM)	IGROV-1 (μM)	A2780 (μM)
67	1.37	0.48	0.075	1.03	0.036
68	0.4	1.09	0.185	1.24	0.22
69	0.44	1.36	0.28	2.24	0.08
Topotecan (TPT)	1.37	0.48	0.075	1.03	0.036
cDDP	22	20.5	19.57	14.8	4.35

Platinum Based Drugs That Are FDA Approved or under Clinical Trial

Different platinum-based potent anticancer drugs their chemical structure, specific cancer types and current status are shown in Table 54.

Table 54. Platinum-based anticancer drugs with chemical structure, specific cancer types and current status.

Compound Name	Chemical Structure	Type of Cancer	Status	References
Cisplatin		solid neoplasms, including ovarian, testicular, bladder, colorectal, lung and head and neck cancers	FDA-approved	[134]
Carboplatin		Retinoblastoma Lung cancer	FDA-approved	[134]
Oxaliplatin		Medulloblastoma Non-small cell lung cancer	FDA-approved	[134]
Nedaplatin		solid neoplasms, including ovarian, testicular	FDA-approved	[134]
Lobaplatin		metastatic breast cancer, chronic myelogenous leukemia and SCLC	Regional approval CHINA	[135]
Heptaplatin		gastric cancer	Regional approval (Republic of Korea)	[135]

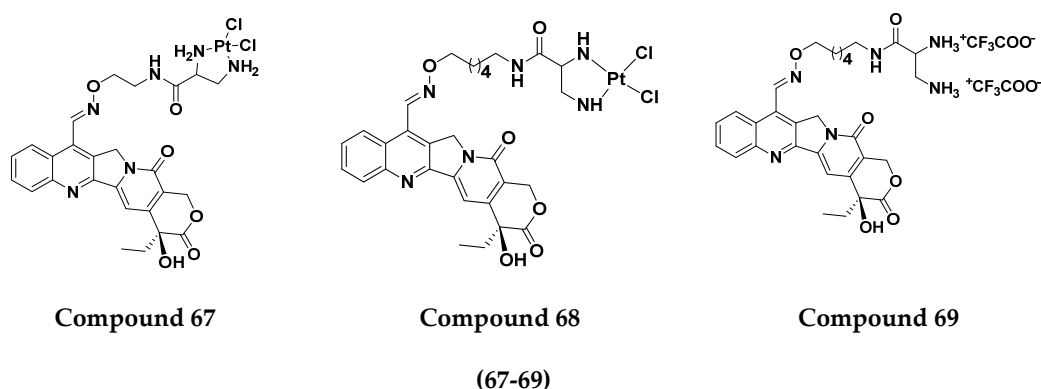


Figure 66. Structure of Camptothecin-linked platinum hybrid derivatives (67–69).

3.11. Hydroxamic Acid Hybrids

Xing Yan et al. (2016) synthesized hybrids of hydroxamic acid with artemisinin and evaluated their anticancer activity against different cell lines. Most of the synthesized compounds showed potent anticancer activity. Among them, compound **70(a)** exhibited excellent activity against various cell lines including HepG2, MCF-7 and HL-60 (human leukemia cell) with IC_{50} values of 2.50, 2.62, and 1.28 μM , respectively, and control suberoylanilide hydroxamic acid (SAHA) IC_{50} values of 0.31, 1.90, and 0.18 μM , respectively. Furthermore, they synthesized 14 compounds. Amongst them, only two compounds **70(a)**, and **70(b)**, showed excellent HDAC (histone deacetylases) selectivity with IC_{50} values of 29.31 and 22.7 μM , respectively. The structure of a hydroxamic acid artemisinin hybrid is shown in Figure 67 and the in vitro cytotoxic activities of hybrid compounds **70(a–c)** are listed in Table 55 [136].

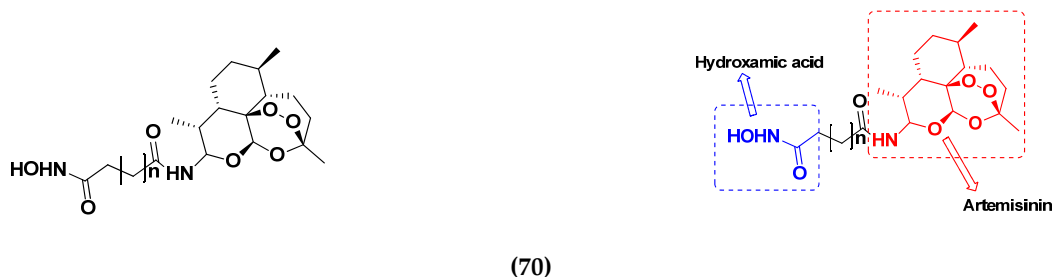


Figure 67. Structure of hydroxamic acid with artemisinin hybrid derivatives (70).

Table 55. In vitro cytotoxic activities of hydroxamic acid with artemisinin hybrid compounds **70(a–c)**.

Compound No.	n	HDAC Inhibiting	Cytotoxicity (μM)		
			HepG2	MCF-2	HC-60
70a	$(-\text{CH}_2)_6$	2.50	2.50	2.62	1.28
70b	$(-\text{CH}_2)_2$	14.17	14.17	10.98	6.41
70c	$(-\text{CH}_2)_3$	>125	84.80	71.64	21.84
SAHA	-	0.35	0.31	1.90	0.18

Yong Ling et al. (2018) synthesized hydroxamate- β -carboline based novel hybrids and evaluated their antiproliferative activity against different cell lines. Most of the synthesized compounds displayed potent anticancer activity. Among them, compound **71(a)** exhibited potent activity against panel of cell lines including HCT116 (human colon cancer cell), SUMM-7721 (human hepatocellular carcinoma cells), HepG2, MCF-7 and Huh-7 (human hepatocellular carcinoma cells) with IC_{50} values of 0.82, 1.06, 0.65, 2.25 and 1.52 μM , respectively, and control SAHA IC_{50} values of 5.53, 5.61, 6.27, 4.48 and 4.95 μM , respectively.

The structure of novel hydroxamate- β -carboline based derivatives is given in Figure 68 and the in vitro cytotoxic activities of hybrid compounds 71(a–d) are listed in Table 56 [137].

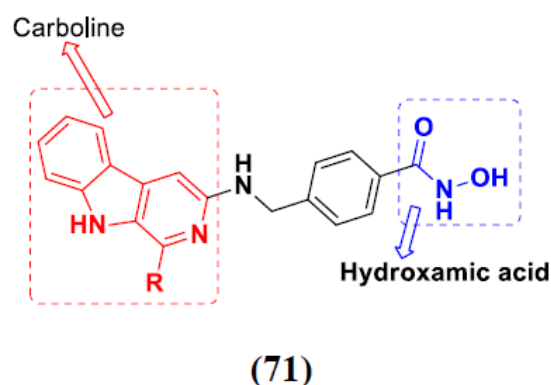


Figure 68. Structure of hydroxamate- β -carboline based hybrid derivatives (71).

Table 56. In vitro cytotoxic activities of hydroxamate- β -carboline based hybrid compounds 71(a–d).

Compounds No.	R	In Vitro Antiproliferative Activity (IC ₅₀ μ M)				
		HCT116	SUMM-7721	HepG2	Mcf-7	Huh-7
71a	3,4,5 (MeO) ₃ -Ph	0.82	1.06	0.65	2.25	1.52
71b	3-MeO-Ph	0.89	1.22	1.02	2.18	1.52
71c	4-Me-Ph	0.78	0.84	0.53	1.56	0.96
71d	4-NO ₂ -Ph	1.41	2.61	1.51	4.03	2.78
SAHA	-	5.53	5.61	6.26	4.48	4.95

M.F.A. Mohamed et al. (2017) synthesized hybrids of hydroxamic acid and chalcone derivatives and evaluate their antiproliferative activity against different cell lines. Most of the synthesized compounds displayed potent anticancer activity. Among them, 72(a) exhibited potent activity against cancer cell lines including HEPG2, MCF-7 and HcF-116 (human colon cancer cell), having IC₅₀ values of 0.62, 2.05 and 2.92 μ M, respectively and control, SAHA having IC₅₀ values of 3.33, 2.18 and 1.23, respectively. The structure of hydroxamic acid based chalcone derivatives is given in Figure 69 and the in vitro cytotoxic activities of hybrid compounds 72(a–d) are listed in Table 57 [138].

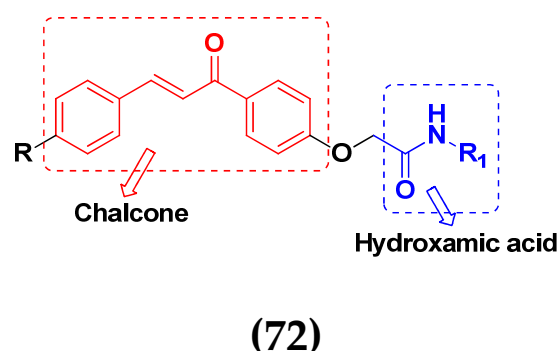
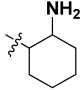


Figure 69. Structure of hydroxamic acid based chalcone derivatives (72).

Chao ding et al. (2017) synthesized and investigated novel 6-(1,2,3-triazol-4-yl) 4-aminoquinazolin derivatives possessing a hydroxamic acid moiety for antiproliferative activity against two cell lines. Most of the synthesized compounds displayed potent anticancer activity. Among them, 73(a) exhibited potent activity against cell lines including

A549 and BT-474 (human breast cancer cells) with IC_{50} values of 0.51 and 3.63 μM , respectively. Controls were lapatinib (IC_{50} : 1.740.28 and 0.100.02) and SAHA (IC_{50} : 2.57 and 2.67). The structure of hydroxamic acid based 4-aminoquinazolin derivatives is given in Figure 70 and the in vitro cytotoxic activities of hybrid compounds 73(a–d) (IC_{50} , μM) are listed in Table 58 [139].

Table 57. In vitro cytotoxic activities of hydroxamic acid based chalcone hybrid compounds 72(a–d).

Compound No.	R	R ₁	Antiproliferative Activity (IC_{50} μM)		
			HeptG2	MCF-7	HCF-116
72a	4-OH ₃	OH	0.620.04	2.050.48	2.920.52
72b	H	OH	3.550.77	2.210.44	2.180.33
72c	4-F	OH	8.721.65	3.200.82	6.741.59
72d	4-OCH ₃		7.172.01	12.992.99	3.020.81
SAHA	-	-	3.330.74	2.180.35	1.230.08

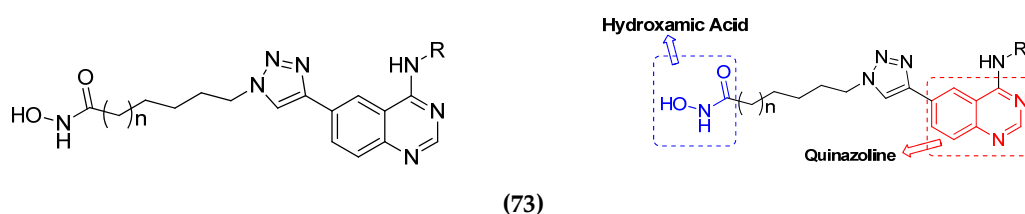
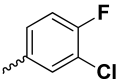
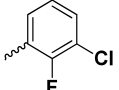
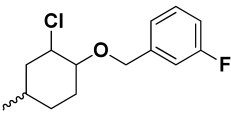
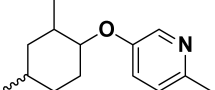


Figure 70. Structure of hydroxamic acid based 4-aminoquinazolin derivatives (73).

Table 58. In vitro cytotoxic activities of hydroxamic acid based 4-aminoquinazolin hybrid compounds 73(a–d).

Compound No.	R	n	Antiproliferative Activity (IC_{50} μM)	
			A549	BT-474
73a		1	0.51	3.63
73b		2	0.63	3.88
73c		2	3.68	2.24
73d		1	8.46	14.65
Lapatinib	-	-	1.74	0.10
SAHA	-	-	2.57	2.67

D.T.M. Dung et al. (2017) synthesized hybrids of indoline-based N-hydroxy prope- namides and evaluated their antiproliferative activity against different cell lines. Most of the synthesized compounds displayed potent anticancer activity. Among them, compound 74(a) exhibited potent activity against three different cell lines including SW620 (colon cancer), Aspe-1 (prostate cancer) and PC-3 at with IC_{50} values 3.05, 6.83 and 7.30 (μM), respectively with control SAHA having IC_{50} values of 1.44, 7.04, 5.30 (μM), respectively.

The structure of hydroxamic acid based indoline derivatives is given in Figure 71 and the in vitro cytotoxic activities of hybrid compounds 74(a–d) are listed in Table 59 [140].

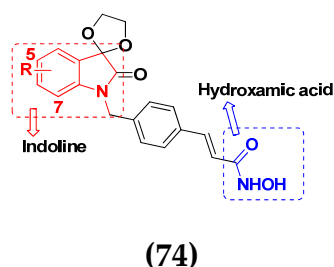


Figure 71. Structure of hydroxamic acid based indoline derivatives (74).

Table 59. In vitro cytotoxic activities of hydroxamic acid based indoline hybrid compounds 74(a–d).

Compound No.	R	Cytotoxicity Cell Line (IC ₅₀ μM)		
		SE620	AsPc-1	PC3
74a	5-Br	3.05	6.83	7.30
74b	5-F	3.30	7.28	11.50
74c	5-Cl	3.42	22.35	17.44
74d	5-CH ₃	3.44	7.47	12.25
SAHA	-	1.44	7.04	5.30

Hydroxamic Acid Based Hybrids That Are FDA Approved or under Clinical Trial

Hydroxamic acid based hybrids that are FDA approved or under clinical trial, and their chemical structure and current status are listed in Table 60.

Table 60. Hydroxamic acid-based hybrid compounds approved or under clinical trials.

Company Name	Compound Name	Drug Structure	Drug Target	Type of Cancer	Status	References
Merck and Co., Inc	Vorinostat (SAHA)		histone deacetylase inhibitor	cutaneous T cell lymphoma	Approved	[141]
Novartis	Panobinostat		non-selective histone deacetylase inhibitor	multiple myeloma	Approved	[142]
4SC AG	Resminostat		histone deacetylase inhibitor	hepatocellular carcinoma	Approved	[143]
Helsinn and MEI Pharma	Pracinostat		histone deacetylase inhibitor	Acute Myeloid Leukemia	Clinical Trial	[144]
Italfarmaco Group's	Givinostat		histone deacetylase inhibitor	chronic lymphocytic leukemia	Clinical Trial	[144]
Xynomic Pharmaceuticals, Inc.	Abexinostat		histone deacetylase inhibitor	Hodgkin's lymphoma	Clinical Trial	[144]

3.12. Ferrocene Hybrids

Quirante et al. (2011) synthesized ferrocene-indole based hybrids (Figure 72) and evaluated their cytotoxic activity against A549 cells using 5-fluorouracil (5-FU) as a positive control. They synthesized 14 molecules, and 12 showed cytotoxic activity at IC₅₀ values

below 100 μM , where 5-FU had an IC_{50} value of $<5 \mu\text{M}$. Among these molecules, ferrocene-indole hybrid **75(a)** showed the strongest cytotoxic activity with an IC_{50} value of $5 \mu\text{M}$. Cytotoxic activities of hybrid compounds **75(a–d)** are listed in Table 61 [145].

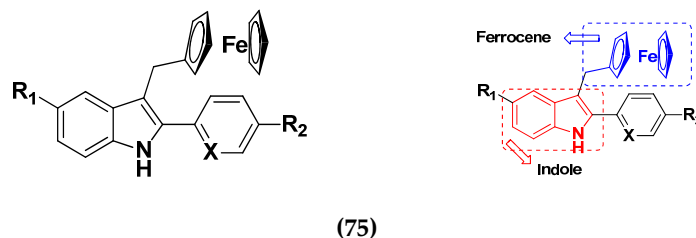


Figure 72. Structure of ferrocene-indole derivatives (75).

Table 61. In vitro cytotoxic activities of ferrocene-indole hybrid compounds **75(a–d)**.

Compounds No.	R ₁	R ₂	X	A549 (μM)
75a	OCH ₃	H	H	5
75b	H	Cl	H	33
75c	Cl	H	N	10
75d	NO ₂	H	H	14
5-Fluorouracil				<5

Xian-Feng Huang et al. (2014) synthesized novel hybrids of ferrocene containing pyrazolyl moieties and evaluated their anti-proliferative activity against different cell lines. Most of the synthesized compounds displayed potent anticancer activity. Among them, compound **76(c)** exhibited potent activity against three different cell lines; A549 (human lung cancer cell), Hep G2 (human liver cancer cell) and MDA-MB-45 (human breast cancer cell) with IC_{50} values of 4.44, 20.82, and 4.89 (μM), respectively. Control 5-Fluoro Uracil had IC_{50} values of 16.2, 17.6, 2.80 and cisplatin 0.87, 0.74 and 1.14, respectively. The structure of ferrocene derivatives containing pyrazolyl moiety is given in Figure 73 and in vitro cytotoxic activities of hybrid compounds **76(a–d)** are listed in Table 62 [146].

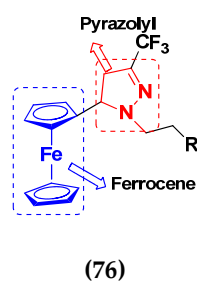
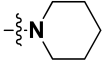

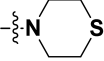
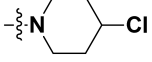
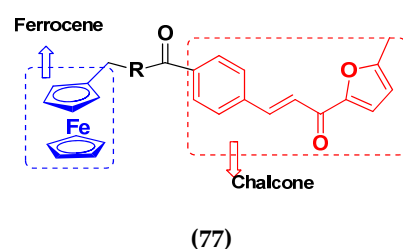


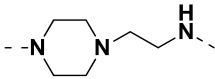
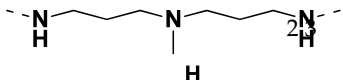
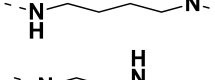
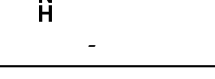
Figure 73. Structure of ferrocene containing a pyrazolyl derivative (76).

Frans J. Smit et al. (2016) synthesized hybrids of ferrocenyl-chalcone amide, and evaluate their antitumor activity against different cell lines. Most of the synthesized compounds displayed potent anticancer activity. Among them, compound **77(a)** exhibited potent activity against three different cell lines, including Tk-10 (renal) UACC-62 (melanoma), and, MCF-7 at IC_{50} 2.4, 3.0 and 2.5 μM , respectively. Control parthenolide (PTD)-had IC_{50} values of 6.4, 15.0 and 5.8, respectively. The structure of ferrocenyl-chalcone amide derivatives are shown in Figure 74 and the in vitro cytotoxic activities of hybrid compounds **77(a–d)** are listed in Table 63 [147].

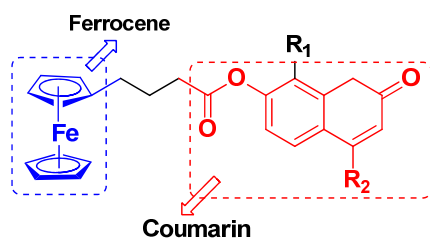
Table 62. In vitro cytotoxic activities of ferrocene containing pyrazolyl hybrid compounds 76(a–d).

Compound No.	R	Antitumor Activity (μM)		
		A549	HepG2	MDA-MB-45
76a		4.47	26.70	4.50
76b		5.31	10.89	5.39
76c		4.44	20.82	4.89
76d		7.93	8.43	6.98
5-FU	-	16.8	17.6	2.80
Cisplatin	-	0.87	0.74	1.14

**Figure 74.** Structure of ferrocenyl-chalcone amide derivative (77).**Table 63.** In vitro cytotoxic activities of ferrocenyl-chalcone amide hybrid compounds 77(a–d).

Compound No.	R	Anticancer Activity IC_{50} (μM)		
		TK-10	UACC-62	MCF-7
77a		2.4	3.0	2.5
77b		2.8	6.0	2.8
77c		2.5	3.0	2.8
77d		2.5	3.5	3.0
PTD	-	6.4	15.0	5.8

J.N. Wei et al. (2019) synthesized novel hybrids of ferrocene-coumarin moiety and evaluate their antiproliferative activity against six different human cancer cell lines. Most of the synthesized compounds displayed potent anticancer activity. Among them, compound 78(a) exhibited potent activity against six different cell lines: BIU-87 (Human Bladder Cancer cell), SGC-790 (human cancer gastric cells), EC9706 and ECa1090 (human esophageal cancer cells), MCF-7 (human breast adenocarcinoma cells) and Jurkat (human leukemia cell) with IC_{50} values 1.09, 10.61, 25.89, 36.38, 12.10 and 53.01 (μM), respectively. Control adriamycin had IC_{50} values of 6.09, 5.44, 8.56, 6.52, 7.95, 4.50 μM , respectively. The structure of ferrocene-coumarin derivatives is given in Figure 75 and the in vitro cytotoxic activities of hybrid compounds 78(a–d) are listed in Table 64 [148].



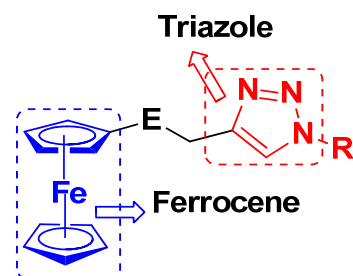
(78)

Figure 75. Structure of ferrocene-coumarin moiety derivative (78).

Table 64. In vitro cytotoxic activities of ferrocene-coumarin hybrid compounds 78(a–d).

Compound No.	Name	Anticancer Activity IC ₅₀ (μM)					
		BIU-87	SGC-7901	EC-9706	ECa-109	MCF-7	Jurkat
78a	4-Methyl-7-hydroxy-8-nitrocoumarin-ferrocene butyrate conjugate	1.09	1.061	25.89	36.38	12.10	53.01
78b	4-Methyl-7-hydroxycoumarin-ferrocene butyrate conjugate	4.48	16.61	41.26	27.97	15.34	54.90
78c	7-Hydroxycoumarin-ferrocene butyrate conjugate	5.24	7.46	82.83	42.47	28.10	55.77
78d	7-Hydroxy-8-nitrocoumarin-ferrocene butyrate conjugate	15.27	19.78	N	40.00	23.91	38.81
Adriamycin	-	6.09	5.44	8.56	6.52	7.90	4.50

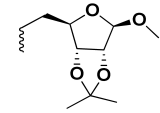
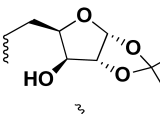
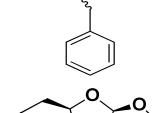
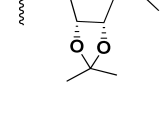
S. Panaka et al. (2016) synthesized hybrids of ferrocenyl chalcogeno (sugar) triazole conjugates and evaluated their antitumor activity against different cell lines. Most of the synthesized compounds displayed potent anticancer activity. Among them, compound 79(a) exhibited potent activity against five different cell lines including A549 (human lung cancer cell), MDA-MB-231 (human breast cancer cell), MCF-7 (human breast adenocarcinoma cell), HeLa (immortal human cell) and HEK-293T (normal non-tumorigenic human embryonic kidney) at IC₅₀ values 2.9, 3.35, 5.58 and 11.6 (μM), respectively. A control, doxorubicin, had IC₅₀ values of 0.36, 0.47, 0.98 and 0.89, respectively. The structure of ferrocenyl-chalcogeno (sugar) triazole conjugates is given in Figure 76 and the in vitro cytotoxic activities of hybrid compounds 79(a–d) (IC₅₀, μM) are listed in Table 65 [149].



(79)

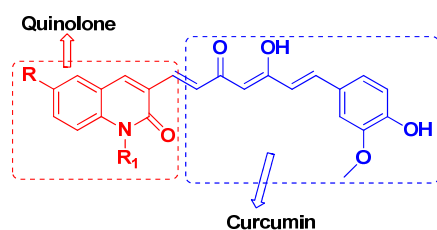
Figure 76. Structure of ferrocene-chalcogeno (sugar) triazole conjugate derivatives (79).

Table 65. In vitro cytotoxic activities of ferrocene-chalcogeno (sugar) triazole conjugate compounds 79(a–d).

Compound No.	E	R	Anticancer Activity IC ₅₀ (μM)				
			A549	MDA-MB-231	MCF-7	HeLa	HEK-293T
79a	Se (Selenium)		2.9	3.35	5.85	11.6	-
79b	Se (Selenium)		3.71	>200	>200	18.3	-
79c	S (Sulphur)		11.6	>200	>200	14.8	-
79d	S (Sulphur)		>200	9.7	>200	>200	-
Doxorubicin			0.39	0.47	0.98	0.89	-

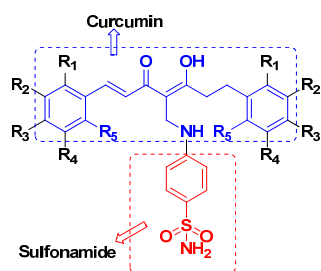
3.13. Curcumin-Based Hybrids

Saiharish Raghavan et al. (2015) synthesized hybrids of curcumin and quinolone and evaluated their anticancer activity against different cell lines. Most of the synthesized compounds displayed potent anticancer activity. Among them, compound **80(a)** exhibited potent activity against four different cell lines including A549 (human lung cancer cell), MCF-7 (human breast adenocarcinoma cell), SKOV3 (ovarian cancer cell line) and H460 (human lung cancer cell) at IC₅₀ values 23.9, 36.2, 12.8, 21.75, respectively. The structure of curcumin-quinolone derivatives is given in Figure 77 and in vitro cytotoxic activities of hybrid compounds **80(a–d)** are listed in Table 66 [150].

**(80)****Figure 77.** Structure of curcumin-quinolone derivatives (**80**).**Table 66.** In vitro cytotoxic activities of curcumin-quinolone hybrid compounds **80(a–d)**.

Compound No.	R	R ₁	Anticancer Activity IC ₅₀ (μM)			
			A549	MCF-9	SKOV3	H460
80a	-CH ₃	$\begin{matrix} \text{H}_2 \\ \\ -\text{C} \cdot \text{C} \equiv \text{CH} \end{matrix}$	23.9	36.2	12.8	21.75
80b	-H	$\begin{matrix} \text{H}_2 \\ \\ -\text{C} \cdot \text{C} \equiv \text{CH} \end{matrix}$	21.3	151.56	19	25.4
80c	-OCH ₃	$\begin{matrix} \text{H}_2 \\ \\ -\text{C} \cdot \text{C} \equiv \text{CH} \end{matrix}$	20.6	>100	14.04	38.14
80d	-F	$\begin{matrix} \text{H}_2 \\ \\ -\text{C} \cdot \text{C} \equiv \text{CH} \end{matrix}$	40.45	25.0	>100	44.3

G. Banupriya et al. (2018) synthesized hybrids of curcumin and sulfonamides and evaluated their anticancer activity against two cell lines. Most of the synthesized compounds displayed potent anticancer activity. Among them, compound **81(a)** exhibited potent activity against two different cell lines including A549 (human lung cancer cell) and AGS (human gastric adenocarcinoma cell) at IC_{50} values 1.29 and 10.16 (μM), respectively with control Curcumin at IC_{50} values 25.33 and 20.76, respectively. The structure of curcumin-sulfonamide derivatives is given in Figure 78 and in vitro cytotoxic activities of hybrid compounds **81(a–d)** are listed in Table 67 [151].



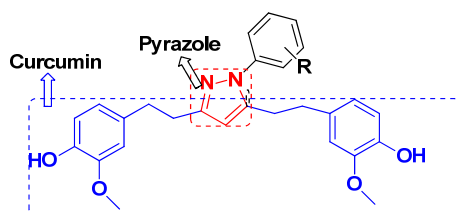
(81)

Figure 78. Structure of curcumin-sulfonamide derivatives (81).

Table 67. In vitro cytotoxic activities of curcumin-sulfonamide hybrid compounds **81(a–d)**.

Compound No.	R_1	R_2	R_3	R_4	R_5	Anticancer Activity IC_{50} (μM)	
						A549	AGS
81a	H	OMe	OH	H	H	1.29	10.16
81b	H	H	Me	H	H	6.25	11.94
81c	H	H	Cl	H	H	12.56	22.31
Curcumin	-	-	-	-	-	25.33	20.76

H.R. Puneeth et al. (2016) synthesized hybrids of curcumin-pyrazole and evaluated their anticancer activity against different cell lines. Most of the synthesized compounds displayed potent anticancer activity. Among them, compound **82(a)** exhibited potent activity against four different cell lines including HeLa (human cervical cell), MCF-7 (human breast adenocarcinoma cell), K562 (human immortalized myelogenous leukemia cell) and HEK293T (normal non-tumorigenic human embryonic kidney) at IC_{50} values 45.54, 34.99, 25.55 and >1000 (μM), respectively with control Paclitaxel at IC_{50} values 11.61, 9.12, 8.43 and 1.43 (μM), respectively. The structure of curcumin-pyrazole derivatives is given in Figure 79 and in vitro cytotoxic activities of hybrid compounds **82(a–c)** (IC_{50} , μM) are listed in Table 68 [152].



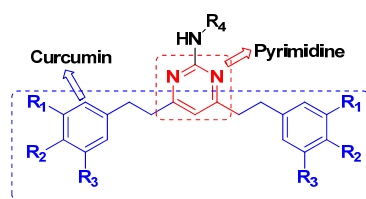
(82)

Figure 79. Structure of curcumin-pyrazole derivative (82).

Table 68. In vitro cytotoxic activities of curcumin-pyrazole hybrid compounds 82(a–c).

Compound No.	R	Anticancer Activity IC ₅₀ (μM)			
		HeLa	MCF-7	K562	HEK293K
82a	o-Cl	45.56	34.99	25.55	>1000
82b	H	42.56	52.88	36.99	NT
82c	o, p-diNO ₂	56.45	43.60	42.35	NT
Paclitaxel	-	0.0061	0.0053	0.0049	NT

Peiju Qui et al. (2013) synthesized hybrids of curcumin, pyrimidine and urea and evaluated their anticancer activity against different cell lines. Most of the synthesized compounds displayed potent anticancer activity. Among them, compound 83(a) exhibited potent activity against two different cell lines including HT29 (human colon adenocarcinoma cell) and HCT116 (human colon cancer cell) at IC₅₀ values 7.10.4 and 6.21.2 (μM), respectively with control 5-fluorouracil at IC₅₀ 11.61, 9.12, 8.43 and 1.43 (μM), respectively. The structure of curcumin pyrimidine derivatives is given in Figure 80 and in vitro cytotoxic activities of hybrid compounds 83(a–c) (IC₅₀, μM) are listed in Table 69 [153].

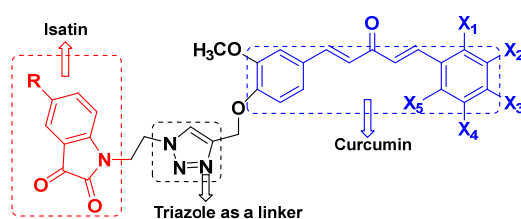


(83)

Figure 80. Structure of curcumin-pyrimidine derivatives (83).**Table 69.** In vitro cytotoxic activities of curcumin-pyrimidine hybrid compounds 83(a–c).

Compound No.	R ₁	R ₂	R ₃	R ₄	Anticancer Activity IC ₅₀ (μM)	
					HT29	HCT116
83a	OCH ₃	OCH ₃	H	CH ₂ CH ₂ OH	7.10.4	6.21.2
83b	OCH ₃	OCH ₃	H	CH ₂ (CH ₂) ₂ OH	12.81.9	9.96.9
83c	OCH ₃	OCH ₃	H	CH ₂ CH ₃	38.525.4	46.423.6

Sahil Sharma et al. (2015) synthesized hybrids of curcumin and isatin and evaluated their anticancer activity against different cell lines. Most of the synthesized compounds displayed potent anticancer activity. Among them, compound 84(a) exhibited potent activity against four different cell lines including THP-1 (Leukemia), COLO-205 (Colon), HCT-(116) and PC-3 (Prostate) at IC₅₀ values of 2.87, 4.15, 1.12 and 5.67 (μM), respectively. The structure of curcumin-isatin derivatives is given in Figure 81 and in vitro cytotoxic activities of hybrid compounds 84(a–c) are listed in Table 70 [154].



(84)

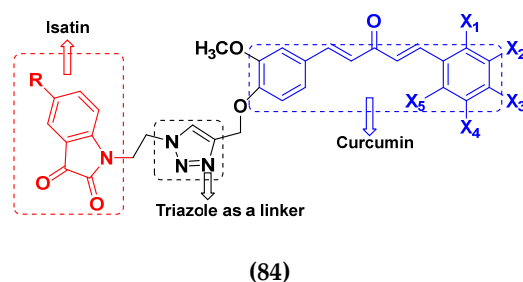
Figure 81. Structure of curcumin-isatin derivatives (84).

Table 70. In vitro cytotoxic activities of curcumin-isatin hybrid compounds **84(a–c)**.

Compound No.	X ₁	X ₂	X ₃	X ₄	X ₅	R	Anticancer Activity IC ₅₀ (μM)			
							THP-1	CoLo-205	HCT-116	PC-3
84a	H	OCH ₃	OCH ₃	OCH ₃	H	H	2.87	4.15	1.12	5.67
84b	H	OCH ₃	OCH ₃	H	H	H	4.31	5.78	2.92	6.44
84c	H	H	OCH ₃	H	H	H	4.96	6.72	3.45	8.95

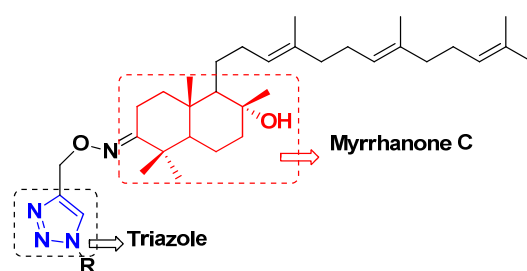
3.14. Triazole-Based Hybrids

Li Ying et al. (2015) synthesized hybrids of triazole, pyrimidine and urea and evaluated their anticancer activity against different cell lines. Most of the synthesized compounds displayed potent anticancer activity. Among them, compound **85(a)** exhibited potent activity against four different cell lines including EC-109 (squamous cell carcinoma cells), MCF-7 (human breast adenocarcinoma cells), MGC-803 (immortal human cells) and B16-F10 (murine melanoma cells) at IC₅₀ 2.96, 3.11, 3.60 and 4.55 (μM), respectively and with control 5-fluorouracil an IC₅₀ of 11.61, 9.12, 8.43 and 1.43 (μM), respectively. The structure of triazole-pyrimidine derivatives is given in Figure 82 and in vitro cytotoxic activities of hybrid compounds **85(a–d)** are listed in Table 71 [155].

**Figure 82.** Structure of triazole-pyrimidine derivatives (**85**).**Table 71.** In vitro cytotoxic activities of triazole-pyrimidine hybrid compounds **85(a–d)**.

Compound No.	R ₁	R ₂	Anticancer Activity IC ₅₀ (μM)			
			EC-109	MCF-7	MGC-803	B16-F10
85a	m-CF ₃	p-Br	2.96	3.11	3.60	4.55
85b	m-CF ₃	7-CH ₃	32.29	6.12	7.58	9.58
85c	m-CF ₃	m,p,m-Tri-OCH ₃	>64	8.14	8.21	24.43
85d	m-CF ₃	p-CH(CH ₃) ₂	24.22	8.62	>64	1.70
5-FU	-	-	11.61	9.12	8.43	1.43

Madasu Chandrashekhar et al. (2016) synthesized hybrids of triazole–myrrhanore Cand evaluated their anticancer activity against different cell lines. Most of synthesized compounds displayed potent anticancer activity. Among them, compound **86(a)** exhibited good anticancer activity against different cell lines including A549 (human lung cancer cell), Hela (human cervical cell), MCF-7 (human breast adenocarcinoma cell), DU-I45 (human prostate cancer cell) and HepG2 (human hepatocellular carcinoma cell) at IC₅₀ 06.16, 07.76, 09.59, 08.83 and 09.52 (μM), respectively, with control doxorubicin 2.81, 2.57, 1.13, 1.41 and 3.01 (μM), respectively. The structure of triazole–myrrhanore C derivatives is given in Figure 83 and in vitro cytotoxic activities of hybrid compounds **86(a–c)** (IC₅₀, μM) are listed in Table 72 [156].



(86)

Figure 83. Structure of triazole–myrrhanore C derivatives (86).

Table 72. In vitro cytotoxic activities of triazole –myrrhanore C hybrid compounds 86(a–c).

Compound No.	R	Anticancer Activity IC ₅₀ (μM)				
		A549	Hela	MCF-7	DU-I45	HepG2
86a		06.16	07.76	09.59	08.83	09.52
86b		08.12	12.83	14.66	11.14	14.08
86c		11.22	22.96	16.59	16.37	34.87
Doxorubicin	-	2.81	2.57	1.13	1.41	3.01

Zahra Najafi et al. (2015) synthesized hybrids of triazole and isoxazole and evaluated their anticancer activity against different cell lines. Most of the synthesized compounds displayed potent anticancer activity. Among them, compound 87(a) exhibited potent activity against two different cell lines including MCF-7 and T47D (breast cancer cell line) at IC₅₀ > 100 and 27.7 μM, respectively with control etoposide at IC₅₀ 7.5 and 7.9, respectively (μM). The structure of triazole-isoxazole derivatives is given in Figure 84 and in vitro cytotoxic activities of hybrid compounds 87(a–b) (IC₅₀, μM) are listed in Table 73 [157].

Table 73. In vitro cytotoxic activities of triazole-isoxazole hybrid compounds 87(a–c).

Compound No.	Ar ₁	Ar ₂	Cytotoxic Activity IC ₅₀ (μM)	
			MCF-7	T47D
87a	Ph		>100	27.7 ± 0.1
87b	Ph		85.7 ± 4.5	>100
Etoposide	-	-	7.5 ± 0.32	7.9 ± 0.45

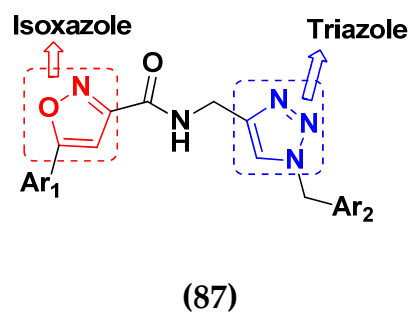


Figure 84. Structure of triazole-isoxazole derivatives (87).

Y.C. Duan et al. (2013) synthesized hybrids of 1,2,3-triazole and dithiocarbamate and evaluated their anticancer activity against different cell lines. Most of the synthesized compounds displayed potent anticancer activity. Among them, compound **88(a)** exhibited potent activity against four different cell lines including MGC-803 (immortal human cell), MCF-7 (human breast adenocarcinoma cells), PC-3 (human pancreatic cancer cell) and EC-109 (squamous cell carcinoma cell) at IC_{50} 0.73, 5.67, 11.61 and 2.44 μ M, respectively with control 5-fluorouracil at IC_{50} 7.01, 7.54, 27.07 and 3.34 μ M, respectively. The structure of triazole-dithiocarbamate derivatives is shown in Figure 85 and in vitro cytotoxic activities of hybrid compounds **88(a–c)** (IC_{50} , μ M) are listed in Table 74 [158].

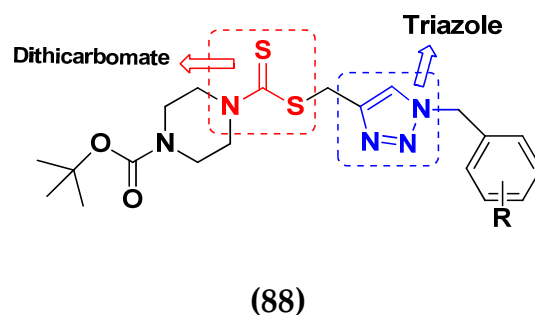


Figure 85. Structure of triazole-dithiocarbamate derivatives (88).

Table 74. In vitro cytotoxic activities of triazole-dithiocarbamate hybrid compounds **88(a–c)**.

Compound No.	R	Anticancer Activity IC_{50} (μ M)			
		MGC-803	MCF-7	PC-3	EC-109
88a	o-F	0.73	5.67	11.61	2.44
88b	o-Cl	0.49	6.09	12.45	11.93
5-FU	-	7.01	7.54	27.07	3.3

R.M. Kumbhare et al. (2015) synthesized hybrids of triazole thiazole and evaluated their anticancer activity against different cell lines. Most of the synthesized compounds displayed potent anticancer activity. Among them, compound **89(a)** exhibited potent activity against four different cell lines including MCF-7 (human breast cancer), A549 (human lung cancer), A375 (human melanoma cancer), and MCF-10A (normal breast epithelial cells) with IC_{50} values of 2.12, 5.48, 4.7 and 29.33 μ M, respectively. Control doxorubicin had comparative IC_{50} 0.12, 3.13, 7.2 and 24.0 μ M and paclitaxel at IC_{50} 2.58, 4.9, 8.0, 38.0 μ M, respectively. The structure of triazole based thiazole derivatives is given in Figure 86 and in vitro cytotoxic activities of hybrid compounds **89(a–c)** are listed in Table 75 [159].

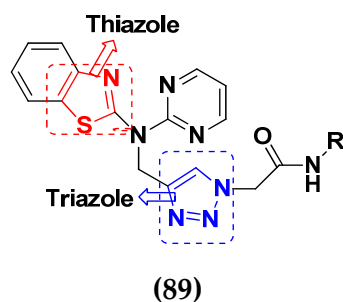


Figure 86. Structure of triazole-thiazole derivative (89).

Table 75. In vitro cytotoxic activities of triazole-thiazole hybrid compounds 89(a–c).

Compound No.	R	Anticancer Activity IC ₅₀ (μM)			
		MCF-7	A549	A375	MCF-10A
89a	5-(CF ₃)-1,2,4-thiadiazole	2.12	5.48	4.7	29.33
89b	4,5-CF ₃ C ₆ H ₄	2.52	4.97	4.67	2.5
89c	2,4-FC ₆ H ₃	3.0	4.45	6.02	2.2
Doxorubicin	-	0.12	3.13	7.2	24.0
Paclitaxel	-	2.58	4.9	8.0	38.0

3.15. Benzimidazole-Based Hybrids

R. Sivaramakarthiskeyan et al. (2020) synthesized hybrids of benzimidazole and pyrazole and evaluated their anticancer activity against different cell lines. Most of the synthesized compounds displayed potent anticancer activity. Among them, compound 90(a) exhibited potent activity against three different cell lines including SW1990 (human pancreatic adenocarcinoma cell), AsPC1 (human pancreatic tumor cell), MRCS (marginal reticular cells) with IC₅₀ values of 30.9, 32.8, 80.0 μM, respectively and control gemcitabine at IC₅₀ values of 35.09, 39.27 and 54.17 μM, respectively. The structure of benzimidazole-pyrazole derivatives is given in Figure 87 and in vitro cytotoxic activities of hybrid compounds 90(a–c) (IC₅₀, μM) are listed in Table 76 [160].

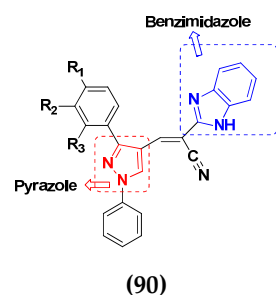


Figure 87. Structure of benzimidazole-pyrazole derivatives (90).

Table 76. In vitro cytotoxic activities of benzimidazole-pyrazole hybrid compounds 90(a–b).

Compound No.	R ₁	R ₂	R ₃	Anticancer Activity IC ₅₀ (μM)		
				SW1990	AsPC1	MRCS
90a	F	H	H	30.9	32.8	80.0
90b	o-Me	H	H	57.6	62.4	>100
Gemcitabine	-	-	-	35.09	39.27	54.17

Kun Pena Shao et al. (2014) synthesized hybrids of benzimidazole–pyrimidine and evaluated their anticancer activity against different cell lines. Most of the synthesized compounds displayed potent anticancer activity. Among them, compound 91a exhibited potent

activity against three different cell lines including MCF-7 (human breast adenocarcinoma cells), MGC-803 (immortal human cells), EC-9706 (esophagus squamous cell carcinoma) and SMMC-7721 (human hepatocellular carcinoma cells) with IC_{50} values of 1.43, 1.33, 3.33, 20.50 (μM), respectively with control 5-Fluorouracil had IC_{50} values 7.12, 3.45, 8.07 and 15.08 (μM), respectively. The structure of benzimidazole-pyrimidine derivatives is given in Figure 88 and in vitro cytotoxic activities of hybrid compounds 91(a–c) (IC_{50} , μM) are listed in Table 77 [161].

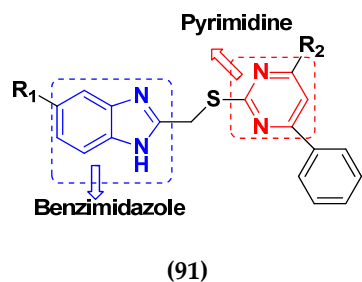


Figure 88. Structure of benzimidazole-pyrimidine derivatives (91).

Table 77. In vitro cytotoxic activities of benzimidazole-pyrimidine hybrid compounds 91(a–c).

Compound No.	R_1	R_2	Anticancer Activity IC_{50} (μM)			
			MCF-7	MGC-803	EC-9706	SMMC-7721
91a	H	4- CH_3 - C_6H_5 -NH-	1.43	1.33	3.33	20.50
91b	H	4- CH_3O - C_6H_5 -NH-	2.90	2.03	5.83	10.55
91c	H	4-F- C_6H_5 -NH-	4.24	2.30	8.55	22.58
5-FU	-	-	7.12	3.45	8.07	15.08

Pankaj Sharma et al. (2016) synthesized hybrids of benzimidazole and thiazolidinedione and evaluated their anticancer activity against different cell lines. Most of the synthesized compounds displayed potent anticancer activity. Among them, compound 92a exhibited potent activity against five different cell lines including PC-3, DU-145 (prostate cancer), MDA MB-231 (breast cancer), A549 (lung cancer) and MCF10A (normal breast epithelial cells) with IC_{50} values of 39.87, 31.41, 29.18, 11.46 and >100 (μM), respectively with control 5-Fluorouracil had IC_{50} values of 45.32, 40.58, 35.98, 30.47 (μM), respectively. The structure of benzimidazole-pyrimidine derivatives is given in Figure 89 and in vitro cytotoxic activities of hybrid compounds 92(a–c) are listed in Table 78 [162].

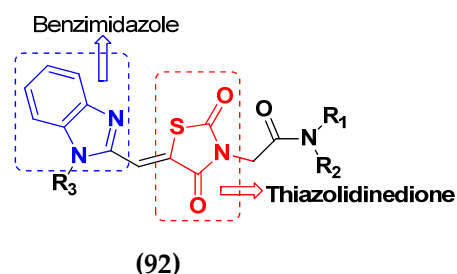
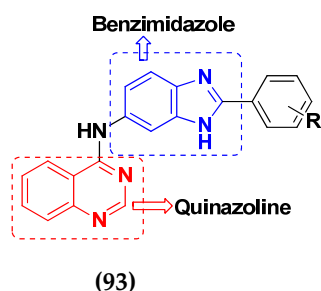


Figure 89. Structure of benzimidazole–thiazolidinedione derivatives (92).

Table 78. In vitro cytotoxic activities of benzimidazole–thiazolidinedione hybrid compounds **92(a–c)**.

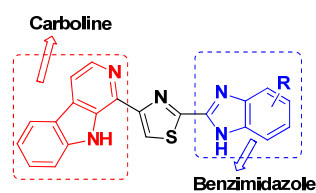
Compound No.	NR ₁ R ₂	R ₃	Anticancer Activity IC ₅₀ (μM)				
			PC-3	DU-145	MDA MB-231	A549	MCF10A
92a	R ₁ = H, R ₂ = 4-phenylthiazol 6,7-dimethoxy-	Methyl	39.87	31.41	29.18	11.46	>100
92b	1,2,3,4-tetrahydroisoquinoline 6,7-dimethoxy-	Ethyl	33.54	>50	>50	29.40	—
92c	1,2,3,4-tetrahydroisoquinoline	Methyl	41.10	37.32	36.03	13.35	>100
5-FU	-	-	45.32	40.58	35.98	30.47	-

Lei Shi et al. (2014) synthesized benzimidazole-quinazoline hybrids and evaluated their anticancer activity against different cell lines. Most of the synthesized compounds displayed potent anticancer activity. Among them, compound **93a** exhibited potent activity against two different cell lines including Hep-G2 (human liver carcinoma cells) and MCF-7 (human breast adenocarcinoma cell) at IC₅₀ 8.7 and 1.5 (μM), respectively. Control galvatinib had IC₅₀ values of 65.5 and 49.6 μM, respectively. The structure of benzimidazole-quinazoline derivatives is given in Figure 90 and in vitro cytotoxic activities of hybrid compounds **93(a–c)** are listed in Table 79 [163].

**Figure 90.** Structure of benzimidazole-quinazoline derivatives (**93**).**Table 79.** In vitro cytotoxic activities of benzimidazole-quinazoline hybrid compounds **93(a–c)**.

Compound No.	R	Proliferative Inhibition IC ₅₀ (μM)	
		Hep-G2	MCF-7
93a	4-F	8.7	12.6
93b	4-Cl	15.8	3.6
93c	4-Br	24.7	8.3
Galvatinib	-	65.5	49.6

Reddymasu Sireesha et al. (2021) synthesized hybrids of benzimidazole and β-carboline and evaluated their anticancer activity against different cell lines. Most of the synthesized compounds displayed potent anticancer activity. Among them, compound **94a** exhibited potent activity against four different cell lines, including MCF-7 (human breast cancer cell line), A549 (a human lung cancer cell line), Colo-205 (a human colon cancer cell line) and A2780 (a human ovarian cancer cell line) with IC₅₀ values of 0.22, 1.55, 1.68 and 1.16 (μM), respectively, with the control etoposide having IC₅₀ values of 2.11, 3.08, 0.13 and 1.31 (μM), respectively. The structure of benzimidazole–β-carboline derivatives is given in Figure 91 and in vitro cytotoxic activities of hybrid compounds **94(a–c)** are listed in Table 80 [164].



(94)

Figure 91. Structure of benzimidazole-β-Carboline derivatives (94).**Table 80.** In vitro cytotoxic activities of benzimidazole-β-Carboline hybrid compounds 94(a–c).

Compound No.	R	Cytotoxicity of Compound IC ₅₀ (μM)			
		MCF-7	A549	Colo-205	A2780
94a	5,6-dicyano	0.220	1.550	1.680	1.160
94b	5,6-dimethoxy	0.0920	0.720	0.340	1.230
94c	5,6-dimethyl	0.810	1.900	0.410	1.800
Etoposide	-	2.110	3.080	0.130	1.310

Benzimidazole Based Hybrids That Are FDA Approved or under Clinical Trials

Benzimidazole based hybrids that are FDA approved/under clinical trials and their current status are given in Table 81.

Table 81. Current status of benzimidazole based hybrids that are approved or under clinical trials.

Company Name	Compound Name	Drug Structure	Drug Target	Type of Cancer	Status	Reference
Eli Lilly and Company	Abemaciclib		cyclin dependent kinase-4 (CDK4) and CDK6 inhibitor	negative metastatic breast cancer	Approved	[165]
AbbVie	Veliparib		PARP inhibitor	ovarian cancer	Clinical Trial	[166]
Allarity Therapeutics	Dovitinib		pan tyrosine kinase inhibitor	prostate cancer	Clinical Trial	[167]
Novartis	Nazartinib		EGFR kinase inhibitor	non-small cell lung cancer	Clinical Trial	[168]

3.16. Isatin Containing Hybrids

In humans and other mammals, isatin is an endogenous compound that has a variety of pharmacological properties, including anticancer activity [169]. Human health is facing several difficulties in the modern medical period, especially with regard to human cancers. As a result, new therapies that selectively target tumor cells will unavoidably be added to the therapeutic arsenal for these cancers [170].

AZIZ et al. (2021) synthesized different sets of isatin-based benzoazine hybrids, i.e., isatin quinoxaline quinazoline and phthalazines hybrids. All the synthesized hybrids were evaluated in vitro for their antiproliferative activity against three human cancer cell lines, namely breast cancer (ZR-75), human colon cancer (HT-29) and lung cancer (A-549). The

structure of isatin-based benzoazine derivatives is given in Figure 92 and in vitro cytotoxic activities of hybrid compounds 95(a–c) are listed in Table 82 [171].

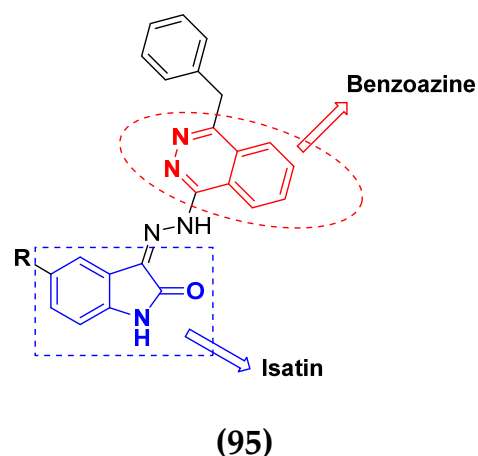


Figure 92. Structure of isatin-based benzoazine derivatives (95).

Table 82. In vitro cytotoxic activities of isatin-based benzoazine hybrid compounds 95(a–c).

Compound No.	R	ZR-75(μM)	HT-29 (μM)	A-549 (μM)	Average IC ₅₀ (μM)
95a	H	13.25	6.69	7.19	9.04
95b	F	5.9	5.31	5.39	5.53
95c	Cl	7.77	6.23	7.02	7.01
Sunitinib		8.31	10.14	5.87	8.11

Meleddu et al. (2017) synthesized isatin-dihydropyrazole derivatives and then evaluated their capability to inhibit tumor cell growth against nine human cancer cell lines, namely A549 (lung carcinoma), IGR39 (melanoma), U87 (glioblastoma), MDA-MB-231 (breast cancer), MCF-7 (breast adenocarcinoma), and BT474 (invasive ductal carcinoma), H1299 (non-small cell lung carcinoma), BxPC-3 (pancreatic adenocarcinoma), SKOV-3 (ovarian cancer) and human foreskin fibroblasts. Sunitinib was the standard drug taken for evaluation of anticancer activity. The structure of dihydropyrazole isatin based hybrids is given in Figure 93 and the in vitro cytotoxicity of hybrid compounds 96(a–d) against human cancer cell lines is shown in Table 83 [172].

Table 83. In vitro cytotoxic activities of isatin-dihydropyrazole hybrid compounds 96(a–d).

Compound No.	Ar	R	EC ₅₀ Values (μM)								
			IGR39	A549	U87	Fibroblasts	MCF-7	BT474	H1299	BxPC-3	SKOV-3
96a		5-Cl	0.33	0.34	0.38	-	0.07	0.09	0.01	0.06	0.06
96b		5-OCH ₃	0.50	0.73	0.67	0.27	0.27	0.24	0.15	0.10	-
96c		5-CH ₃	0.14	0.18	0.23	0.15	0.31	-	-	0.10	-
96d		5-Cl	2.97	-	5.76	-	-	-	-	-	-
Sunitinib	-		-	-	-	0.30	0.96	0.90	1.54	2.5	1.36

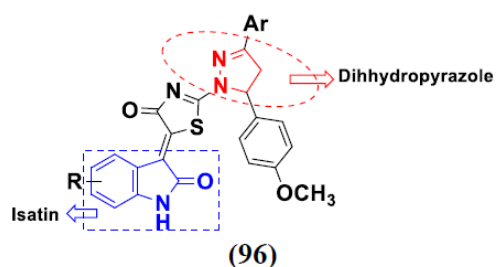


Figure 93. Structure of isatin-dihydropyrazole derivatives (96).

Wagdy et al. (2015) synthesized isatin-pyridine derivatives and tested their anti-proliferative activity against three human tumor cancer cell lines, i.e., hepatocellular carcinoma (HEPG2), lung cancer (A549), and breast cancer (MCF-7) using a sulforhodamine B (SRB) colorimetric assay. Doxorubicin has been used as a reference cytotoxic compound. The structure of pyridine isatin based hybrids is given in Figure 94 and in vitro cytotoxicity of compounds 97(a–c), or 98, 99(a–c) against human cancer cell lines is shown in Table 84 [173].

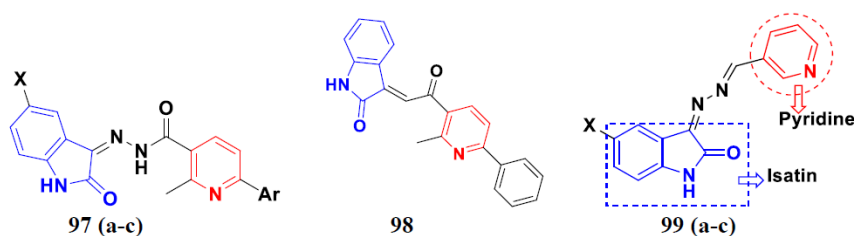


Figure 94. Structure of isatin-pyridine derivatives [97(a–c), 98, and 99 (a–c)].

Table 84. In vitro cytotoxic activities of isatin-pyridine hybrid compounds [97(a–c), 98, 99 (a–c)].

Compound No.	X	Ar	IC ₅₀ (μM)		
			A549	HepG2	MCF-7
97a	H	F-	>200	>200	>200
97b	Cl	F-	>200	>200	>200
97c	Br	F-	>200	>200	>200
98	-	-	19.3	2.5	11.6
99a	H	-	16.8	>200	14.7
99b	F	-	19.7	11.5	10.4
99c	Cl	-	10.8	8.7	6.3
Doxorubicin	-	-	7.6	6.9	6.1

Singh et al. (2015) synthesized isatin-coumarin hybrids which contain triazole as a linker, and investigated their in vitro cytotoxicity activity against four human cancer cell lines (COLO-205, THP-1, HCT-116 and PC-3) using sulforhodamine B19. The cells were given 48 h to multiply in the presence of a test substance. COLO-205, THP-1 and HCT-116 (three of the four cancer cell lines tested) were sensitive to the synthesized hybrids, and the THP-1 cancer cell line was the most susceptible to these hybrids, whereas PC-3 was found to be resistant. The structure of isatin-based coumarin hybrids is given in Figure 95 and in vitro cytotoxicity of compounds 100(a–d) against human cancer cell lines is shown in Table 85 [174].

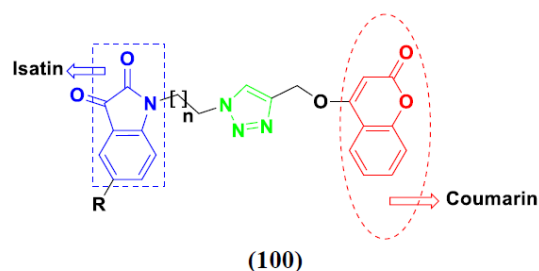


Figure 95. Structure of isatin-based coumarin derivatives (100).

Table 85. In vitro cytotoxic activities of isatin-based coumarin hybrid compounds 100(a–d).

Compound No.	R	n	IC ₅₀ (μM)		
			THP-1	COLO-205	HCT-116
100a	H	1	0.73	3.45	3.04
100b	F	1	1.99	6.67	5.41
100c	Cl	1	5.47	8.87	5.77
100d	Br	1	6.43	10.53	8.09

Wabli et al. (2017) synthesized isatin-indole derivatives and evaluated their antiproliferative activity on three cell lines: ZR-75 (human breast), HT-29 (colon) and A-549 (lung). Compound 101(d) had an average IC₅₀ value of 1.17 μM against the tested human cancer cell lines, making it the most active compound, with a potency approximately seven times greater than that of sunitinib. The structure of isatin-based indole hybrids is given in Figure 96 and in vitro cytotoxicity IC₅₀ (μM) of compounds 101(a–d) against human cancer cell lines is shown in Table 86 [175].

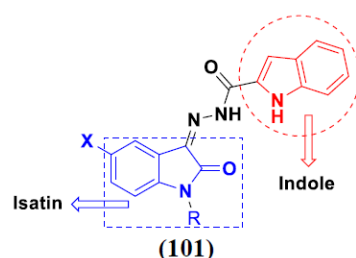


Figure 96. Structure of isatin-indole derivatives (101).

Table 86. In vitro cytotoxic activities of isatin-indole hybrid compounds 101(a–d).

Compound No.	X	R	IC ₅₀ (μM)			Average IC ₅₀ (μM)
			ZR-75	HT-29	A-549	
101a	H	H	22.73	19.74	12.98	18.48
101b	Br	H	21.92	21.93	16.01	19.95
101c	OCH ₃	CH ₃	1.48	5.73	1.93	3.05
101d	Cl		0.74	2.02	0.76	1.17
Sunitinib	-	-	8.31	10.14	5.87	8.11

Panga et al. (2020) synthesized isatin-benzoic acid conjugates and tested their in vitro cytotoxic activity against MCF-7 and HeLa cell lines. All the synthesized isatin-benzoic acid conjugates showed moderate to strong cytotoxicity against both HeLa and MCF-7 cell lines with IC₅₀ values ranging from 4.02 to 17.83 μM and 17.14 to 24.6 μM, respectively. Among all synthesized compounds, 102(b) showed maximum activity on both cell lines. The

structure of isatin-based benzoic acid hybrids is given in Figure 97 and in vitro cytotoxicity of compounds 102(a–d) against human cancer cell lines is shown in Table 87 [176].

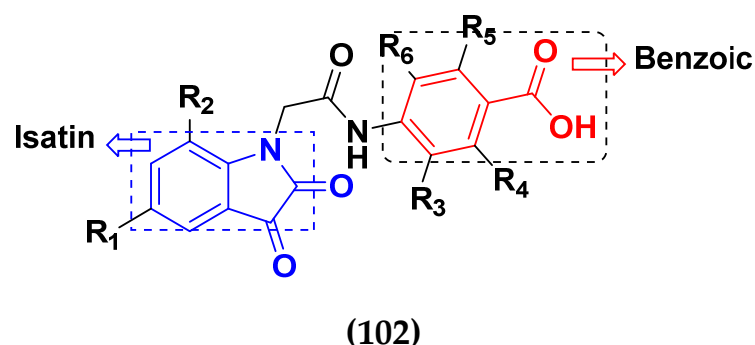


Figure 97. Structure of isatin-benzoic acid derivatives (102).

Table 87. In vitro cytotoxic activities of isatin-benzoic hybrid compounds 102(a–d).

Compound No.	R ₁	R ₂	R ₃	R ₄	R ₅	R ₆	IC ₅₀ (μM)	
							HeLa	MCF-7
102a	I	H	Cl	H	OC ₂ H	H	9.24	6.57
102b	Br	Br	Cl	H	OC ₂ H	H	8.34	5.88
102c	Br	H	H	OCH ₃	H		16.68	11.32
102d	Br	Br	H	OCH ₃	H		10.44	9.46
Vinblastine	-	-	-	-	-	-	7.14	4.02

Eldehna et al. (2016) synthesized isatin-thiazolo benzimidazole hybrids and evaluated their anti-proliferative efficacy against MCF-7 and MDA-MB-231 breast cancer cell lines by using sulforhodamine B colorimetric (SRB) assay. Staurosporine was utilized as a positive control, and the results were shown as IC₅₀ values. Compounds 103(a) and 104(a) had maximum anticancer activity towards the tested cell lines. The structure of isatin-based thiazolo-benzimidazole hybrids is shown in Figure 98, and the in vitro cytotoxicity IC₅₀ (μM) of compounds 103(a–c), 104(a–c) against human cancer cell lines is shown in Table 88 [170].

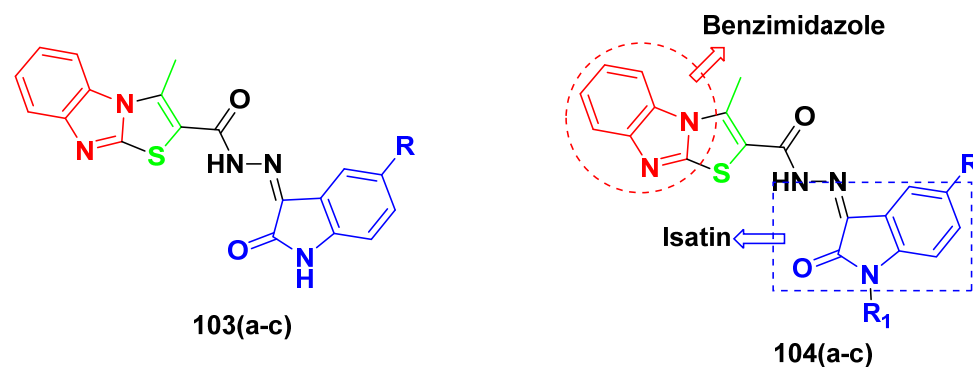
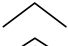
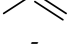


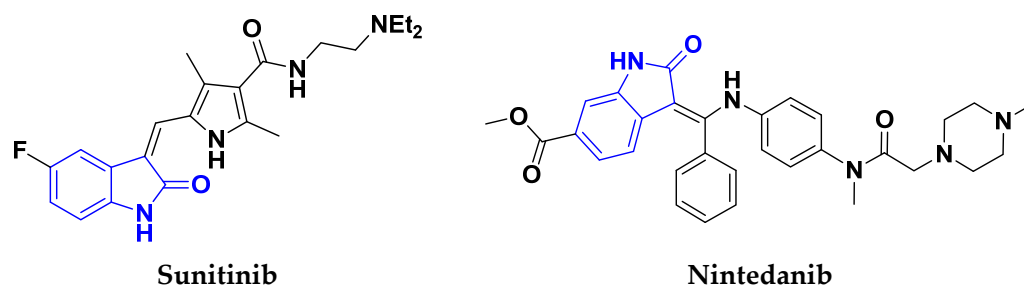
Figure 98. Structure of isatin-thiazolo benzimidazole derivatives (103,104).

Isatin Containing FDA-Approved Hybrids

Isatin containing FDA-approved hybrids are depicted in Figure 99 [177].

Table 88. In vitro cytotoxic activities of isatin-thiazolo benzimidazole hybrid compounds 103(a–c) and, 104(a–c).

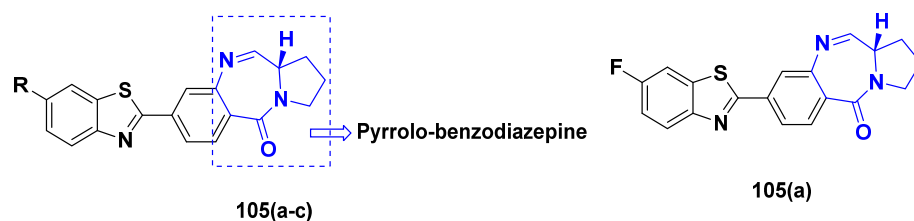
Compound No.	R	R ₁	IC ₅₀ Values	
			MCF	MDA-MB-231
103a	H	-	2.02	6.50
103b	F	-	16.83	42.64
103c	Br	-	9.39	8.62
104a	H	CH ₃	3.01	2.60
104b	H		9.80	18.06
104c	H		1.27	13.73
Staurosporine	-	-	3.81	4.29

**Figure 99.** The isatin moiety as FDA-approved anticancer drug.

3.17. Pyrrolo-Benzodiazepines Based Hybrids

Pyrrolo-benzodiazepines (PBD) are naturally found in many actinomycetes species. PBD block transcription factors and promote DNA replication by binding covalently to DNA, and thus inhibits cell growth [178].

Bose et al. (2012) synthesized hybrids of pyrrole and benzodiazepine and tested cytotoxic activities of the synthesized compounds was in vitro against five tumor cell lines: THP-1 (human acute monocytic leukemia), U-937 (human histiocytic lymphoma), HL-60 (human promyelocytic leukemia), Jurkat (human T-cell leukemia) and A-549 (lung carcinoma). Among the synthesized compounds, 105(a) was the most potent. The structure of pyrrolo-benzodiazepine hybrids is given in Figure 100 and the in vitro cytotoxicity IC₅₀ of compounds 105(a–c) against human cancer cell lines is shown in Table 89 [179].

**Figure 100.** Structure of pyrrolo-benzodiazepine hybrids and the most promising compound 105a.**Table 89.** In vitro cytotoxic activities of pyrrolo-benzodiazepine hybrid compounds 105(a–c).

Compound No.	R	IC ₅₀ Values (μM)				
		THP-1	U-937	HL-60	Jurkat	A-549
105a	F	0.49	3.44	4.13	6.58	nd
105b	OMe	2.14	6.03	6.39	11.27	nd
105c	H	3.09	5.41	7.27	9.43	nd
Etoposide		2.16	17.94	1.83	5.35	17.94
Camptothecin		0.07	1.98	0.60	0.026	0.008

Kamal et al. (2012) synthesized pyrrolo-benzodiazepine conjugated with benzoindolone derivatives. The synthesized derivatives were assessed for their anticancer activity in human cancer cell lines of the lung, skin, colon and prostate by using the MTT assay. These new conjugates exhibited encouraging anticancer activity, with IC_{50} values ranging from 1.05 to 36.49 μ M. Doxorubicin and DC81, the positive controls, displayed IC_{50} values in the range of 0.03–2.51 μ M and 0.86–1.65 μ M, respectively. Compound **106(d)** had the maximum anticancer activity. The structure of pyrrolo-benzodiazepine-based benzoindolone hybrids is given in Figure 101 and in vitro cytotoxicity of compounds **106(a–d)** against human cancer cell lines is shown in Table 90 [180].

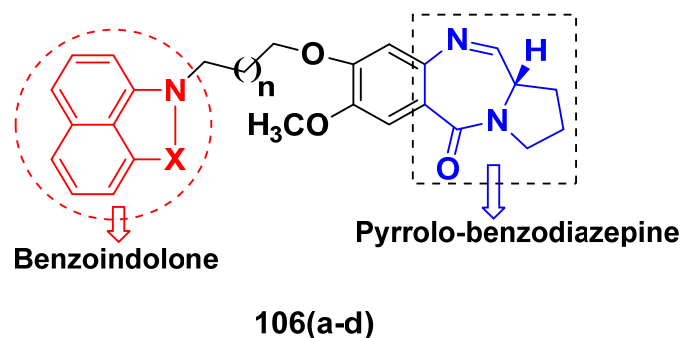


Figure 101. Structure of pyrrolo-benzodiazepine-based benzoindolone derivative (**106**).

Table 90. In vitro cytotoxic activities of pyrrolo-benzodiazepine-based benzoindolone compounds **106(a–d)**.

Compound No.	X	n	IC ₅₀ (μ M)			
			A431	A549	Colo-205	PC-3
106a	CO	1	3.04	13.85	8.65	7.67
106b	CO	2	1.34	9.80	3.31	3.23
106c	CO	3	3.71	21.94	9.76	15.45
106d	SO ₂	4	1.72	1.05	1.21	1.52
DC-81	-	-	1.65	1.11	0.86	1.19
Dox	-	-	0.03	1.02	1.69	2.51

Li et al. (2021) synthesized new pyrrolo [2,1-c] [1,4] benzodiazepine-3,11-dione (PBD) derivatives and evaluated their HDAC6 inhibitory effect. When R = H, the activity of the linker with the benzene ring was moderate. However, when the linker was extended by one methylene, the compound's activity drastically dropped (**107a** vs. **107b**). The structure of pyrrolo-benzodiazepine-dione hybrids is given in Figure 102 and the in vitro IC_{50} of compounds [**107(a–c)**,**108(a–c)**] against HDAC6 enzyme is shown in Table 91 [181].

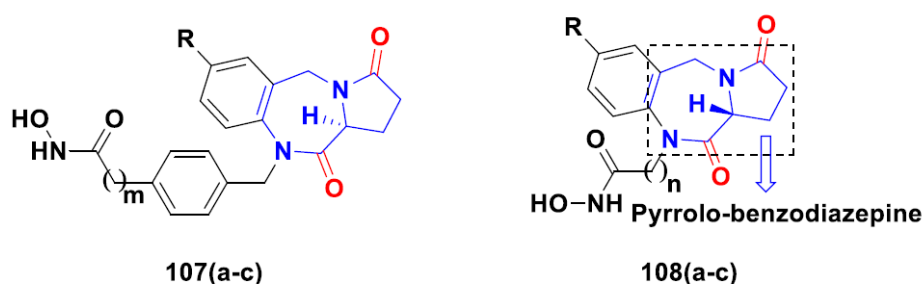
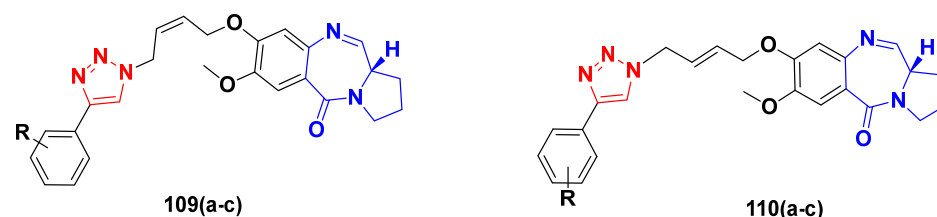


Figure 102. Structure of pyrrolo-benzodiazepine-dione derivatives [**107(a–c)**,**108(a–c)**].

Table 91. In vitro cytotoxic activities of pyrrolo-benzodiazepine-dione hybrid compounds [107(a-c),108(a-c)].

Compound No.	R	m/n	IC ₅₀ Value (nM)
			HDAC6 Enzyme
107a	H	0	38.80
107b	H	1	147
107c	H	3	>300
108a	Cl	5	23.77
108b	Cl	6	27.80
108c	Cl	7	137.77
Tubacin	-	-	5.36
Tubastatin A	-	-	22.36

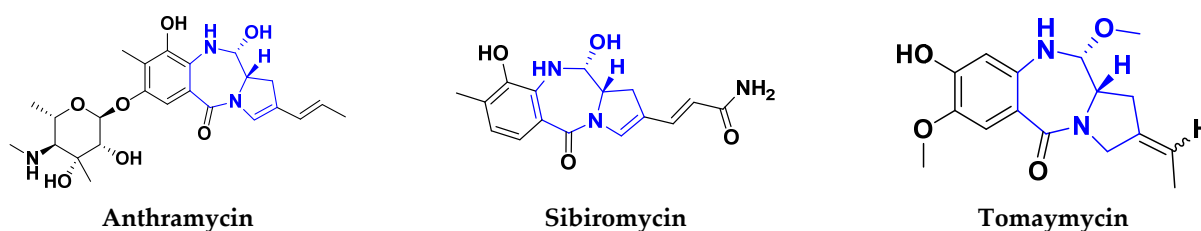
Chen et al. (2013) synthesized a new series of PBD-triazole hybrids and their cytotoxicity was investigated on various mouse and human cells, taking tubastatin A as a positive control. Cis-hybrids (109a–c) were much more cytotoxic than trans isomers (110a–c) in sensitive melanoma (A375). Compound 109a exhibited a higher inhibitory activity compared to that of other agents on A375 cells. The structure of triazole pyrrolo-benzodiazepine hybrids is given in Figure 103 and the in vitro cytotoxicity of compounds [109(a–c), 110(a–c)] against cancer cell lines is shown in Table 92 [182].

**Figure 103.** Structure of triazole-pyrrolo-benzodiazepines derivative [109(a–c),110(a–c)].**Table 92.** In vitro cytotoxic activities of triazole-pyrrolo-benzodiazepines hybrid compounds [109(a–c),110(a–c)].

Compound No.	R	IC ₅₀ Value
		A375
109a	H	2.2
109b	2-OCH ₃	4.2
109c	3-OCH ₃	3.6
110a	H	4.5
110b	2-OCH ₃	5.2
110c	3-OCH ₃	5.3

FDA Approved Drugs Containing Pyrrolo-Benzodiazepines

FDA approved drugs containing pyrrolo-benzodiazepines include tomaymycin, sibiromycin and neothramycin, which are depicted in Figure 104 [178].

**Figure 104.** Pyrrolo-benzodiazepine containing FDA approved anticancer drug.

3.18. Chalcone-Based Hybrids

Chalcone compounds are one of the most important fundamental categories of natural products as they are abundant within tea leaves, fruits and vegetables, fruits, and are of great interest because of their pharmacological effectiveness in treating many diseases. Some of the naturally occurring chalcones are depicted in Figure 105 [183].

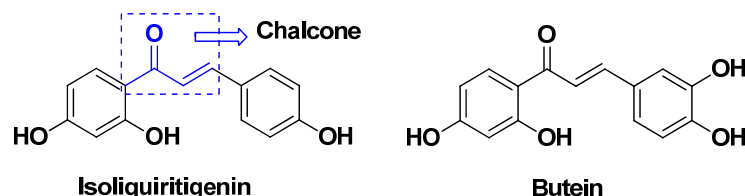


Figure 105. Naturally occurring phytoconstituents containing chalcone.

One of the most significant bioactive substances with a chalcone structure (isoliquiritigenin) was isolated from liquorice roots. Butein, a physiologically active flavonoid found in *Rhus verniciflua* (Stokes' bark), has been shown to have strong anticancer effects on a variety of cancer types.

Chalcone-based hybrid compounds have the potential to improve selectivity and anti-cancer activity while also overcoming drug resistance. Therefore, combining the chalcone moiety with additional anticancer pharmacophores is a promising strategy for creating new anticancer drugs. In recent times, a number of chalcone hybrids have been prepared and evaluated for their cytotoxic activity; some of them are found to have remarkable activity both in vitro and in vivo [184].

Zahrani et al. (2020) synthesized chalcone-based phenothiazine derivatives and evaluated their cytotoxic activity against two carcinoma cell lines (human breast cancer cell line MCF-7 and human hepatocellular carcinoma HEPG-2 cells) compared with anticancer standard drugs cisplatin and doxorubicin under the similar conditions following the MTT (methylthiazol-tetrazolium) colorimetric assay. **111(a)** and **111(b)** were the most effective compounds with IC_{50} values of 7.14 $\mu\text{g}/\text{mL}$ and 7.6 g/mL , respectively. The structure of chalcone based phenothiazine hybrids is shown in Figure 106 and the in vitro cytotoxicity of compounds **111(a–d)** against cancer cell lines is shown in Table 93 [183].

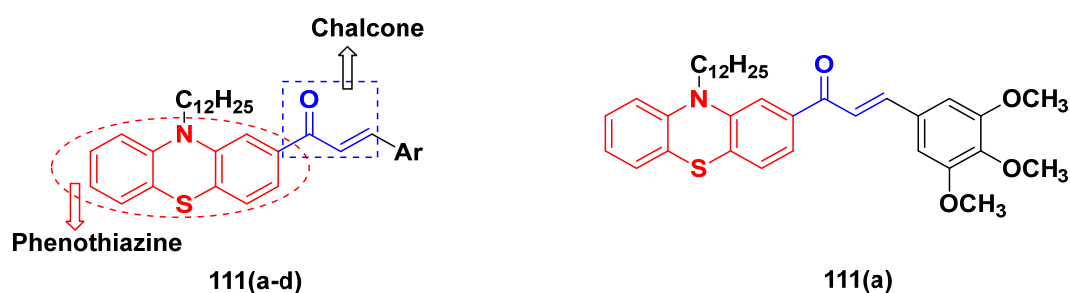
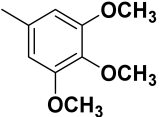
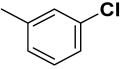
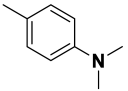
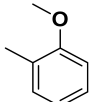
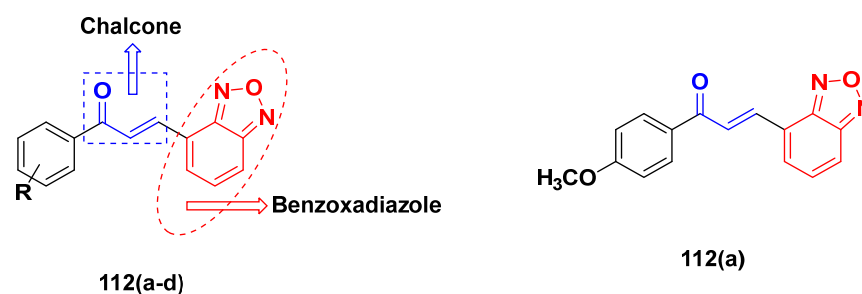


Figure 106. Structure of chalcone-based phenothiazine hybrids and the most promising compound **111a**.

Shivapriya et al. (2021) produced chalcone benzoxadiazole hybrids and evaluated their cytotoxic activity against the human epidermal carcinoma (KB) cell line using MTT assay. Chalcone-benzoxadiazole hybrids were prepared through the Claisen–Schmidt condensation reaction. The structure of chalcone-based benzoxadiazole hybrids is given in Figure 107 and the in vitro cytotoxicity of compounds **112(a–d)** against cancer cell lines is shown in Table 94 [185].

Table 93. In vitro cytotoxic activities of chalcone-based phenothiazine hybrid compounds [111(a–d),111(a)].

Compound No.	Ar	IC ₅₀ (μM)	
		MCF-7	HepG-2
111a		12	7.6
111b		13.8	7.14
111c		15.4	11.6
111d		19.2	14.7
Cisplatin	-	5.71	3.67
Doxorubicin	-	0.35	0.36

**Figure 107.** Structure of chalcone-based benzoxadiazole hybrids and the most promising compound 112a.**Table 94.** In vitro cytotoxic activities of chalcone-based benzoxadiazole hybrid compounds [112(a–d),112(a)].

Compound No.	R	IC ₅₀ (μM)
		KB
112a	4-OCH ₃	15
112b	4-F	15
112c	4-Br	15
112d	4-Cl	31

Alswah (2017) et al., designed and synthesized a series of triazolo-quinoxaline-chalcone derivatives **113a–d**, and evaluated their cytotoxic activity against three target cell lines: human breast adenocarcinoma (MCF-7), human colon carcinoma (HCT-116) and human hepatocellular carcinoma (HEPG-2) using the MTT assay method with doxorubicin as a reference drug. The initial results showed that some of the chalcones exhibited significant antiproliferative effects against most of the cell lines, with selective or non-selective behavior, with IC₅₀ values found to be in the 1.65 to 34.28 μM range. Compound **113(a)** showed maximum cytotoxic activity towards given cell lines. The structure of chalcone-based triazolo-quinoxaline hybrids is given in Figure 108 and the in vitro cytotoxicity of synthesized hybrids against cancer cell lines are shown in Table 95 [186].

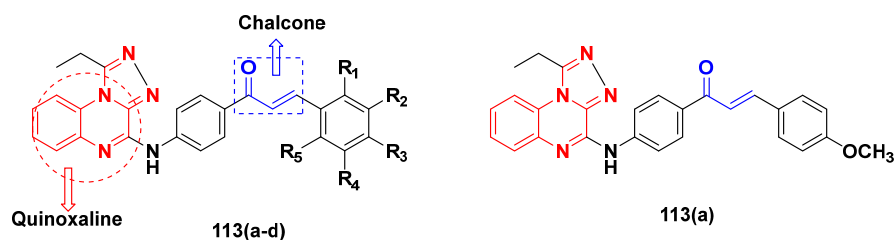


Figure 108. Structure of chalcone-based triazolo-quinoxaline hybrids and the most promising compound 113a.

Table 95. In vitro cytotoxic activities of chalcone-based triazolo-quinoxaline hybrid compounds [113(a–d),113(a)].

Compound No.	R ₁	R ₂	R ₃	R ₄	R ₅	IC ₅₀ (μM)		
						MCF-7	HCT-116	HepG-2
113a	H	H	OCH ₃	H	H	8.23	9.57	34.28
113b	H	H	H	H	H	58.92	57.49	105.21
113c	OCH ₃	H	H	H	H	24.04	25.60	30.72
113d	OH	H	H	H	H	22.17	19.76	17.32
Doxorubicin	-	-	-	-	-	0.27	1.55	0.22

Yepes et al. (2021) synthesized a new series of hybrid molecules by inclusion of two scaffolds: chalcone and melatonin. To achieve this goal, biologically active chalcone was attached via a non-hydrolyzable thioalkoxy linker to the corresponding melatonin bioisostere scaffold. The anticancer activity of the synthesized hybrids was evaluated against an in vitro model of colorectal cancer. In this study, two cell lines were used, i.e., the non-malignant (CHO-K1) and human colon adenocarcinoma cells (SW480). The reference drug used was 5-FU. Compound 114(a) maximum activity. The structure of chalcone based melatonin hybrids is given in Figure 109 and in vitro cytotoxicity of compounds 114(a–d) against cancer cell lines is shown in Table 96 [187].

Table 96. In vitro cytotoxic activities of chalcone based melatonin hybrid compounds [114(a–d),114(a)].

Compound No.	R	24 h		48 h	
		IC ₅₀ (μM) SW480 Cells	IC ₅₀ (μM) CHO-K1 Cells	IC ₅₀ (μM) SW480 Cells	IC ₅₀ (μM) CHOK1 Cells
114a		1.26	6.40	0.24	0.16
114b		29.49	20.48	4.14	4.95
114c		30.46	10.12	2.43	1.13
114d		49.82	>100	1.77	10.61
5-fluorouracil	-	-	543.5	174.3	173.2

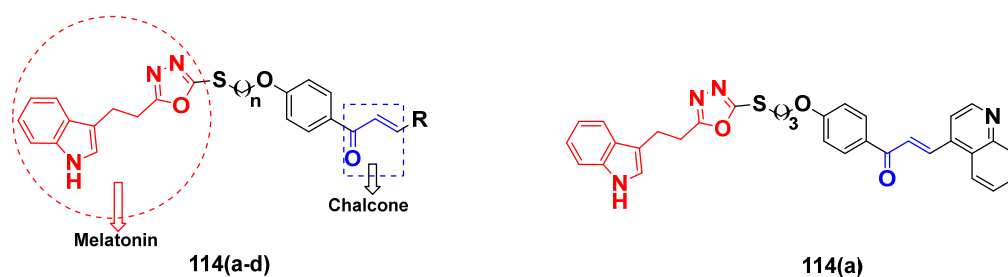


Figure 109. Structure of chalcone based melatonin hybrids and the most promising compound **114a**.

Ma et al. (2021) synthesized chalcone-based quinoxalin as anti-cancer hybrids. All of the synthesized compounds (**115a–e**) were tested *in vitro* for their anticancer activities against, PC12, BPH-1 and MCF-7 cells using the MTT assay. With IC_{50} values in the micro molar range (9.1–98.7 mM) against all tested cancer cells, all synthesized compounds demonstrated moderate to good antiproliferative activity and compound **115(e)** showed maximum cytotoxic activity. The structure of chalcone-based quinoxalin hybrids is given in Figure 110 and the *in vitro* cytotoxicity of compounds **115(a–e)** against cancer cell lines is shown in Table 97 [188].

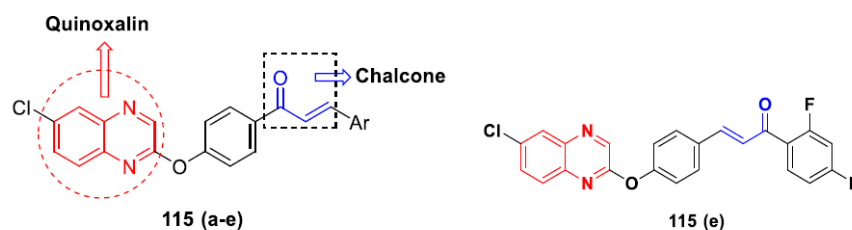


Figure 110. Structure of chalcone-based quinoxalin hybrids and the most promising compound **115e**.

Table 97. *In vitro* cytotoxic activities of chalcone-based quinoxaline hybrid compounds [**115(a–e)**,**115(e)**].

Compound No.	Ar	IC_{50} Value (mM)		
		BPH-1	PC12	MCF-7
115a		48.5	42.1	72.4
115b		54.8	48.5	54.8
115c		64.2	73.1	80.9
115d		76.9	81.1	77.3
115e		10.4	16.7	9.1
Doxorubicin		14.1	22.5	9.2

3.19. Coumarin-Based Hybrids

The coumarin scaffold (2H-1-benzopyran-2-one) is extensive in nature, and its derivatives exhibit various antibacterial, antifungal, antimalarial, and anticancer pharmacological properties.

Kamaldeep Paul et al. (2013) synthesized coumarin-benzimidazole hybrids. The synthesized compounds showed potent activity against leukemia cancer cells (CCRF-CEM, HL-60(TB), K-562, RPMI-8226), colon cancer cells (HCT-116, HCT-15), melanoma cancer cells (LOX IMVI, UACC-257) and breast cancer cells (MCF7, T-47D). The compounds containing substitution (NR_1R_2) were the most potent with inhibition of most of the cell lines. The compound with ethanolamine as a substituent (NR_1R_2) at position 7 of the coumarin-benzimidazole scaffold, was the most potent synthesized compound. The structure of coumarin-benzimidazole hybrids is given in Figure 111 and the in vitro % growth inhibition of compounds **116(a–e)** against cancer cell lines is shown in Table 98 [189].

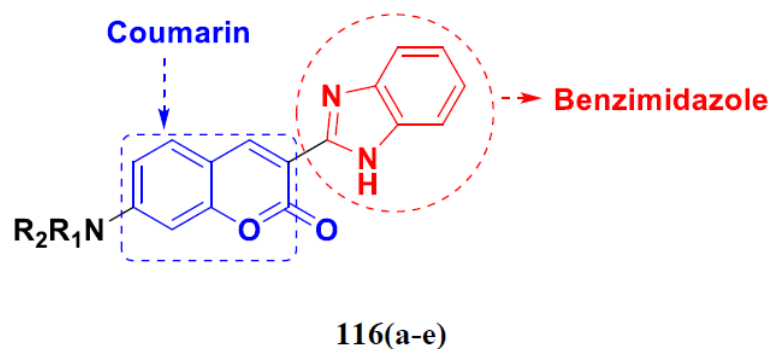


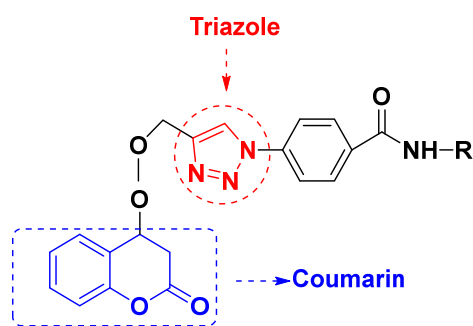
Figure 111. Structure of coumarin-benzimidazole derivatives **116(a–e)**.

Table 98. In vitro cytotoxic activities of coumarin-benzimidazole hybrid compounds **116(a–e)**.

Compound No.	Substitution	% Growth Inhibition	Maximal Inhibition	
116a	$NR_1R_2 =$ Ethylenediamine		20.5	Colon Cancer
			33.98	Breast Cancer
116b	$NR_1R_2 =$ Ethanolamine		80.51	Leukemia
116c	$NR_1R_2 =$ Morpholine		62.12	Breast Cancer
116d	$NR_1R_2 =$ Methylpiperazine		56.39	Leukemia
116e	$NR_1R_2 = 2-$ Aminoethylmorpholine		23.26	Small cell lung cancer
			22.91	CNS Cancer
5-FU			47.9	Leukemia

R. An et al. synthesized amide containing 1,2,3-triazole hybrids, which showed moderate to excellent activity against MDB-MB 231 cell lines under both normoxic and hypoxic conditions. The structure of coumarin-triazole hybrids is given in Figure 112 and the in vitro IC_{50} of compounds **117(a–e)** against cancer cell lines are shown in Table 99 [190].

H.A. Elshemy et al., (2017) synthesized coumarin-chalcone hybrids having anticancer activity against HEPG2, leukemia, and WI-38 cell lines. All coumarin-chalcone hybrids had potent activity against HEPG2 and K562, and weak activity against WI-38 cell. Among the coumarin-chalcone hybrids, 4-methoxyphenyl chalcone **118(a)** was more potent than 3,4-dimethoxyphenyl chalcone **118(b)**, which showed higher activity than chalcone with 3,4,5-trimethoxyphenyl moiety **118(c)**.



117(a-e)

Figure 112. Structure of coumarin containing 1,2,3-triazole derivatives 117(a–e).

Table 99. In vitro cytotoxic activities of coumarin containing 1,2,3-triazole hybrid compounds 117(a–e).

Compound No.	Substitution	IC ₅₀ (mM)		IC ₅₀ normoxia/IC ₅₀ hypoxia
		Hypoxia	Normoxic	
117a		23.47	24.41	1.04
117b		75.21	73.77	0.98
117c		6.72	6.78	1.01
117d		0.03	1.34	46.31
117e		73.82	91.61	1.24
Dox		0.60	1.07	1.79

In the coumarin-acrylohydrazone series, compound **119(c)** showed the highest activity against a leukemia cell line (k562) while compound (**119a** and **119b**) showed potent activity against the HEPG2 cell line and moderate activity against the WI-38 cell line. The structure of coumarin containing chalcone hybrids is shown in Figure 113 and the in vitro IC₅₀ (μM) of compounds [**118(a–c)**,**119(a–c)**] against cancer cell lines is shown in Table 100 [191].

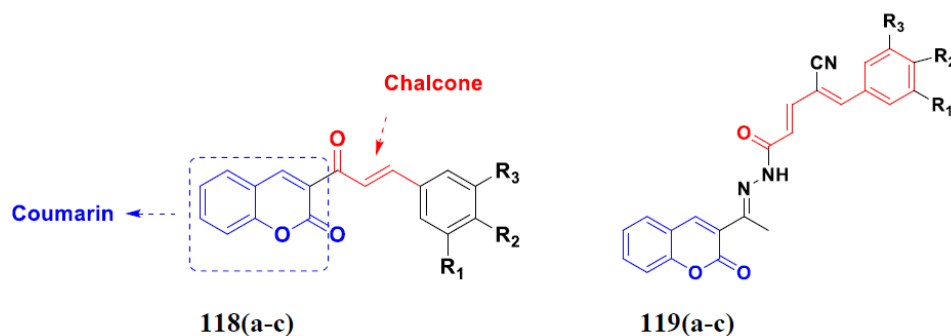
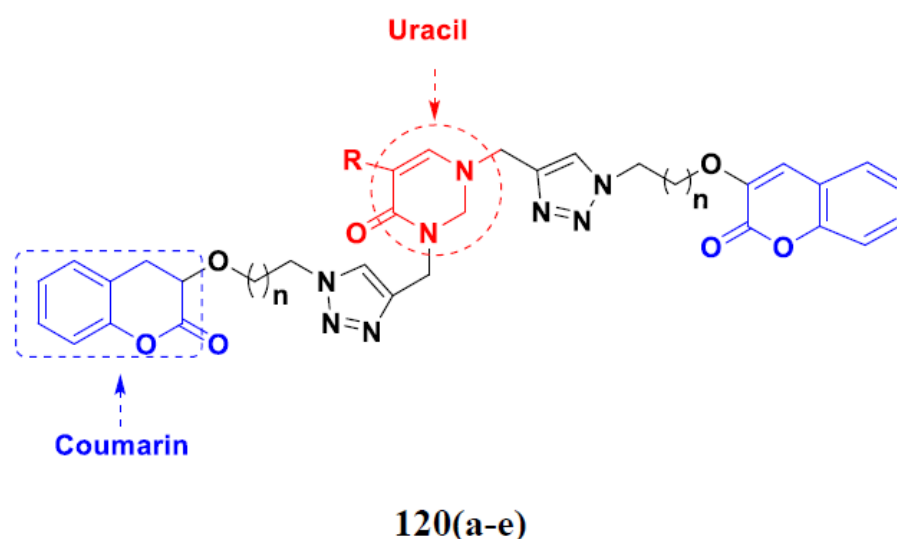


Figure 113. Structure of coumarin containing chalcone derivative [**118(a–c)**,**119(a–c)**].

Table 100. In vitro cytotoxic activities of coumarin containing chalcone hybrid compounds [118(a–c),119(a–c)].

Compound No.	Substitution			IC ₅₀ (μM)		
	R ₁	R ₂	R ₃	HEPG2	Leukemia K562	WI-38
118a	H	OCH ₃	H	0.65	1.09	292.7
118b	OCH ₃	OCH ₃	H	0.82	0.93	33.09
118c	OCH ₃	OCH ₃	OCH ₃	2.02	1.36	9.55
119a	H	OCH ₃	H	0.77	3.96	48.4
119b	OCH ₃	OCH ₃	H	0.93	8.71	3.3
119c	OCH ₃	OCH ₃	OCH ₃	1.57	0.49	11.1
Cisplatin				2.56	2.02	NA

Mohit Sanduja et al. (2020) synthesized uracil-coumarin-based compounds as potent anticancer hybrid compounds. The uracil-coumarin hybrid compounds inhibited the MCF-7 cancer cell proliferation more effectively compared to standard 5-FU. The most potent compound 120b (GI₅₀ = 1.55 μM) contained A with fluorine atom as R with two carbon chain lengths between triazole and coumarin moieties. The structure of coumarin containing uracil hybrids is given in Figure 114, and in vitro GI₅₀ (μM) of compounds 120(a–e) against cancer cell lines is shown in Table 101 [192].

**Figure 114.** Structure of coumarin-based uracil derivatives 120(a–e).**Table 101.** In vitro cytotoxic activities of coumarin-based uracil hybrid compounds 120(a–e).

Compound No.	Substitution (R)	n	MCF-7(GI ₅₀ . μM)
120a	H	1	10.99
120b	F	1	1.55
120c	Cl	1	2.57
120d	Br	1	3.34
120e	I	1	3.96
5-FU			7.28

Zhuo zing et al., (2018) synthesized novel coumarin-based furoxin hybrids which had potent activity against Hela cell proliferation. The compound 121(e) had the highest antiproliferative activity and was more potent than standard, doxorubicin. The structure of coumarin containing furoxin hybrids is given in Figure 115 and the in vitro IC₅₀ of compounds 121(a–e) against cancer cell lines is shown in Table 102 [193].

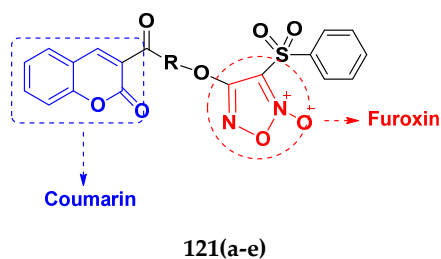


Figure 115. Structure of coumarin-based furoxin derivatives **121(a-e)**.

Table 102. In vitro cytotoxic activities of coumarin-based furoxin hybrid compounds **121(a-e)**.

Compound No.	Substitution [®]	IC ₅₀ (μM)
121a	—(CH ₂) ₂ —O	32.32
121b	—(CH ₂) ₃ —O	4.85
121c	—(CH ₂) ₄ —O	5.16
121d	—CH ₂ ·C≡C—CH ₂ ·O—	5.95
121e	—(CH ₂) ₂ O—(CH ₂) ₂ O	4.72
Dox		10.21

3.20. Nitrogen Mustard Based Hybrids

Shengtao Xu et al. (2014) synthesized natural oridonin bearing nitrogen mustard hybrid as potential anticancer compound. The hybrid showed activity against the multidrug resistant cell lines SW620/AD300 and NCL-H460/MX20. Compound **122(b)** induced apoptosis and affected cell cycle progression in human hepatoma (Bel-7402) cells. The structure of nitrogen mustard containing oridonin hybrids is given in Figure 116 and the in vitro IC₅₀ of compounds **122(a-d)** against the cancer cell line (Bel-7402) is shown in Table 103 [194].

Table 103. In vitro cytotoxic activities of nitrogen mustard-containing oridonin hybrid compounds **122(a-d)**.

Compound No.	Substitution (R ₁)	IC ₅₀ (μM) against Bel-7502
122a		8.35
122b		0.50
122c		1.43
122d		7.91
Chlorambucil		49.31

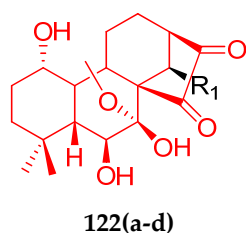


Figure 116. Structure of nitrogen mustard contain oridonin derivatives **122(a–d)**.

Laczkowski et al. (2016) synthesized nitrogen mustard-based thiazole hybrid drugs that showed antiproliferative activity against human cancer cell lines MV4-11, A549, MCF-7 and HCT-116. Among the all derivatives, **123(a–e)** was most potent and exhibited activity against human leukemia (MV4-11) cells. The compounds **123(b)** and **123(e)** had potent activity against MCF-7 and HCT116. The structure of nitrogen mustard contain thiazole hybrids is given in Figure 117 and the in vitro IC_{50} of compounds **123(a–e)** against cancer cell lines is shown in Table 104 [195].

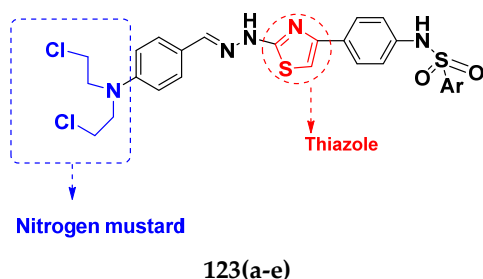


Figure 117. Structure of nitrogen mustard-containing thiazole derivatives **123(a–e)**.

Table 104. In vitro cytotoxic activities of nitrogen mustard-containing thiazole hybrid compounds **123(a–e)**.

Compound No.	Substitution (Ar)	IC_{50} ($\mu\text{g/mL}$)	Log P
123a		3.63	6.15
123b		3.95	5.74
123c		3.29	6.80
123d		4.26	6.35
123e		2.17	6.53
Cisplatin		0.31	-

Kolesinska et al. (2012) synthesized hybrids containing a nitrogen mustard-triazine scaffold as potent anticancer compounds. These were prepared by rearrangement of mono, bis and tris-(1,3,5-triazin-2-yl)-1,4-diazacyclo [2.2.2] octanium chlorides leading to the formation of 2-chloroethylamino fragments attached to 1,3,5-triazine via one, two or three piperazine, respectively. Their cytotoxicity and alkylating activity depended on substituents on the triazine ring and nitrogen mustard. Among the above mentioned compounds, **124(b)** and **124(d)** were the most potent. The structure of nitrogen mustard-containing triazine

hybrids is shown in Figure 118 and the in vitro IC₅₀ of compounds 124(a–d) against cancer cell lines is shown in Table 105 [196].

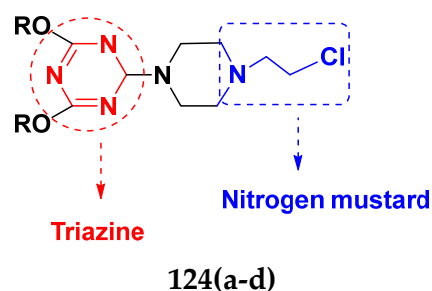


Figure 118. Structure of nitrogen mustard-containing triazine derivatives 124(a–d).

Table 105. In vitro cytotoxic activities of nitrogen mustard-containing triazine hybrid compounds 124(a–d).

Compound No.	Substitution (R)	IC ₅₀ (µg/mL)		
		Breast Cancer (T47D)	Prostate Cancer (LNCaP)	Colorectal Cancer (SW707)
124a	CH ₃	27.86	15.78	32.98
124b	C ₆ H ₅ CH ₂	1.40	0.99	3.45
124c	CF ₃ CH ₂	96.84	18.27	96.84
124d	C ₆ H ₅	2.60	1.47	2.93

Acharya et al. (2017) synthesized androstene oxime-nitrogen mustard hybrids and nitrogen mustard conjugates of various steroidal oximes. The conjugation was achieved by oxime-ester linkage. The 17-E-steroidal oxime benzoic acid mustard ester, 3β acetoxy-17E-[p-(N,N-bis(2-chloroethyl)amino)benzoyloxiamino-androst-5ene 125(a) showed the highest growth inhibition on IGROV (ovarian cancer cells) with a GI₅₀ of 0.937 µg/mL. The structure of androstene oxime-nitrogen mustard hybrids is shown in Figure 119 and the in vitro GI₅₀ (µg/mL) of compounds (125(a-b),126(a-b)) against cancer cell lines is shown in Table 106 [197].

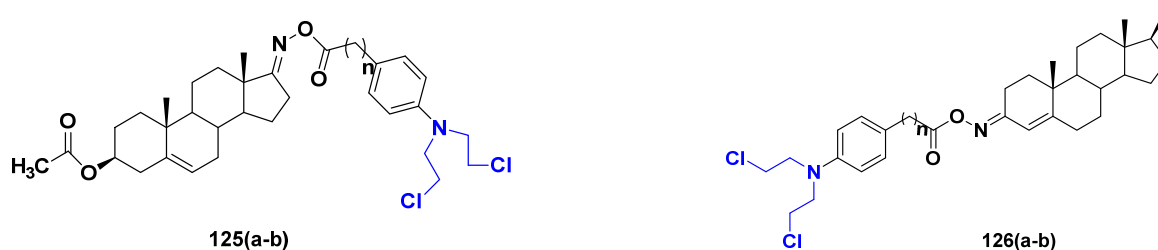


Figure 119. Structure of androstane oxime-nitrogen mustard hybrids [125(a-b),126(a-b)].

Table 106. In vitro cytotoxic activities of androstane oxime-nitrogen mustard hybrid compounds [125(a-b),126(a-b)].

Compound No.	Substitution (n)	GI ₅₀ (µM)	
		K-562	HL-60
125a	0	3.90	7.01
125b	1	13.6	36.0
126a	0	12.4	32.2
126b	1	40.1	61.2

3.21. Pyrazole-Based Hybrids

Hassan et al. (2021) synthesized indole-pyrazole hybrids as anticancer agents. The newly synthesized hybrids were screened for their cytotoxicity activities in vitro against four human cancer types, i.e., colorectal (HCT-116), breast carcinoma (MCF-7), liver carcinoma (HepG2) and lung carcinoma (A549). Among all indole-pyrazole hybrids, **126a** and **126b** showed excellent anticancer activity against the HepG2 cancer cell line with an IC_{50} of 6.1 and 7.9 μM , respectively. The structure of the pyrazole-based indole hybrid is given in Figure 120 and the in vitro IC_{50} of compounds **127(a–e)** against cancer cell lines are shown in Table 107 [198].

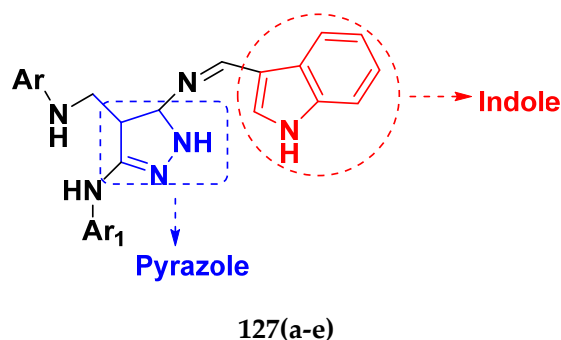


Figure 120. Structure of pyrazole-based indole derivatives **127(a–e)**.

Table 107. In vitro cytotoxic activities of pyrazole-based indole hybrid compounds **127(a–e)**.

Compound No.	Substitution		IC_{50} (μM)			
	Ar	Ar ₁	HCT-116	MCF-7	HepG2	A549
127a	C ₆ H ₅	C ₆ H ₅	17.4	10.6	6.1	23.7
127b	4-CH ₃ -C ₆ H ₄	C ₆ H ₅	19.6	14.5	7.9	14.1
127c	H	4-CH ₃ -O-C ₆ H ₄	31.9	22.2	35.8	43.4
127d	C ₆ H ₅	4-CH ₃ -O-C ₆ H ₄	25.3	17.4	27.2	58.7
127e	4-CH ₃ -C ₆ H ₄	4-CH ₃ -O-C ₆ H ₄	37.4	16.2	25.8	40.8
Dox	-	-	40.0	64.8	24.7	58.1

Somaia et al. (2015) synthesized benzofuran-pyrazole-based hybrids as anticancer drugs. The newly synthesized compounds showed remarkable growth inhibitory activity against leukemia (CCRF-CEM), A549 (lung carcinoma), and HCT-116 (colorectal carcinoma) cells. Compound **128c** showed good src inhibition activity at 10 μM and was found to be most potent compound. The structure of benzofuran-pyrazole hybrids is given in Figure 121 and in vitro IC_{50} of compounds **128(a–d)** against cancer cell lines is shown in Table 108 [199].

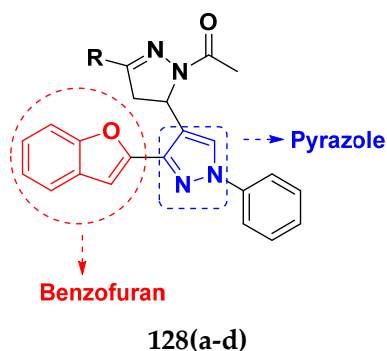
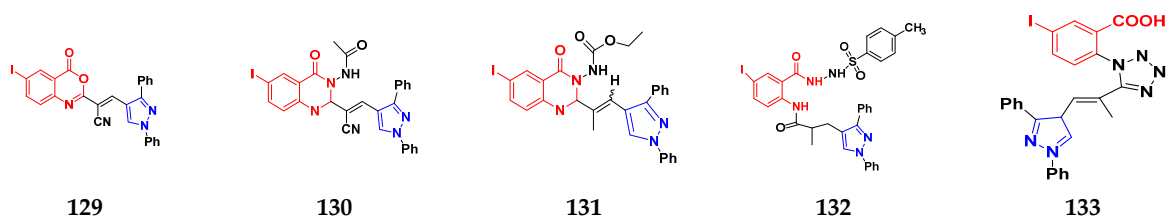


Figure 121. Structure of benzofuran-pyrazole-based derivatives **128(a–d)**.

Table 108. In vitro cytotoxic activities of benzofuran-pyrazole-based hybrid compounds 128(a–d).

Compound No.	Substitution (R)	Cell Growth Promotion Percentage (At 10^{-5} M Concentration)		
		CCRM-CEM	A549/ATCC	HCT-116
128a	4-Cl-C ₆ H ₄ -	-	-	-
128b	Cyclohexyl	-	-	-
128c	2-pyroryl	90.65	62.56	27.86
128d	2-furyl	78.58	93.57	74.8

Abdelaal et al. (2021) synthesized quinazoline-pyrazole hybrids as potential antiproliferative agents. The newly synthesized compounds showed activity against hepatocellular carcinoma (liver) HEPG2, mammary gland (breast) MCF-7 and colon cancer HCT-116 cells. The structure of quinazoline-pyrazole hybrids is given in Figure 122 and the in vitro IC₅₀ of compounds (129–133) against cancer cell lines is shown in Table 109 [200].

**Figure 122.** Structure of quinazoline-pyrazole-based derivatives (129–131) and pyrazole derivative (132–133).**Table 109.** In vitro cytotoxic activities of quinazoline-pyrazole-based compounds (129–131) and pyrazole derivatives (132–133).

Compound No.	IC ₅₀ (μM)		
	HePG2	HCT-116	MCF-7
129	65.14	45.95	79.88
130	4.99	6.83	4.63
131	16.18	11.78	18.72
132	6.85	3.46	9.07
133	73.11	88.60	69.16

Washim Akhtar et al. (2021) synthesized 15 novel pyrazoline-pyrazole hybrids, all of which showed activity in the MTT growth inhibition assay against five cancer cells lines: MCF-7, A549, SiHa, COLO205 and HePG2 cells. Compound 134 (b) was found to active against A549, SiHa, COLO205 and HePG2 cell lines with IC₅₀ values of 4.94, 4.54, 4.98 and 2.09 μM, respectively, and was non-toxic against normal cells. The structure of pyrazoline-pyrazole hybrids is given in Figure 123 and in vitro IC₅₀ of compounds 134(a–e) against cancer cell lines is shown in Table 110 [201].

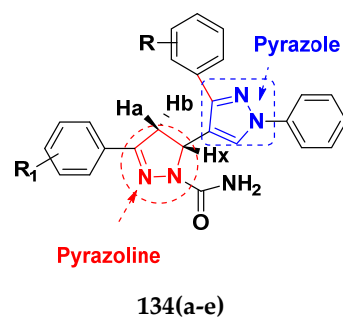
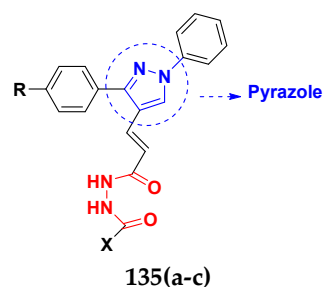
**Figure 123.** Structure of pyrazoline-pyrazole-based derivatives 134(a–e).

Table 110. In vitro cytotoxic activities of pyrazoline-pyrazole-based hybrid compounds **134(a–e)**.

Compound No.	Substitution		IC ₅₀ (μM)				
	R	R ₁	MCF-7	A549	SiHa	COLO205	HepG2
134a	4-Cl	4-OCH ₃	31.38	15.30	4.54	12.95	>50
134b	H	4-OCH ₃	27.37	4.94	4.58	4.86	2.09
134c	H	4-F	29.31	10.27	5.67	6.69	8.56
134d	H	4-Cl	30.05	11.50	6.40	7.16	>50
134e	H	H	>50	26.25	>50	31.27	>50
5-FU			2.08	4.35	5.78	4.00	19.01

Garima Verma et al. (2018) synthesized pyrazole acrylic acid-based oxadiazole and amide hybrids as anticancer and antimalarial agents. The anticancer activity of newly synthesized compounds was measured using the sulforhodamine B assay. Compounds **135(a–c)** demonstrated promising results against all tested cell lines. The non-cyclized compounds (amide derivatives) favored anticancer activity. The structure of pyrazole acrylic acid based oxadiazole hybrids is shown in Figure 124 and the in vitro IC₅₀ of compounds **135(a–c)** against cancer cell lines is shown in Table 111 [202].

**Figure 124.** Structure of pyrazole acrylic acid-based oxadiazole derivatives **135(a–c)**.**Table 111.** In vitro cytotoxic activities of pyrazole acrylic acid-based oxadiazole hybrid compounds **135(a–c)**.

Compound No.	Substitution		IC ₅₀ (μM)			
	R	X	HCT-116	SW-620	MCF-7	HT-29
135a	4-CH ₃		1.8	3.6	2.0	4.4
135b	4-CH ₃		10	>10	10.9	8.5
135c	H		1.9	5.0	6.4	4.6
Paclitaxel			0.004	0.006	0.006	0.005

3.22. Pyridine-Based Hybrids

Chetan B. Sangani et al. (2014) synthesized biquinoline-pyridine hybrids as potential EGFR and HER-2 kinase inhibitors by base catalyzed cyclocondensation through one potent multicomponent reaction. All the synthesized compounds were tested against A549 (adenocarcinomic human alveolar basal epithelial) and Hep G2 (liver cancer) cell lines. Enzyme inhibitory activity was measured against HER-2. Compound **136(d)** was found to be most potent compound. The structure of biquinoline-pyridine hybrids is given in Figure 125 and the in vitro IC₅₀ of compounds **136(a–e)** against cancer cell lines is shown in Table 112 [203].

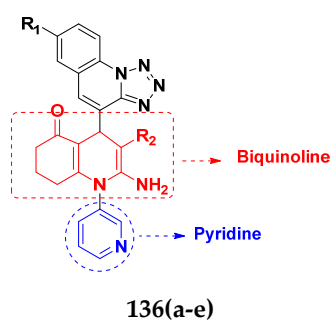


Figure 125. Structure of biquinoline-pyridine hybrid derivative **136(a-e)**.

Table 112. In vitro cytotoxic activities of biquinoline-pyridine hybrid compounds **136(a-e)**.

Compound No.	Substitution		IC ₅₀ (μM)
	R ₁	R ₂	
136a	H	CN	4.8
136b	OCH ₃	CN	5.4
136c	H	COOMe	1.1
136d	CH ₃	COOEt	0.09
136e	OCH ₃	COOEt	0.2
Erlotinib			0.03

W.M. Eldehna et al. (2015) synthesized isatin-pyridine hybrids as potential antiproliferative agents. They showed antiproliferative activity against hepatocellular carcinoma (HEPG2), lung cancer (A549) and breast cancer (MCF-7) cell lines. Compound **137** showed the most potent activity against HEPG2 with an IC₅₀ of 2.5 μM, while compound **138(c)** was the most potent compound against A549 and MCF-7 cell line with IC₅₀ values of 10.8 and 6.3 μM, respectively. The structure of isatin-pyridine hybrids is shown in Figure 126 and the in vitro IC₅₀ of compounds [**137,138(a-d)**] against cancer cell lines is shown in Table 113 [173].

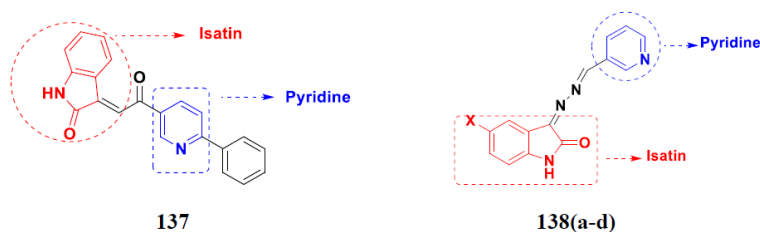


Figure 126. Structure of isatin-pyridine derivative [**137,138(a-d)**].

Table 113. In vitro cytotoxic activities of isatin-pyridine hybrid compounds [**137,138(a-d)**].

Compounds No.	Substitution (X)	IC ₅₀ (μM)		
		HepG2	A549	MCF-7
138a	H	NA	16.8	14.7
138b	F	11.5	19.7	10.4
138c	Cl	8.7	10.8	6.3
138d	Br	59.1	85	14.9
Dox		6.9	7.6	6.1

E.K. Hamza et al. (2020) synthesized pyrazolo [3,4] pyridine hybrids as potential anticancer agents. The activity of the newly synthesized compounds was evaluated in vitro against two human cancer cell lines (HCT116 and MCF-7). Compounds **139(a-d)** showed activity against HCT116 and compounds **140(a-d)** showed activity against MCF-7 cancer

cell lines. The structure of pyrazolo [3,4] pyridine hybrids is shown in Figure 127 and the in vitro IC_{50} (μM) of compounds [139(a–d),140(a–d)] against cancer cell lines is shown in Table 114 [204].

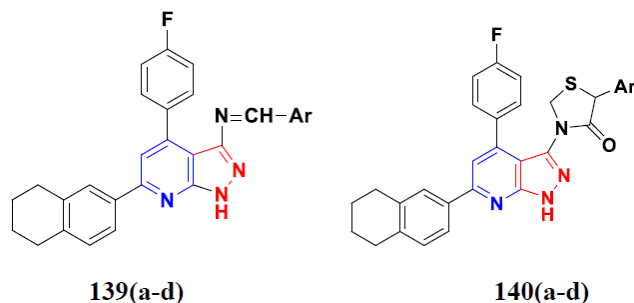


Figure 127. Structure of pyrazolo [3,4] pyridine derivatives [139(a–d),140(a–d)].

Table 114. In vitro cytotoxic activities of pyrazolo [3,4] pyridine hybrid compounds [139(a–d),140(a–d)].

Compound No.	Substitution (Ar)	IC_{50} (μM)	
		HCT116 *	MCF-7 **
139a, 140a		6.4	70.9
139a, 140b		19.8	55
139c, 140c		8.1	48.7
139d, 140d		9.8	32.6
Dox		9.5	65.6

* 139(a–d), ** 140(a–d).

4. Conclusions

For a very long time, medicinal chemists from all over the world have been trying to develop new and effective cancer treatments. Combination therapy and hybrid chemotherapeutics have become more common, because a complex disease such as cancer cannot be properly treated with a single drug. This study presents rational approaches behind the design of anticancer agents employing molecular hybridization. This method has potential because it combines two moieties to create new molecular scaffolds. Molecular hybridization offers a wide range of applications since it can produce compounds with distinct and/or multiple modes of action and minimal side effects. The few examples included in this article are not intended to be an exhaustive collection of anticancer hybrids, but to provide a quick explanation of the idea and its potential uses for researchers working in this field.

Author Contributions: Conceptualization: P.K., M.G. and M.J.; data collection: P.S., H.P. and J.P.Y.; writing the manuscript: A.K.S. and A.K.; sketching of figures: P.P. and H.S.; data interpretation: S.T. and A.-H.E.; writing, review and final editing of the manuscript: A.V. and H.K. All authors have read and agreed to the published version of the manuscript.

Funding: The APC was funded by King Abdullah University of Science and Technology (KAUST), Thuwal, Jeddah, Saudi Arabia.

Institutional Review Board Statement: Not applicable.

Informed Consent Statement: Not applicable.

Data Availability Statement: All the data given in this manuscript has been taken from published research articles, given in the list of references and are available online.

Acknowledgments: The authors are thankful to Central University of Punjab for providing infra-structural facilities for the successful completion of this study. Prateek Pathak and Maria Grishina also acknowledge Ministry of Science and Higher Education of Russia (Grant FENU-2020-0019).

Conflicts of Interest: The authors declare no competing interest.

Abbreviations

EGFR	Epidermal Growth Factor Receptor
EMA	European Medicines Agency
FDA	Food and Drug Administration
HDAC	Histone Deacetylases
MDR	Multidrug Resistance
PDGF	Platelet Derived Growth Factor
SAHA	Suberoylanilide Hydroxamic Acid
VEGFR-2	Vascular Endothelial Growth Factor Receptor-2
WHO	World Health Organization

References

- Rana, A.; Alex, J.M.; Chauhan, M.; Joshi, G.; Kumar, R. A review on pharmacophoric designs of antiproliferative agents. *Med. Chem. Res.* **2015**, *24*, 903–920. [[CrossRef](#)]
- Kori, S. An overview: Several causes of breast cancer. *Epidemol. Int. J.* **2018**, *2*, 000107. [[CrossRef](#)]
- Hassanpour, S.H.; Dehghani, M. Review of cancer from perspective of molecular. *J. Cancer Res. Pract.* **2017**, *4*, 127–129. [[CrossRef](#)]
- Sung, H.; Ferlay, J.; Siegel, R.L.; Laversanne, M.; Soerjomataram, I.; Jemal, A.; Bray, F. Global cancer statistics 2020: GLOBOCAN estimates of incidence and mortality worldwide for 36 cancers in 185 countries. *Cancer J. Clin.* **2021**, *71*, 209–249. [[CrossRef](#)]
- Philip, C.C.; Mathew, A.; John, M.J. Cancer care: Challenges in the developing world. *Cancer Res. Treat.* **2018**, *1*, 58–62.
- Penny, L.K.; Wallace, H.M. The challenges for cancer chemoprevention. *Chem. Soc. Rev.* **2015**, *44*, 8836–8847. [[CrossRef](#)]
- Zugazagoitia, J.; Guedes, C.; Ponce, S.; Ferrer, I.; Molina-Pinelo, S.; Paz-Ares, L. Current challenges in cancer treatment. *Clin. Ther.* **2016**, *38*, 1551–1566. [[CrossRef](#)]
- Zhong, L.; Li, Y.; Xiong, L.; Wang, W.; Wu, M.; Yuan, T.; Yang, W.; Tian, C.; Miao, Z.; Wang, T. Small molecules in targeted cancer therapy: Advances, challenges, and future perspectives. *Signal Transduct. Target. Ther.* **2021**, *6*, 201. [[CrossRef](#)]
- Chakraborty, S.; Rahman, T. The difficulties in cancer treatment. *Ecancermedicalscience* **2012**, *6*, ed16.
- Shalini; Kumar, V. Have molecular hybrids delivered effective anticancer treatments and what should future drug discovery focus on? *Expert Opin. Drug Discov.* **2021**, *16*, 335–363. [[CrossRef](#)]
- Bass, A.K.; El-Zoghbi, M.S.; Nageeb, E.S.M.; Mohamed, M.F.; Badr, M.; Abuo-Rahma, G.E.D.A. Comprehensive review for anticancer hybridized multitargeting HDAC inhibitors. *Eur. J. Med. Chem.* **2021**, *209*, 112904. [[CrossRef](#)]
- Gediya, L.K.; Njar, V.C. Promise and challenges in drug discovery and development of hybrid anticancer drugs. *Expert Opin. Drug Discov.* **2009**, *4*, 1099–1111. [[CrossRef](#)]
- Moustafa, A.M.Y.; Bakare, S.B. Synthesis of some hybrid 7-hydroxy quinolinone derivatives as anti breast cancer drugs. *Res. Chem. Intermed.* **2019**, *45*, 3895–3912. [[CrossRef](#)]
- Nepali, K.; Sharma, S.; Sharma, M.; Bedi, P.; Dhar, K. Rational approaches, design strategies, structure activity relationship and mechanistic insights for anticancer hybrids. *Eur. J. Med. Chem.* **2014**, *77*, 422–487. [[CrossRef](#)]
- Decker, M. Hybrid molecules incorporating natural products: Applications in cancer therapy, neurodegenerative disorders and beyond. *Curr. Med. Chem.* **2011**, *18*, 1464–1475. [[CrossRef](#)]
- Kerru, N.; Singh, P.; Koorbanally, N.; Raj, R.; Kumar, V. Recent advances (2015–2016) in anticancer hybrids. *Eur. J. Med. Chem.* **2017**, *142*, 179–212. [[CrossRef](#)]
- Szumilak, M.; Wiktorowska-Owczarek, A.; Stanczak, A. Hybrid drugs—A strategy for overcoming anticancer drug resistance? *Molecules* **2021**, *26*, 2601. [[CrossRef](#)]
- Abbot, V.; Sharma, P.; Dhiman, S.; Noolvi, M.N.; Patel, H.M.; Bhardwaj, V. Small hybrid heteroaromatics: Resourceful biological tools in cancer research. *RSC Adv.* **2017**, *7*, 28313–28349. [[CrossRef](#)]
- Fortin, S.; Bérubé, G. Advances in the development of hybrid anticancer drugs. *Expert Opin. Drug Discov.* **2013**, *8*, 1029–1047. [[CrossRef](#)]
- Mishra, S.; Singh, P. Hybrid molecules: The privileged scaffolds for various pharmaceuticals. *Eur. J. Med. Chem.* **2016**, *124*, 500–536.
- Zheng, W.; Zhao, Y.; Luo, Q.; Zhang, Y.; Wu, K.; Wang, F. Multi-targeted anticancer agents. *Curr. Top. Med. Chem.* **2017**, *17*, 3084–3098. [[CrossRef](#)] [[PubMed](#)]

22. Chamseddine, I.M.; Rejniak, K.A. Hybrid modeling frameworks of tumor development and treatment. *Wiley Interdiscip. Rev. Syst. Biol. Med.* **2020**, *12*, e1461. [[CrossRef](#)] [[PubMed](#)]
23. Alagarsamy, V.; Chitra, K.; Saravanan, G.; Solomon, V.R.; Sulthana, M.; Narendhar, B. An overview of quinazolines: Pharmacological significance and recent developments. *Eur. J. Med. Chem.* **2018**, *151*, 628–685. [[CrossRef](#)] [[PubMed](#)]
24. Das, D.; Hong, J. Recent advancements of 4-aminoquinazoline derivatives as kinase inhibitors and their applications in medicinal chemistry. *Eur. J. Med. Chem.* **2019**, *170*, 55–72. [[CrossRef](#)]
25. Cheng, W.; Zhu, S.; Ma, X.; Qiu, N.; Peng, P.; Sheng, R.; Hu, Y. Design, synthesis and biological evaluation of 6-(nitroimidazole-1H-alkyloxy)-4-anilinoquinazolines as efficient EGFR inhibitors exerting cytotoxic effects both under normoxia and hypoxia. *Eur. J. Med. Chem.* **2015**, *89*, 826–834. [[CrossRef](#)]
26. Zhang, Y.; Gao, H.; Liu, R.; Liu, J.; Chen, L.; Li, X.; Zhao, L.; Wang, W.; Li, B. Quinazoline-1-deoxynojirimycin hybrids as high active dual inhibitors of EGFR and α -glucosidase. *Bioorg. Med. Chem. Lett.* **2017**, *27*, 4309–4313. [[CrossRef](#)]
27. Zhang, H.Q.; Gong, F.H.; Ye, J.Q.; Zhang, C.; Yue, X.H.; Li, C.G.; Xu, Y.G.; Sun, L.P. Design and discovery of 4-anilinoquinazoline-urea derivatives as dual TK inhibitors of EGFR and VEGFR-2. *Eur. J. Med. Chem.* **2017**, *125*, 245–254. [[CrossRef](#)]
28. Yadav, R.R.; Guru, S.K.; Joshi, P.; Mahajan, G.; Mintoo, M.J.; Kumar, V.; Bharate, S.S.; Mondhe, D.M.; Vishwakarma, R.A.; Bhushan, S. 6-Aryl substituted 4-(4-cyanomethyl) phenylamino quinazolines as a new class of isoform-selective PI3K- α inhibitors. *Eur. J. Med. Chem.* **2016**, *122*, 731–743. [[CrossRef](#)]
29. Ding, H.W.; Deng, C.L.; Li, D.D.; Liu, D.D.; Chai, S.M.; Wang, W.; Zhang, Y.; Chen, K.; Li, X.; Wang, J. Design, synthesis and biological evaluation of novel 4-aminoquinazolines as dual target inhibitors of EGFR-PI3K α . *Eur. J. Med. Chem.* **2018**, *146*, 460–470. [[CrossRef](#)]
30. Fan, Y.H.; Ding, H.W.; Liu, D.D.; Song, H.R.; Xu, Y.N.; Wang, J. Novel 4-aminoquinazoline derivatives induce growth inhibition, cell cycle arrest and apoptosis via PI3K α inhibition. *Bioorg. Med. Chem.* **2018**, *26*, 1675–1685. [[CrossRef](#)]
31. Fröhlich, T.; Reiter, C.; Ibrahim, M.M.; Beutel, J.; Hutterer, C.; Zeitträger, I.; Bahsi, H.; Leidenberger, M.; Friedrich, O.; Kappes, B. Synthesis of novel hybrids of quinazoline and artemisinin with high activities against Plasmodium falciparum, human cytomegalovirus, and leukemia cells. *ACS Omega* **2017**, *2*, 2422–2431. [[CrossRef](#)]
32. Yang, S.M.; Urban, D.J.; Yoshioka, M.; Strovel, J.W.; Fletcher, S.; Wang, A.Q.; Xu, X.; Shah, P.; Hu, X.; Hall, M.D. Discovery and lead identification of quinazoline-based BRD4 inhibitors. *Bioorg. Med. Chem. Lett.* **2018**, *28*, 3483–3488. [[CrossRef](#)]
33. Lee, H.A.; Hyun, S.A.; Byun, B.; Chae, J.H.; Kim, K.S. Electrophysiological mechanisms of vandetanib-induced cardiotoxicity: Comparison of action potentials in rabbit Purkinje fibers and pluripotent stem cell-derived cardiomyocytes. *PLoS ONE* **2018**, *13*, e0195577. [[CrossRef](#)]
34. Cheng, C.C.; Chang, J.; Huang, S.C.C.; Lin, H.C.; Ho, A.S.; Lim, K.H.; Chang, C.C.; Huang, L.; Chang, Y.C.; Chang, Y.F. YM155 as an inhibitor of cancer stemness simultaneously inhibits autophosphorylation of epidermal growth factor receptor and G9a-mediated stemness in lung cancer cells. *PLoS ONE* **2017**, *12*, e0182149. [[CrossRef](#)]
35. Han, W.; Pan, H.; Chen, Y.; Sun, J.; Wang, Y.; Li, J.; Ge, W.; Feng, L.; Lin, X.; Wang, X. EGFR tyrosine kinase inhibitors activate autophagy as a cytoprotective response in human lung cancer cells. *PLoS ONE* **2011**, *6*, e18691. [[CrossRef](#)]
36. Tabasum, S.; Singh, R.P. Fisetin suppresses migration, invasion and stem-cell-like phenotype of human non-small cell lung carcinoma cells via attenuation of epithelial to mesenchymal transition. *Chem. Biol. Interact.* **2019**, *303*, 14–21. [[CrossRef](#)]
37. Eno, M.R.; El-Gendy, B.E.D.M.; Cameron, M.D. P450 3A-catalyzed O-dealkylation of lapatinib induces mitochondrial stress and activates Nrf2. *Chem. Res. Toxicol.* **2016**, *29*, 784–796. [[CrossRef](#)]
38. Pham, H.T.T.; Maurer, B.; Prchal-Murphy, M.; Grausenburger, R.; Grundschober, E.; Javaheri, T.; Nivarthi, H.; Boersma, A.; Kolbe, T.; Elabd, M. STAT5B N642H is a driver mutation for T cell neoplasia. *J. Clin. Investig.* **2018**, *128*, 387–401. [[CrossRef](#)]
39. Sun, H.; Mediwala, S.N.; Szafran, A.T.; Mancini, M.A.; Marcelli, M. CUDC-101, a novel inhibitor of full-length androgen receptor (fAR) and androgen receptor variant 7 (AR-V7) activity: Mechanism of action and in vivo efficacy. *Horm. Cancer* **2016**, *7*, 196–210. [[CrossRef](#)]
40. Zhou, Y.; Li, Y.; Ni, H.M.; Ding, W.X.; Zhong, H. Nrf2 but not autophagy inhibition is associated with the survival of wild-type epidermal growth factor receptor non-small cell lung cancer cells. *Toxicol. Appl. Pharmacol.* **2016**, *310*, 140–149. [[CrossRef](#)]
41. Kumari, A.; Singh, R.K. Medicinal chemistry of indole derivatives: Current to future therapeutic prospectives. *Bioorg. Chem.* **2019**, *89*, 103021. [[CrossRef](#)] [[PubMed](#)]
42. Dadashpour, S.; Emami, S. Indole in the target-based design of anticancer agents: A versatile scaffold with diverse mechanisms. *Eur. J. Med. Chem.* **2018**, *150*, 9–29. [[CrossRef](#)] [[PubMed](#)]
43. Zhang, Y.; Yang, P.; Chou, C.J.; Liu, C.; Wang, X.; Xu, W. Development of N-hydroxycinnamide-based histone deacetylase inhibitors with an indole-containing cap group. *ACS Med. Chem. Lett.* **2013**, *4*, 235–238. [[CrossRef](#)] [[PubMed](#)]
44. Li, X.; Inks, E.S.; Li, X.; Hou, J.; Chou, C.J.; Zhang, J.; Jiang, Y.; Zhang, Y.; Xu, W. Discovery of the first N-hydroxycinnamide-based histone deacetylase 1/3 dual inhibitors with potent oral antitumor activity. *J. Med. Chem.* **2014**, *57*, 3324–3341. [[CrossRef](#)]
45. Mehndiratta, S.; Hsieh, Y.L.; Liu, Y.M.; Wang, A.W.; Lee, H.Y.; Liang, L.Y.; Kumar, S.; Teng, C.M.; Yang, C.R.; Liou, J.P. Indole-3-ethylsulfamoylphenylacrylamides: Potent histone deacetylase inhibitors with anti-inflammatory activity. *Eur. J. Med. Chem.* **2014**, *85*, 468–479. [[CrossRef](#)]
46. Panathur, N.; Dalimba, U.; Koushik, P.V.; Alvala, M.; Yogeewari, P.; Sriram, D.; Kumar, V. Identification and characterization of novel indole based small molecules as anticancer agents through SIRT1 inhibition. *Eur. J. Med. Chem.* **2013**, *69*, 125–138. [[CrossRef](#)]

47. Lee, J.; More, K.N.; Yang, S.A.; Hong, V.S. 3, 5-bis (aminopyrimidinyl) indole derivatives: Synthesis and evaluation of pim kinase inhibitory activities. *Bull. Korean Chem. Soc.* **2014**, *35*, 2123–2129. [[CrossRef](#)]
48. Mirzaei, H.; Shokrzadeh, M.; Modanloo, M.; Ziar, A.; Riazi, G.H.; Emami, S. New indole-based chalconoids as tubulin-targeting antiproliferative agents. *Bioorg. Chem.* **2017**, *75*, 86–98. [[CrossRef](#)]
49. Zhou, Y.; Duan, K.; Zhu, L.; Liu, Z.; Zhang, C.; Yang, L.; Li, M.; Zhang, H.; Yang, X. Synthesis and cytotoxic activity of novel hexahydropyrrolo [2, 3-b] indole imidazolium salts. *Bioorg. Med. Chem. Lett.* **2016**, *26*, 460–465. [[CrossRef](#)]
50. Kumar, D.; Kumar, N.M.; Tantak, M.P.; Ogura, M.; Kusaka, E.; Ito, T. Synthesis and identification of α -cyano bis (indolyl) chalcones as novel anticancer agents. *Bioorg. Med. Chem. Lett.* **2014**, *24*, 5170–5174. [[CrossRef](#)]
51. Kumar, S.; Gu, L.; Palma, G.; Kaur, M.; Singh-Pillay, A.; Singh, P.; Kumar, V. Design, synthesis, anti-proliferative evaluation and docking studies of 1 H-1, 2, 3-triazole tethered ospemifene–isatin conjugates as selective estrogen receptor modulators. *New J. Chem.* **2018**, *42*, 3703–3713. [[CrossRef](#)]
52. Sharma, B.; Singh, A.; Gu, L.; Saha, S.T.; Singh-Pillay, A.; Cele, N.; Singh, P.; Kaur, M.; Kumar, V. Diastereoselective approach to rationally design tetrahydro- β -carboline–isatin conjugates as potential SERMs against breast cancer. *RSC Adv.* **2019**, *9*, 9809–9819. [[CrossRef](#)]
53. Lindsay, C.R.; MacPherson, I.R.; Cassidy, J. Current status of cediranib: The rapid development of a novel anti-angiogenic therapy. *Future Oncol.* **2009**, *5*, 421–432. [[CrossRef](#)]
54. Song, F.; Hu, B.; Cheng, J.W.; Sun, Y.F.; Zhou, K.Q.; Wang, P.X.; Guo, W.; Zhou, J.; Fan, J.; Chen, Z. Anlotinib suppresses tumor progression via blocking the VEGFR2/PI3K/AKT cascade in intrahepatic cholangiocarcinoma. *Cell Death Dis.* **2020**, *11*, 573. [[CrossRef](#)]
55. Heldin, C.H.; Vanlandewijck, M.; Moustakas, A. Regulation of EMT by TGF β in cancer. *FEBS Lett.* **2012**, *586*, 1959–1970. [[CrossRef](#)]
56. Yaseen, A.; Chen, S.; Hock, S.; Rosato, R.; Dent, P.; Dai, Y.; Grant, S. Resveratrol sensitizes acute myelogenous leukemia cells to histone deacetylase inhibitors through reactive oxygen species-mediated activation of the extrinsic apoptotic pathway. *Mol. Pharmacol.* **2012**, *82*, 1030–1041. [[CrossRef](#)]
57. Kato, Y.; Salumbides, B.C.; Wang, X.F.; Qian, D.Z.; Williams, S.; Wei, Y.; Sanni, T.B.; Atadja, P.; Pili, R. Antitumor effect of the histone deacetylase inhibitor LAQ824 in combination with 13-cis-retinoic acid in human malignant melanoma. *Mol. Cancer Ther.* **2007**, *6*, 70–81. [[CrossRef](#)]
58. Gluszyńska, A. Biological potential of carbazole derivatives. *Eur. J. Med. Chem.* **2015**, *94*, 405–426. [[CrossRef](#)]
59. Issa, S.; Prandina, A.; Bedel, N.; Rongved, P.; Yous, S.; Le Borgne, M.; Bouaziz, Z. Carbazole scaffolds in cancer therapy: A review from 2012 to 2018. *J. Enzyme Inhib. Med. Chem.* **2019**, *34*, 1321–1346. [[CrossRef](#)]
60. Liu, L.X.; Wang, X.Q.; Zhou, B.; Yang, L.J.; Li, Y.; Zhang, H.B.; Yang, X.D. Synthesis and antitumor activity of novel N-substituted carbazole imidazolium salt derivatives. *Sci. Rep.* **2015**, *5*, 13101. [[CrossRef](#)]
61. Mongre, R.K.; Mishra, C.B.; Prakash, A.; Jung, S.; Lee, B.S.; Kumari, S.; Hong, J.T.; Lee, M.S. Novel carbazole-piperazine hybrid small molecule induces apoptosis by targeting BCL-2 and inhibits tumor progression in lung adenocarcinoma in vitro and xenograft mice model. *Cancers* **2019**, *11*, 1245. [[CrossRef](#)] [[PubMed](#)]
62. Rawjewski, R.A. Formulations of Indole-3-Carbinol Derived Antitumor Agents with Increased Oral Bioavailability. U.S. Patent 13/263,838, 19 July 2012.
63. Tucker, J.; Sviridov, S.; Brodsky, L.; Burkhart, C.; Purmal, A.; Gurova, K.; Gudkov, A. Carbazole Compounds and Therapeutic Uses of the Compounds. U.S. Patent 8,765,738, 4 June 2015.
64. Narayanan, R.; Miller, D.D.; Ponnusamy, T.; Hwang, D.J.; Pagadala, J.; Duke, C.B.; Coss, C.C.; Dalton, J.T.; He, Y. Selective Androgen Receptor Degradator (SARD) Ligands and Methods of Use Thereof. U.S. Patent 9,815,776 B2, 14 November 2017.
65. Ruiz-Ceja, K.A.; Chirino, Y.I. Current FDA-approved treatments for non-small cell lung cancer and potential biomarkers for its detection. *Biomed. Pharmacother.* **2017**, *90*, 24–37. [[CrossRef](#)] [[PubMed](#)]
66. Stone, R.M.; Manley, P.W.; Larson, R.A.; Capdeville, R. Midostaurin: Its odyssey from discovery to approval for treating acute myeloid leukemia and advanced systemic mastocytosis. *Blood Adv.* **2018**, *2*, 444–453. [[CrossRef](#)] [[PubMed](#)]
67. Huang, Y.C.; Chao, D.K.; Chao, K.C.; Chen, Y.J. Oral small-molecule tyrosine kinase inhibitor midostaurin (PKC412) inhibits growth and induces megakaryocytic differentiation in human leukemia cells. *Toxicol. Vitr.* **2009**, *23*, 979–985. [[CrossRef](#)]
68. Zhang, J.; Ren, L.; Yang, X.; White, M.; Greenhaw, J.; Harris, T.; Wu, Q.; Bryant, M.; Papoian, T.; Mattes, W. Cytotoxicity of 34 FDA approved small-molecule kinase inhibitors in primary rat and human hepatocytes. *Toxicol. Lett.* **2018**, *291*, 138–148. [[CrossRef](#)]
69. Hawkins, W.; Mitchell, C.; McKinstry, R.; Gilfor, D.; Starkey, J.; Dai, Y.; Dawson, K.; Ramakrishnan, V.; Roberts, J.D.; Yacoub, A. Transient exposure of mammary tumors to PD184352 and UCN-01 causes tumor cell death in vivo and prolonged suppression of tumor re-growth. *Cancer Biol. Ther.* **2005**, *4*, 1275–1284. [[CrossRef](#)]
70. Kumar, S.; Narasimhan, B. Therapeutic potential of heterocyclic pyrimidine scaffolds. *Chem. Cent. J.* **2018**, *12*, 38. [[CrossRef](#)]
71. Kaur, R.; Kaur, P.; Sharma, S.; Singh, G.; Mehndiratta, S.; MS Bedi, P.; Nepali, K. Anticancer pyrimidines in diverse scaffolds: A review of patent literature. *Recent Pat. Anticancer. Drug Discov.* **2015**, *10*, 23–71. [[CrossRef](#)]
72. Combs, A.P.; Li, Y.L.; Mei, S.; Yue, E.W. Substituted Diamino-Pyrimidine and Diamino-Pyridine Derivatives as PI3K Inhibitors. U.S. Patent 9,108,984, 18 August 2015.
73. Bloor, A.; Cheung, M.; Harris, P.A.; Hinkle, K.; Laudeman, C.P.; Stafford, J.A.; Veal, J.M. Chemical Compounds. Patent GB201201758D0, 1 February 2012.

74. Hogberg, M.; Dahlstedt, E.; Smitt, O.; Johansson, T. Novel Pyrimidine Derivatives. Patent WO2012127032, 27 September 2012.
75. Liu, J.; Mao, L.; Wang, X.; Xu, X.; Zhao, L. Pyrazolopyrimidine Derivatives and Uses as Anticancer Agents. Patent WO2012/097196 A, 19 July 2012.
76. Tanaka, M.; Zhang, C.; Shokat, K.M.; Burlingame, A.L.; Hansen, K.; Bateman, R.L.; DiMugno, S.G. Pyrazolo Pyrimidine Derivatives and Methods of Use Thereof. Patent US201313862348A, 12 March 2013.
77. Liang, C. mTOR Selective Kinase Inhibitors. U.S. Patent US20130072481, 21 March 2013.
78. Dorsch, D.; Hoelzemann, G.; Schiemann, K.; Wegener, A. Triazolo [4, 5-d] Pyrimidine Derivatives. Patent WO2013110309A1, 1 August 2013.
79. El-Sayed, N.S.; El-Bendary, E.R.; El-Ashry, S.M.; El-Kerdawy, M.M. Synthesis and antitumor activity of new sulfonamide derivatives of thiadiazolo [3, 2-a] pyrimidines. *Eur. J. Med. Chem.* **2011**, *46*, 3714–3720. [[CrossRef](#)]
80. Shao, H.; Shi, S.; Foley, D.W.; Lam, F.; Abbas, A.Y.; Liu, X.; Huang, S.; Jiang, X.; Baharin, N.; Fischer, P.M. Synthesis, structure–activity relationship and biological evaluation of 2, 4, 5-trisubstituted pyrimidine CDK inhibitors as potential anti-tumour agents. *Eur. J. Med. Chem.* **2013**, *70*, 447–455. [[CrossRef](#)]
81. Fares, M.; Abou-Seri, S.M.; Abdel-Aziz, H.A.; Abbas, S.E.S.; Youssef, M.M.; Eladwy, R.A. Synthesis and antitumor activity of pyrrolo [2, 3-d] pyrimidine and pyrido [2, 3-d] [1, 2, 4] triazolo [4, 3-a] pyrimidine derivatives that induce apoptosis through G1 cell-cycle arrest. *Eur. J. Med. Chem.* **2014**, *83*, 155–166. [[CrossRef](#)]
82. Kurumurthy, C.; Rao, P.S.; Rao, P.S.; Narsaiah, B.; Velatooru, L.; Pamanji, R.; Rao, J.V. Synthesis of novel alkyltriazole tagged pyrrolo [2, 3-d] pyrimidine derivatives and their anticancer activity. *Eur. J. Med. Chem.* **2011**, *46*, 3462–3468. [[CrossRef](#)]
83. Nagender, P.; Reddy, G.M.; Kumar, R.N.; Poornachandra, Y.; Kumar, C.G.; Narsaiah, B. Synthesis, cytotoxicity, antimicrobial and anti-biofilm activities of novel pyrazolo [3, 4-b] pyridine and pyrimidine functionalized 1, 2, 3-triazole derivatives. *Bioorg. Med. Chem. Lett.* **2014**, *24*, 2905–2908. [[CrossRef](#)]
84. Huang, Y.Y.; Wang, L.Y.; Chang, C.H.; Kuo, Y.H.; Kaneko, K.; Takayama, H.; Kimura, M.; Juang, S.H.; Wong, F.F. One-pot synthesis and antiproliferative evaluation of pyrazolo [3, 4-d] pyrimidine derivatives. *Tetrahedron* **2012**, *68*, 9658–9664. [[CrossRef](#)]
85. Han, M.; Shen, J.; Wang, L.; Wang, Y.; Zhai, X.; Li, Y.; Liu, M.; Li, Z.; Zuo, D.; Wu, Y. 5-chloro-N4-(2-(isopropylsulfonyl) phenyl)-N2-(2-methoxy-4-(4-(4-methylpiperazin-1-yl) methyl)-1H-1, 2, 3-triazol-1-yl) phenyl) pyrimidine-2, 4-diamine (WY-135), a novel ALK inhibitor, induces cell cycle arrest and apoptosis through inhibiting ALK and its downstream pathways in Karpas299 and H2228 cells. *Chem. Biol. Interact.* **2018**, *284*, 24–31.
86. The, I.; Ruijtenberg, S.; Bouchet, B.P.; Cristobal, A.; Prinsen, M.B.; van Mourik, T.; Koreth, J.; Xu, H.; Heck, A.J.; Akhmanova, A. Rb and FZR1/Cdh1 determine CDK4/6-cyclin D requirement in *C. elegans* and human cancer cells. *Nat. Commun.* **2015**, *6*, 5906. [[CrossRef](#)]
87. Ceribelli, M.; Kelly, P.N.; Shaffer, A.L.; Wright, G.W.; Xiao, W.; Yang, Y.; Mathews Griner, L.A.; Guha, R.; Shinn, P.; Keller, J.M. Blockade of oncogenic I κ B kinase activity in diffuse large B-cell lymphoma by bromodomain and extraterminal domain protein inhibitors. *Proc. Natl. Acad. Sci. USA* **2014**, *111*, 11365–11370. [[CrossRef](#)]
88. Matsui, T.; Miyamoto, K.; Yamanaka, K.; Okai, Y.; Kaushik, E.P.; Harada, K.; Wagoner, M.; Shinozawa, T. Cell-based two-dimensional morphological assessment system to predict cancer drug-induced cardiotoxicity using human induced pluripotent stem cell-derived cardiomyocytes. *Toxicol. Appl. Pharmacol.* **2019**, *383*, 114761. [[CrossRef](#)]
89. Chu, X.M.; Wang, C.; Liu, W.; Liang, L.L.; Gong, K.K.; Zhao, C.Y.; Sun, K.L. Quinoline and quinolone dimers and their biological activities: An overview. *Eur. J. Med. Chem.* **2019**, *161*, 101–117. [[CrossRef](#)]
90. Zhao, D.; Hamilton, J.P.; Pham, G.M.; Crisovan, E.; Wiegert-Rininger, K.; Vaillancourt, B.; DellaPenna, D.; Buell, C.R. De novo genome assembly of *Camptotheca acuminata*, a natural source of the anticancer compound camptothecin. *GigaScience* **2017**, *6*, gix065. [[CrossRef](#)]
91. Afzal, O.; Kumar, S.; Haider, M.R.; Ali, M.R.; Kumar, R.; Jaggi, M.; Bawa, S. A review on anticancer potential of bioactive heterocycle quinoline. *Eur. J. Med. Chem.* **2015**, *97*, 871–910. [[CrossRef](#)] [[PubMed](#)]
92. Sidoryk, K.; Świtalska, M.; Jaromin, A.; Cmoch, P.; Bujak, I.; Kaczmarska, M.; Wietrzyk, J.; Dominguez, E.G.; Żarnowski, R.; Andes, D.R. The synthesis of indolo [2, 3-b] quinoline derivatives with a guanidine group: Highly selective cytotoxic agents. *Eur. J. Med. Chem.* **2015**, *105*, 208–219. [[CrossRef](#)] [[PubMed](#)]
93. Gedawy, E.M.; Kassab, A.E.; El-Malah, A.A. Synthesis and anticancer activity of novel tetrahydroquinoline and tetrahydropyrimidoquinoline derivatives. *Med. Chem. Res.* **2015**, *24*, 3387–3397. [[CrossRef](#)]
94. González-Sánchez, I.; Solano, J.D.; Loza-Mejía, M.A.; Olvera-Vázquez, S.; Rodríguez-Sotres, R.; Morán, J.; Lira-Rocha, A.; Cerbón, M.A. Antineoplastic activity of the thiazolo [5, 4-b] quinoline derivative D3CLP in K-562 cells is mediated through effector caspases activation. *Eur. J. Med. Chem.* **2011**, *46*, 2102–2108. [[CrossRef](#)]
95. Luniewski, W.; Wietrzyk, J.; Godlewska, J.; Switalska, M.; Piskozub, M.; Peczynska-Czoch, W.; Kaczmarek, L. New derivatives of 11-methyl-6-[2-(dimethylamino) ethyl]-6H-indolo [2, 3-b] quinoline as cytotoxic DNA topoisomerase II inhibitors. *Bioorg. Med. Chem. Lett.* **2012**, *22*, 6103–6107. [[CrossRef](#)]
96. Jin, X.Y.; Chen, H.; Li, D.D.; Li, A.L.; Wang, W.Y.; Gu, W. Design, synthesis, and anticancer evaluation of novel quinoline derivatives of ursolic acid with hydrazide, oxadiazole, and thiadiazole moieties as potent MEK inhibitors. *J. Enzyme Inhib. Med. Chem.* **2019**, *34*, 955–972. [[CrossRef](#)]
97. Solomon, V.R.; Pundir, S.; Lee, H. Examination of novel 4-aminoquinoline derivatives designed and synthesized by a hybrid pharmacophore approach to enhance their anticancer activities. *Sci. Rep.* **2019**, *9*, 6315. [[CrossRef](#)]

98. Kumar, K.; Schniper, S.; González-Sarriás, A.; Holder, A.A.; Sanders, N.; Sullivan, D.; Jarrett, W.L.; Davis, K.; Bai, F.; Seeram, N.P. Highly potent anti-proliferative effects of a gallium (III) complex with 7-chloroquinoline thiosemicarbazone as a ligand: Synthesis, cytotoxic and antimalarial evaluation. *Eur. J. Med. Chem.* **2014**, *86*, 81–86. [[CrossRef](#)]
99. Capozzi, M.; De Divitiis, C.; Ottaiano, A.; von Arx, C.; Scala, S.; Tatangelo, F.; Delrio, P.; Tafuto, S. Lenvatinib, a molecule with versatile application: From preclinical evidence to future development in anticancer treatment. *Cancer Manag. Res.* **2019**, *11*, 3847–3860. [[CrossRef](#)]
100. Dong, H.; Wade, M.G. Application of a nonradioactive assay for high throughput screening for inhibition of thyroid hormone uptake via the transmembrane transporter MCT8. *Toxicol. Vitro.* **2017**, *40*, 234–242. [[CrossRef](#)]
101. Pereyra, C.E.; Dantas, R.F.; Ferreira, S.B.; Gomes, L.P.; Silva, F.P., Jr. The diverse mechanisms and anticancer potential of naphthoquinones. *Cancer Cell Int.* **2019**, *19*, 207. [[CrossRef](#)]
102. Powis, G. Free radical formation by antitumor quinones. *Free Radic. Biol. Med.* **1989**, *6*, 63–101. [[CrossRef](#)]
103. Marković, V.; Debeljak, N.; Stanojković, T.; Kolundžija, B.; Sladić, D.; Vujčić, M.; Janović, B.; Tanić, N.; Perović, M.; Tešić, V. Anthraquinone–chalcone hybrids: Synthesis, preliminary antiproliferative evaluation and DNA-interaction studies. *Eur. J. Med. Chem.* **2015**, *89*, 401–410. [[CrossRef](#)]
104. Jiang, X.; Wang, M.; Song, S.; Xu, Y.; Miao, Z.; Zhang, A. Design, synthesis, and anticancer activities of new compounds bearing the quinone–pyran–lactone tricyclic pharmacophore. *RSC Adv.* **2015**, *5*, 27502–27508. [[CrossRef](#)]
105. Ali, I.; Lone, M.N.; Aboul-Enein, H.Y. Imidazoles as potential anticancer agents. *Med. Chem. Comm.* **2017**, *8*, 1742–1773. [[CrossRef](#)]
106. Wan, W.C.; Chen, W.; Liu, L.X.; Li, Y.; Yang, L.J.; Deng, X.Y.; Zhang, H.B.; Yang, X.D. Synthesis and cytotoxic activity of novel hybrid compounds between 2-alkylbenzofuran and imidazole. *Med. Chem. Res.* **2014**, *23*, 1599–1611. [[CrossRef](#)]
107. Bhatnagar, A.; Sharma, P.; Kumar, N. A review on “Imidazoles”: Their chemistry and pharmacological potentials. *Int. J. Pharm. Tech. Res.* **2011**, *3*, 268–282.
108. Narasimhan, B.; Sharma, D.; Kumar, P. Biological importance of imidazole nucleus in the new millennium. *Med. Chem. Res.* **2011**, *20*, 1119–1140. [[CrossRef](#)]
109. Yang, X.D.; Wan, W.C.; Deng, X.Y.; Li, Y.; Yang, L.J.; Li, L.; Zhang, H.B. Design, synthesis and cytotoxic activities of novel hybrid compounds between 2-phenylbenzofuran and imidazole. *Bioorg. Med. Chem. Lett.* **2012**, *22*, 2726–2729. [[CrossRef](#)]
110. Chen, W.; Deng, X.Y.; Li, Y.; Yang, L.J.; Wan, W.C.; Wang, X.Q.; Zhang, H.B.; Yang, X.D. Synthesis and cytotoxic activities of novel hybrid 2-phenyl-3-alkylbenzofuran and imidazole/triazole compounds. *Bioorg. Med. Chem. Lett.* **2013**, *23*, 4297–4302. [[CrossRef](#)]
111. Al-Blewi, F.; Shaikh, S.A.; Naqvi, A.; Aljohani, F.; Aouad, M.R.; Ihmaid, S.; Rezki, N. Design and synthesis of novel imidazole derivatives possessing triazole pharmacophore with potent anticancer activity, and in silico ADMET with GSK-3 β molecular docking investigations. *Int. J. Mol. Sci.* **2021**, *22*, 1162. [[CrossRef](#)]
112. Hu, Y.; Li, N.; Zhang, J.; Wang, Y.; Chen, L.; Sun, J. Artemisinin-indole and artemisinin-imidazole hybrids: Synthesis, cytotoxic evaluation and reversal effects on multidrug resistance in MCF-7/ADR cells. *Bioorg. Med. Chem. Lett.* **2019**, *29*, 1138–1142. [[CrossRef](#)]
113. Song, W.J.; Yang, X.D.; Zeng, X.H.; Xu, X.L.; Zhang, G.L.; Zhang, H.B. Synthesis and cytotoxic activities of novel hybrid compounds of imidazole scaffold-based 2-substituted benzofurans. *RSC Adv.* **2012**, *2*, 4612–4615. [[CrossRef](#)]
114. Di Martino, S.; Rainone, A.; Troise, A.; Di Paolo, M.; Pugliese, S.; Zappavigna, S.; Grimaldi, A.; Valente, D. Overview of FDA-approved anti cancer drugs used for targeted therapy. *WCRJ* **2015**, *2*, e553WCRJ.
115. Sun, J.; Wei, Q.; Zhou, Y.; Wang, J.; Liu, Q.; Xu, H. A systematic analysis of FDA-approved anticancer drugs. *BMC Syst. Biol.* **2017**, *11*, 87. [[CrossRef](#)]
116. Khojasteh Poor, F.; Keivan, M.; Ramazii, M.; Ghaedrahmati, F.; Anbiyaiee, A.; Panahandeh, S.; Khoshnam, S.E.; Farzaneh, M. Mini review: The FDA-approved prescription drugs that target the MAPK signaling pathway in women with breast cancer. *Breast Dis.* **2021**, *40*, 51–62. [[CrossRef](#)] [[PubMed](#)]
117. Tan, H.W.; Mo, H.Y.; Lau, A.T.; Xu, Y.M. Selenium species: Current status and potentials in cancer prevention and therapy. *Int. J. Mol. Sci.* **2018**, *20*, 75. [[CrossRef](#)]
118. He, X.; Zhong, M.; Li, S.; Li, X.; Li, Y.; Li, Z.; Gao, Y.; Ding, F.; Wen, D.; Lei, Y. Synthesis and biological evaluation of organoselenium (NSAIDs–SeCN and SeCF₃) derivatives as potential anticancer agents. *Eur. J. Med. Chem.* **2020**, *208*, 112864. [[CrossRef](#)]
119. Gandin, V.; Khalkar, P.; Braude, J.; Fernandes, A.P. Organic selenium compounds as potential chemotherapeutic agents for improved cancer treatment. *Free Radic. Biol. Med.* **2018**, *127*, 80–97. [[CrossRef](#)]
120. Jardim, G.A.; da Cruz, E.H.; Valença, W.O.; Lima, D.J.; Cavalcanti, B.C.; Pessoa, C.; Rafique, J.; Braga, A.L.; Jacob, C.; da Silva Júnior, E.N. Synthesis of selenium–quinone hybrid compounds with potential antitumor activity via Rh-catalyzed CH bond activation and click reactions. *Molecules* **2017**, *23*, 83. [[CrossRef](#)]
121. An, B.; Zhang, S.; Hu, J.; Pan, T.; Huang, L.; Tang, J.C.O.; Li, X.; Chan, A.S. The design, synthesis and evaluation of selenium-containing 4-anilinoquinazoline hybrids as anticancer agents and a study of their mechanism. *Org. Biomol. Chem.* **2018**, *16*, 4701–4714. [[CrossRef](#)] [[PubMed](#)]
122. Tang, H.; Liang, Y.; Cheng, J.; Ding, K.; Wang, Y. Bifunctional chiral selenium-containing 1, 4-diarylazetid-2-ones with potent antitumor activities by disrupting tubulin polymerization and inducing reactive oxygen species production. *Eur. J. Med. Chem.* **2021**, *221*, 113531. [[CrossRef](#)] [[PubMed](#)]
123. Huang, S.; Sheng, X.; Bian, M.; Yang, Z.; Lu, Y.; Liu, W. Synthesis and *in vitro* anticancer activities of selenium N-heterocyclic carbene compounds. *Chem. Biol. Drug Des.* **2021**, *98*, 435–444. [[CrossRef](#)] [[PubMed](#)]

124. Rottenberg, S.; Disler, C.; Perego, P. The rediscovery of platinum-based cancer therapy. *Nat. Rev. Cancer* **2021**, *21*, 37–50. [[CrossRef](#)]
125. Ndagi, U.; Mhlongo, N.; Soliman, M.E. Metal complexes in cancer therapy—an update from drug design perspective. *Drug Des. Dev. Ther.* **2017**, *11*, 599–616. [[CrossRef](#)]
126. Ciarimboli, G. Anticancer Platinum Drugs Update. *Biomolecules* **2021**, *11*, 1637. [[CrossRef](#)]
127. Zajda, J.; Wróblewska, A.; Ruzik, L.; Matczuk, M. Methodology for characterization of platinum-based drug's targeted delivery nanosystems. *J. Control. Release* **2021**, *335*, 178–190. [[CrossRef](#)]
128. Johnstone, T.C.; Park, G.Y.; Lippard, S.J. Understanding and improving platinum anticancer drugs—phenanthriplatin. *Anticancer Res.* **2014**, *34*, 471–476.
129. Graham, L.A.; Suryadi, J.; West, T.K.; Kucera, G.L.; Bierbach, U. Synthesis, aqueous reactivity, and biological evaluation of carboxylic acid ester-functionalized platinum–acridine hybrid anticancer agents. *J. Med. Chem.* **2012**, *55*, 7817–7827. [[CrossRef](#)]
130. Zhao, J.; Gou, S.; Sun, Y.; Fang, L.; Wang, Z. Antitumor platinum (II) complexes containing platinum-based moieties of present platinum drugs and furoxan groups as nitric oxide donors: Synthesis, DNA interaction, and cytotoxicity. *Inorg. Chem.* **2012**, *51*, 10317–10324. [[CrossRef](#)]
131. Liu, Z.; Li, Z.; Du, T.; Chen, Y.; Wang, Q.; Li, G.; Liu, M.; Zhang, N.; Li, D.; Han, J. Design, synthesis and biological evaluation of dihydro-2-quinolone platinum (IV) hybrids as antitumor agents displaying mitochondria injury and DNA damage mechanism. *Dalton Trans.* **2021**, *50*, 362–375. [[CrossRef](#)]
132. Chen, Y.; Wang, Q.; Li, Z.; Liu, Z.; Zhao, Y.; Zhang, J.; Liu, M.; Wang, Z.; Li, D.; Han, J. Naproxen platinum (iv) hybrids inhibiting cyclooxygenases and matrix metalloproteinases and causing DNA damage: Synthesis and biological evaluation as antitumor agents in vitro and in vivo. *Dalton Trans.* **2020**, *49*, 5192–5204. [[CrossRef](#)]
133. Cincinelli, R.; Musso, L.; Dallavalle, S.; Artali, R.; Tinelli, S.; Colangelo, D.; Zunino, F.; De Cesare, M.; Beretta, G.L.; Zaffaroni, N. Design, modeling, synthesis and biological activity evaluation of camptothecin-linked platinum anticancer agents. *Eur. J. Med. Chem.* **2013**, *63*, 387–400. [[CrossRef](#)]
134. Zhou, J.; Kang, Y.; Chen, L.; Wang, H.; Liu, J.; Zeng, S.; Yu, L. The drug-resistance mechanisms of five platinum-based antitumor agents. *Front. Pharmacol.* **2020**, *11*, 343. [[CrossRef](#)]
135. Dilruba, S.; Kalayda, G.V. Platinum-based drugs: Past, present and future. *Cancer Chemother. Pharmacol.* **2016**, *77*, 1103–1124. [[CrossRef](#)]
136. Ha, V.T.; Kien, V.T.; Binh, L.H.; Tien, V.D.; My, N.T.T.; Nam, N.H.; Baltas, M.; Hahn, H.; Han, B.W.; Thao, D.T.; et al. Design, synthesis and biological evaluation of novel hydroxamic acids bearing artemisinin skeleton. *Bioorg. Chem.* **2016**, *66*, 63–71. [[CrossRef](#)]
137. Ling, Y.; Guo, J.; Yang, Q.; Zhu, P.; Miao, J.; Gao, W.; Peng, Y.; Yang, J.; Xu, K.; Xiong, B.; et al. Development of novel β -carboline-based hydroxamate derivatives as HDAC inhibitors with antiproliferative and antimetastatic activities in human cancer cells. *Eur. J. Med. Chem.* **2018**, *144*, 398–409. [[CrossRef](#)]
138. Mohamed, M.F.A.; Shaykoon, M.S.A.; Abdelrahman, M.H.; Elsadek, B.E.M.; Aboaraia, A.S.; Abu-Rahma, G. Design, synthesis, docking studies and biological evaluation of novel chalcone derivatives as potential histone deacetylase inhibitors. *Bioorg. Chem.* **2017**, *72*, 32–41. [[CrossRef](#)]
139. Ding, C.; Chen, S.; Zhang, C.; Hu, G.; Zhang, W.; Li, L.; Chen, Y.Z.; Tan, C.; Jiang, Y. Synthesis and investigation of novel 6-(1,2,3-triazol-4-yl)-4-aminoquinazolin derivatives possessing hydroxamic acid moiety for cancer therapy. *Bioorg. Med. Chem.* **2017**, *25*, 27–37. [[CrossRef](#)]
140. Dung, D.T.M.; Dung, P.T.P.; Oanh, D.T.K.; Vu, T.K.; Hahn, H.; Han, B.W.; Pyo, M.; Kim, Y.G.; Han, S.B.; Nam, N.H. Exploration of novel 5'(7')-substituted-2'-oxospiro[1,3]dioxolane-2,3'-indoline-based N-hydroxypropenamides as histone deacetylase inhibitors and antitumor agents. *Arab. J. Chem.* **2017**, *10*, 465–472. [[CrossRef](#)]
141. Bubna, A.K. Vorinostat-An Overview. *Indian J. Dermatol.* **2015**, *60*, 419. [[CrossRef](#)]
142. Moore, D. Panobinostat (Farydak): A Novel Option for the Treatment of Relapsed Or Relapsed and Refractory Multiple Myeloma. *Pharm. Ther.* **2016**, *41*, 296–300.
143. Tak, W.Y.; Ryoo, B.Y.; Lim, H.Y.; Kim, D.Y.; Okusaka, T.; Ikeda, M.; Hidaka, H.; Yeon, J.E.; Mizukoshi, E.; Morimoto, M.; et al. Phase I/II study of first-line combination therapy with sorafenib plus resminostat, an oral HDAC inhibitor, versus sorafenib monotherapy for advanced hepatocellular carcinoma in east Asian patients. *Investig. New Drugs* **2018**, *36*, 1072–1084. [[CrossRef](#)]
144. Alam, M.A. Methods for Hydroxamic Acid Synthesis. *Curr. Org. Chem.* **2019**, *23*, 978–993. [[CrossRef](#)]
145. Quirante, J.; Dubar, F.; González, A.; Lopez, C.; Cascante, M.; Cortés, R.; Forfar, I.; Pradines, B.; Biot, C. Ferrocene–indole hybrids for cancer and malaria therapy. *J. Organomet. Chem.* **2011**, *696*, 1011–1017. [[CrossRef](#)]
146. Huang, X.F.; Wang, L.Z.; Tang, L.; Lu, Y.X.; Wang, F.; Song, G.Q.; Ruan, B.F. Synthesis, characterization and antitumor activity of novel ferrocene derivatives containing pyrazolyl-moiety. *J. Organomet. Chem.* **2014**, *749*, 157–162. [[CrossRef](#)]
147. Smit, F.J.; Bezuidenhout, J.J.; Bezuidenhout, C.C.; N'Da, D.D. Synthesis and *in vitro* biological activities of ferrocenyl–chalcone amides. *Med. Chem. Res.* **2016**, *25*, 568–584. [[CrossRef](#)]
148. Wei, J.N.; Jia, Z.D.; Zhou, Y.Q.; Chen, P.H.; Li, B.; Zhang, N.; Hao, X.Q.; Xu, Y.; Zhang, B. Synthesis, characterization and antitumor activity of novel ferrocene-coumarin conjugates. *J. Organomet. Chem.* **2019**, *902*, 120968. [[CrossRef](#)]
149. Panaka, S.; Trivedi, R.; Jaipal, K.; Giribabu, L.; Sujitha, P.; Kumar, C.G.; Sridhar, B. Ferrocenyl chalcogeno (sugar) triazole conjugates: Synthesis, characterization and anticancer properties. *J. Organomet. Chem.* **2016**, *813*, 125–130. [[CrossRef](#)]

150. Raghavan, S.; Manogaran, P.; Gadepalli Narasimha, K.K.; Kalpattu Kuppasami, B.; Mariyappan, P.; Gopalakrishnan, A.; Venkatraman, G. Synthesis and anticancer activity of novel curcumin–quinolone hybrids. *Bioorg. Med. Chem. Lett.* **2015**, *25*, 3601–3605. [[CrossRef](#)]
151. Banupriya, G.; Sribalan, R.; Padmini, V. Synthesis and characterization of curcumin-sulfonamide hybrids: Biological evaluation and molecular docking studies. *J. Mol. Struct.* **2018**, *1155*, 90–100. [[CrossRef](#)]
152. Puneeth, H.R.; Ananda, H.; Kumar, K.S.S.; Rangappa, K.S.; Sharada, A.C. Synthesis and antiproliferative studies of curcumin pyrazole derivatives. *Med. Chem. Res.* **2016**, *25*, 1842–1851. [[CrossRef](#)]
153. Qiu, P.; Xu, L.; Gao, L.; Zhang, M.; Wang, S.; Tong, S.; Sun, Y.; Zhang, L.; Jiang, T. Exploring pyrimidine-substituted curcumin analogues: Design, synthesis and effects on EGFR signaling. *Bioorg. Med. Chem.* **2013**, *21*, 5012–5020. [[CrossRef](#)] [[PubMed](#)]
154. Sharma, S.; Gupta, M.K.; Saxena, A.K.; Bedi, P.M.S. Triazole linked mono carbonyl curcumin-isatin bifunctional hybrids as novel anti tubulin agents: Design, synthesis, biological evaluation and molecular modeling studies. *Bioorg. Med. Chem.* **2015**, *23*, 7165–7180. [[CrossRef](#)]
155. Ma, L.Y.; Wang, B.; Pang, L.P.; Zhang, M.; Wang, S.Q.; Zheng, Y.C.; Shao, K.P.; Xue, D.Q.; Liu, H.M. Design and synthesis of novel 1,2,3-triazole–pyrimidine–urea hybrids as potential anticancer agents. *Bioorg. Med. Chem. Lett.* **2015**, *25*, 1124–1128. [[CrossRef](#)]
156. Chandrashekar, M.; Nayak, V.L.; Ramakrishna, S.; Mallavadhani, U.V. Novel triazole hybrids of myrrhanone C, a natural polydopane triterpene: Synthesis, cytotoxic activity and cell based studies. *Eur. J. Med. Chem.* **2016**, *114*, 293–307. [[CrossRef](#)]
157. Najafi, Z.; Mahdavi, M.; Safavi, M.; Saeedi, M.; Alinezhad, H.; Pordeli, M.; Kabudanian Ardestani, S.; Shafiee, A.; Foroumadi, A.; Akbarzadeh, T. Synthesis and In vitro Cytotoxic Activity of Novel Triazole-Isoxazole Derivatives. *J. Heterocycl. Chem.* **2015**, *52*, 1743–1747. [[CrossRef](#)]
158. Duan, Y.C.; Ma, Y.C.; Zhang, E.; Shi, X.J.; Wang, M.M.; Ye, X.W.; Liu, H.M. Design and synthesis of novel 1,2,3-triazole-dithiocarbamate hybrids as potential anticancer agents. *Eur. J. Med. Chem.* **2013**, *62*, 11–19. [[CrossRef](#)]
159. Kumbhare, R.M.; Dadmal, T.L.; Ramaiah, M.J.; Kishore, K.S.V.; Pushpa Valli, S.N.C.V.L.; Tiwari, S.K.; Appalanaidu, K.; Rao, Y.K.; Bhadra, M.P. Synthesis and anticancer evaluation of novel triazole linked N-(pyrimidin-2-yl)benzo[d]thiazol-2-amine derivatives as inhibitors of cell survival proteins and inducers of apoptosis in MCF-7 breast cancer cells. *Bioorg. Med. Chem. Lett.* **2015**, *25*, 654–658. [[CrossRef](#)]
160. Sivaramakarthykeyan, R.; Iniyaval, S.; Saravanan, V.; Lim, W.M.; Mai, C.W.; Ramalingan, C. Molecular Hybrids Integrated with Benzimidazole and Pyrazole Structural Motifs: Design, Synthesis, Biological Evaluation, and Molecular Docking Studies. *ACS Omega* **2020**, *5*, 10089–10098. [[CrossRef](#)]
161. Shao, K.P.; Zhang, X.Y.; Chen, P.J.; Xue, D.Q.; He, P.; Ma, L.Y.; Zheng, J.X.; Zhang, Q.R.; Liu, H.M. Synthesis and biological evaluation of novel pyrimidine–benzimidazol hybrids as potential anticancer agents. *Bioorg. Med. Chem. Lett.* **2014**, *24*, 3877–3881. [[CrossRef](#)]
162. Sharma, P.; Srinivasa Reddy, T.; Thummuri, D.; Senwar, K.R.; Praveen Kumar, N.; Naidu, V.G.M.; Bhargava, S.K.; Shankaraiah, N. Synthesis and biological evaluation of new benzimidazole-thiazolidinedione hybrids as potential cytotoxic and apoptosis inducing agents. *Eur. J. Med. Chem.* **2016**, *124*, 608–621. [[CrossRef](#)]
163. Shi, L.; Wu, T.T.; Wang, Z.; Xue, J.Y.; Xu, Y.G. Discovery of quinazolin-4-amines bearing benzimidazole fragments as dual inhibitors of c-Met and VEGFR-2. *Bioorg. Med. Chem.* **2014**, *22*, 4735–4744. [[CrossRef](#)]
164. Sireesha, R.; Sreenivasulu, R.; Chandrasekhar, C.; Jadav, S.S.; Pavani, Y.; Rao, M.V.B.; Subbarao, M. Design, synthesis, anticancer evaluation and binding mode studies of benzimidazole/benzoxazole linked β -carboline derivatives. *J. Mol. Struct.* **2021**, *1226*, 129351. [[CrossRef](#)]
165. Kim, E.S. Abemaciclib: First Global Approval. *Drugs* **2017**, *77*, 2063–2070. [[CrossRef](#)]
166. Ghisoni, E.; Giannone, G.; Tuninetti, V.; Genta, S.; Scotto, G.; Aglietta, M.; Sangiolo, D.; Mittica, G.; Valabrega, G. Veliparib: A new therapeutic option in ovarian cancer? *Future Oncol.* **2019**, *15*, 1975–1987. [[CrossRef](#)]
167. Choi, Y.J.; Kim, H.S.; Park, S.H.; Kim, B.S.; Kim, K.H.; Lee, H.J.; Song, H.S.; Shin, D.Y.; Lee, H.Y.; Kim, H.G.; et al. Phase II Study of Dovitinib in Patients with Castration-Resistant Prostate Cancer (KCSG-GU11-05). *Cancer Res. Treat.* **2018**, *50*, 1252–1259. [[CrossRef](#)] [[PubMed](#)]
168. Cui, J.; Xiao, Z.; Zhang, L.L. Clinical efficacy and safety of nazartinib for epidermal growth factor receptor mutated non-small cell lung cancer: Study protocol for a prospective, multicenter, open-label. *Medicine* **2021**, *100*, e25992. [[CrossRef](#)]
169. Karthikeyan, C.; Solomon, V.R.; Lee, H.; Trivedi, P.J.B.; Nutrition, P. Design, synthesis and biological evaluation of some isatin-linked chalcones as novel anti-breast cancer agents: A molecular hybridization approach. *Biomed. Prev. Nutr.* **2013**, *3*, 325–330. [[CrossRef](#)]
170. Eldehna, W.M.; El Hassab, M.A.; Abo-Ashour, M.F.; Al-Warhi, T.; Elaasser, M.M.; Safwat, N.A.; Suliman, H.; Ahmed, M.F.; Al-Rashood, S.T.; Abdel-Aziz, H.A.J.B.C. Development of isatin-thiazolo [3, 2-a] benzimidazole hybrids as novel CDK2 inhibitors with potent in vitro apoptotic anti-proliferative activity: Synthesis, biological and molecular dynamics investigations. *Bioorg. Chem.* **2021**, *110*, 104748. [[CrossRef](#)]
171. Abdel-Aziz, H.A.; Eldehna, W.M.; Keeton, A.B.; Piazza, G.A.; Kadi, A.A.; Attwa, M.W.; Abdelhameed, A.S.; Attia, M.I.J.D.D. Development; Therapy, Isatin-benzoxazine molecular hybrids as potential antiproliferative agents: Synthesis and in vitro pharmacological profiling. *Drug Des. Dev. Ther.* **2017**, *11*, 2333–2346. [[CrossRef](#)] [[PubMed](#)]

172. Meleddu, R.; Petrikaite, V.; Distinto, S.; Arridu, A.; Angius, R.; Serusi, L.; Škarnulytė, L.; Endriulaitytė, U.; Paškevičiūtė, M.; Cottiglia, F.J.A.M.C.L. Investigating the anticancer activity of isatin/dihydropyrazole hybrids. *ACS Med. Chem. Lett.* **2018**, *10*, 571–576. [[CrossRef](#)] [[PubMed](#)]
173. Eldehna, W.M.; Altoukhy, A.; Mahrous, H.; Abdel-Aziz, H.A. Design, synthesis and QSAR study of certain isatin-pyridine hybrids as potential anti-proliferative agents. *Eur. J. Med. Chem.* **2015**, *90*, 684–694. [[CrossRef](#)] [[PubMed](#)]
174. Singh, H.; Singh, J.V.; Gupta, M.K.; Saxena, A.K.; Sharma, S.; Nepali, K.; Bedi, P.M.S.J.B.; Letters, M.C. Triazole tethered isatin-coumarin based molecular hybrids as novel antitubulin agents: Design, synthesis, biological investigation and docking studies. *Bioorg. Med. Chem. Lett.* **2017**, *27*, 3974–3979. [[CrossRef](#)]
175. Al-Wabli, R.I.; Almomen, A.A.; Almutairi, M.S.; Keeton, A.B.; Piazza, G.A.; Attia, M.I. New Isatin–Indole Conjugates: Synthesis, Characterization, and a Plausible Mechanism of Their in vitro Antiproliferative Activity. *Drug Des. Dev. Ther.* **2020**, *14*, 483–495. [[CrossRef](#)]
176. Panga, S.; Podila, N.K.; Asres, K.; Ciddi, V. Synthesis and anticancer activity of new isatin-benzoic acid conjugates. *Ethiop. Pharm. J.* **2016**, *31*, 75–92. [[CrossRef](#)]
177. Cheke, R.S.; Patil, V.M.; Firke, S.D.; Ambhore, J.P.; Ansari, I.A.; Patel, H.M.; Shinde, S.D.; Pasupuleti, V.R.; Hassan, M.I.; Adnan, M.J.P. Therapeutic Outcomes of Isatin and Its Derivatives against Multiple Diseases: Recent Developments in Drug Discovery. *Pharmaceuticals* **2022**, *15*, 272. [[CrossRef](#)]
178. Ferguson, L.; Bhakta, S.; Fox, K.R.; Wells, G.; Brucoli, F.J.M. Synthesis and Biological Evaluation of a Novel C8-Pyrrolobenzodiazepine (PBD) Adenosine Conjugate. A Study on the Role of the PBD Ring in the Biological Activity of PBD-Conjugates. *Molecules* **2020**, *25*, 1243. [[CrossRef](#)]
179. Bose, D.S.; Idrees, M.; Todewale, I.K.; Jakka, N.; Rao, J.V. Hybrids of privileged structures benzothiazoles and pyrrolo [2, 1-c][1, 4] benzodiazepin-5-one, and diversity-oriented synthesis of benzothiazoles. *Eur. J. Med. Chem.* **2012**, *50*, 27–38. [[CrossRef](#)]
180. Kamal, A.; Ramakrishna, G.; Nayak, V.L.; Raju, P.; Rao, A.S.; Viswanath, A.; Vishnuvardhan, M.; Ramakrishna, S.; Srinivas, G. Design and synthesis of benzo [c, d] indolone-pyrrolobenzodiazepine conjugates as potential anticancer agents. *Bioorg. Med. Chem.* **2012**, *20*, 789–800. [[CrossRef](#)]
181. Li, Y.; Quan, J.; Song, H.; Li, D.; Ma, E.; Wang, Y.; Ma, C. Novel pyrrolo [2, 1-c][1, 4] benzodiazepine-3, 11-dione (PBD) derivatives as selective HDAC6 inhibitors to suppress tumor metastasis and invasion in vitro and in vivo. *Bioorg. Chem.* **2021**, *114*, 105081. [[CrossRef](#)]
182. Chen, C.Y.; Lee, P.H.; Lin, Y.Y.; Yu, W.T.; Hu, W.P.; Hsu, C.C.; Lin, Y.T.; Chang, L.S.; Hsiao, C.T.; Wang, J.-J.; et al. Synthesis, DNA-binding abilities and anticancer activities of triazole-pyrrolo [2, 1-c][1, 4] benzodiazepines hybrid scaffolds. *Bioorg. Med. Chem. Lett.* **2013**, *23*, 6854–6859. [[CrossRef](#)]
183. Al Zahrani, N.A.; El-Shishtawy, R.M.; Elaasser, M.M.; Asiri, A.M. Synthesis of novel chalcone-based phenothiazine derivatives as antioxidant and anticancer agents. *Molecules* **2020**, *25*, 4566. [[CrossRef](#)]
184. Ouyang, Y.; Li, J.; Chen, X.; Fu, X.; Sun, S.; Wu, Q. Chalcone Derivatives: Role in Anticancer Therapy. *Biomolecules* **2021**, *11*, 894. [[CrossRef](#)]
185. Sivapriya, S.; Sivakumar, K.; Manikandan, H. Anticancer effects of chalcone-benzoxadiazole hybrids on KB human cancer cells. *Chem. Data Collect.* **2021**, *35*, 100762. [[CrossRef](#)]
186. Alswah, M.; Bayoumi, A.H.; Elgamal, K.; Elmorsy, A.; Ihmaid, S.; Ahmed, H.E.A. Design, synthesis and cytotoxic evaluation of novel chalcone derivatives bearing triazolo [4, 3-a]-quinoxaline moieties as potent anticancer agents with dual EGFR kinase and tubulin polymerization inhibitory effects. *Molecules* **2017**, *23*, 48. [[CrossRef](#)]
187. Yepes, A.F.; Arias, J.D.; Cardona-G, W.; Herrera-R, A.; Moreno, G. New class of hybrids based on chalcone and melatonin: A promising therapeutic option for the treatment of colorectal cancer. *Med. Chem. Res.* **2021**, *30*, 2240–2255. [[CrossRef](#)]
188. Ma, X.; Wang, D.; Wei, G.; Zhou, Q.; Gan, X. Synthesis and anticancer activity of chalcone–quinoxalin conjugates. *Synth. Commun.* **2021**, *51*, 1363–1372. [[CrossRef](#)]
189. Paul, K.; Bindal, S.; Luxami, V. Synthesis of new conjugated coumarin–benzimidazole hybrids and their anticancer activity. *Bioorg. Med. Chem. Lett.* **2013**, *23*, 3667–3672. [[CrossRef](#)]
190. An, R.; Hou, Z.; Li, J.T.; Yu, H.N.; Mou, Y.H.; Guo, C. Design, synthesis and biological evaluation of novel 4-substituted coumarin derivatives as antitumor agents. *Molecules* **2018**, *23*, 2281. [[CrossRef](#)]
191. Elshemy, H.A.; Zaki, M.A. Design and synthesis of new coumarin hybrids and insight into their mode of antiproliferative action. *Bioorg. Med. Chem.* **2017**, *25*, 1066–1075. [[CrossRef](#)] [[PubMed](#)]
192. Sanduja, M.; Gupta, J.; Singh, H.; Pagare, P.P.; Rana, A. Uracil-coumarin based hybrid molecules as potent anticancer and antibacterial agents. *J. Saudi Chem. Soc.* **2020**, *24*, 251–266. [[CrossRef](#)]
193. Zhang, Z.; Bai, Z.W.; Ling, Y.; He, L.Q.; Huang, P.; Gu, H.X.; Hu, R.F. Design, synthesis and biological evaluation of novel furoxan-based coumarin derivatives as antitumor agents. *Med. Chem. Res.* **2018**, *27*, 1198–1205. [[CrossRef](#)]
194. Xu, S.; Pei, L.; Wang, C.; Zhang, Y.K.; Li, D.; Yao, H.; Wu, X.; Chen, Z.S.; Sun, Y.; Xu, J. Novel hybrids of natural oridonin-bearing nitrogen mustards as potential anticancer drug candidates. *ACS Med. Chem. Lett.* **2014**, *5*, 797–802. [[CrossRef](#)]
195. Łączkowski, K.Z.; Świtalska, M.; Baranowska-Łączkowska, A.; Plech, T.; Paneth, A.; Misiura, K.; Wietrzyk, J.; Czaplinska, B.; Mrozek-Wilczkiewicz, A.; Malarz, K. Thiazole-based nitrogen mustards: Design, synthesis, spectroscopic studies, DFT calculation, molecular docking, and antiproliferative activity against selected human cancer cell lines. *J. Mol. Struct.* **2016**, *1119*, 139–150. [[CrossRef](#)]

196. Kolesinska, B.; Barszcz, K.; Kaminski, Z.J.; Drozdowska, D.; Wietrzyk, J.; Switalska, M. Synthesis and cytotoxicity studies of bifunctional hybrids of nitrogen mustards with potential enzymes inhibitors based on melamine framework. *J. Enzyme Inhib. Med. Chem.* **2012**, *27*, 619–627. [[CrossRef](#)]
197. Acharya, P.C.; Bansal, R. Synthesis of androstene oxime-nitrogen mustard bioconjugates as potent antineoplastic agents. *Steroids* **2017**, *123*, 73–83. [[CrossRef](#)]
198. Hassan, A.S.; Moustafa, G.O.; Awad, H.M.; Nossier, E.S.; Mady, M.F. Design, synthesis, anticancer evaluation, enzymatic assays, and a molecular modeling study of novel pyrazole–indole hybrids. *ACS Omega* **2021**, *6*, 12361–12374. [[CrossRef](#)]
199. Abd El-Karim, S.S.; Anwar, M.M.; Mohamed, N.A.; Nasr, T.; Elseginy, S.A. Design, synthesis, biological evaluation and molecular docking studies of novel benzofuran–pyrazole derivatives as anticancer agents. *Bioorg. Chem.* **2015**, *63*, 1–12. [[CrossRef](#)]
200. Abdalha, A.A.; Hekal, M.H. An efficient synthesis and evaluation of some novel quinazolinone-pyrazole hybrids as potential antiproliferative agents. *Synth. Commun.* **2021**, *51*, 2498–2509. [[CrossRef](#)]
201. Akhtar, W.; Marella, A.; Alam, M.M.; Khan, M.F.; Akhtar, M.; Anwer, T.; Khan, F.; Naematullah, M.; Azam, F.; Rizvi, M.A. Design and synthesis of pyrazole–pyrazoline hybrids as cancer-associated selective COX-2 inhibitors. *Archiv. Der. Pharmazie.* **2021**, *354*, 2000116. [[CrossRef](#)]
202. Verma, G.; Chashoo, G.; Ali, A.; Khan, M.F.; Akhtar, W.; Ali, I.; Akhtar, M.; Alam, M.M.; Shaquiquzzaman, M. Synthesis of pyrazole acrylic acid based oxadiazole and amide derivatives as antimalarial and anticancer agents. *Bioorg. Chem.* **2018**, *77*, 106–124. [[CrossRef](#)]
203. Sangani, C.B.; Makawana, J.A.; Duan, Y.T.; Yin, Y.; Teraiya, S.B.; Thumar, N.J.; Zhu, H.L. Design, synthesis and molecular modeling of biquinoline–pyridine hybrids as a new class of potential EGFR and HER-2 kinase inhibitors. *Bioorg. Med. Chem. Lett.* **2014**, *24*, 4472–4476. [[CrossRef](#)]
204. Hamza, E.K.; Hamdy, N.A.; Zarie, E.S.; Fakhr, I.M.; Elwahy, A.H.; Awad, H.M. Synthesis and in vitro evaluation of novel tetralin-pyrazolo [3, 4-b] pyridine hybrids as potential anticancer agents. *J. Heterocycl. Chem.* **2020**, *57*, 182–196. [[CrossRef](#)]